Defence Research and Development Canada
Recherche et développement pour la défense Canada

DEFENCE R&D DÉFENSE

Database of ion mobility and tandem mass spectrometric data: characterization of chemical warfare agents, hydrolysis products and related compounds

Paul A. D'Agostino and Claude L. Chenier
DRDC Suffield

Defence R&D Canada

Technical Report

DRDC Suffield TR 2012-010

August 2012

Canada

Database of ion mobility and tandem mass spectrometric data: characterization of chemical warfare agents, hydrolysis products and related compounds

Paul A. D'Agostino and Claude L. Chenier
DRDC Suffield

Defence R&D Canada – Suffield

Technical Report
DRDC Suffield TR 2012-010
August 2012

Principal Author

Paul A. D'Agostino
Defence Scientist

Approved by

Scott Duncan
HHPS

Approved for release by

Robin Clewley
DRP Chair

Abstract

The unambiguous identification of chemical warfare agents requires the acquisition of data from at least two spectrometric/spectroscopic techniques, a requirement that typically results in multiple analyses on different instrumentation. It is now possible to acquire both ion mobility spectrometric (IMS) and tandem mass spectrometric (MS^n, where n = 2 or 3) data during a single instrumental analysis using the Synapt HDMS. Chemical warfare agents, hydrolysis products and related compounds were analysed using the time-aligned parallel (TAP) fragmentation approach which yields both IMS and MS^n data during a single instrumental analysis. Compounds were characterized and differentiated on the basis of their acquired IMS profiles and high resolution MS^n data, which contained evidence of the $[M+H]^+$ ion and typically three or more characteristic product ions. Examples of the usefulness of this identification method for chemical warfare agents are provided as well as an application demonstrating the unambiguous identification of the sarin hydrolysis products, isopropyl methylphosphonic acid and methylphosphonic acid, in the fill of an old rocket recovered from the CFB Suffield Military Training Range. This summary report also contains a 55 entry IMS and MS^n database, created following characterization of available chemical warfare agents, hydrolysis products and related compounds.

Résumé

L'identification non ambiguë d'agents de guerre chimique requiert l'acquisition de données obtenues au moyen d'au moins deux techniques spectrométriques/spectroscopiques, une exigence qui conduit habituellement à plusieurs analyses avec des appareils différents. Il est maintenant possible d'acquérir des données de spectrométrie de mobilité ionique (SMI) et des données de spectrométrie de masse en tandem (SM^n, avec n = 2 ou 3) lors une seule analyse au moyen de l'appareil Synapt HDMS. Nous avons analysé des agents de guerre chimique, leurs produits d'hydrolyse et des composés apparentés en suivant une approche de fragmentation parallèle alignée dans le temps (PAT) qui permet d'obtenir des données de SMI et de SM^n lors d'une même analyse expérimentale. Les composés ont été caractérisés et différenciés en se basant sur les profils de SMI et les données de SM^n haute résolution obtenus, qui comportaient des signatures de l'ion $[M+H]^+$ et, typiquement, de trois ions produits caractéristiques ou plus. Nous donnons des exemples de l'utilité de cette méthode d'identification d'agents de guerre chimique, ainsi que d'une application montrant l'identification non ambiguë de produits d'hydrolyse du sarin, l'acide isopropyl(méthyl)phosphonique et l'acide méthylphosphonique, dans la charge d'une vieille roquette récupérée sur le champ de tir d'entraînement militaire de la BFC Suffield. Le présent rapport contient aussi une base de données de SMI et de SM^n à 55 entrées, créée suite à la caractérisation des agents de guerre chimique, des produits d'hydrolyse et des composés apparentés disponibles.

This page intentionally left blank.

Executive summary

Database of ion mobility and tandem mass spectrometric data: characterization of chemical warfare agents, hydrolysis products and related compounds

D'Agostino, P.A.; Chenier, C.L.; DRDC Suffield TR 2012-010; Defence R&D Canada – Suffield; August 2012.

Introduction: The unambiguous identification of chemical warfare agents requires the acquisition of data from at least two spectrometric/spectroscopic techniques, a requirement that typically results in multiple analyses on different instrumentation. It is now possible to acquire both ion mobility spectrometric (IMS) and tandem mass spectrometric (MS^n, where n = 2 or 3) data during a single instrumental analysis using a newly developed commercial time-of-flight mass spectrometer.

Results: Chemical warfare agents, hydrolysis products and related compounds were analysed using the time-aligned parallel (TAP) fragmentation approach which yields both IMS and MS^n data during a single instrumental analysis. Compounds were characterized and differentiated on the basis of their acquired IMS profiles and high resolution MS^n data, which contained evidence of the $[M+H]^+$ ion and typically three or more characteristic product ions. Examples of the usefulness of this identification method for chemical warfare agents are provided as well as a practical application demonstrating the unambiguous identification of the sarin hydrolysis products, isopropyl methylphosphonic acid and methylphosphonic acid, in the fill of an old rocket recovered from the CFB Suffield Military Training Range

Significance: Use of this new analytical approach should reduce both the time and instrumentation typically required for unambiguous identification of chemical warfare agents in samples collected by Canadian Forces personnel. This summary report also contains a 55 entry IMS and MS^n database, created following characterization of available chemical warfare agents, hydrolysis products and related compounds. The data contained in the database will facilitate the unambiguous identification of individual compounds contained in the database. In addition, data collected using the TAP experimental approach could aid in the structural elucidation of previously non-traditional agents or other unknowns present in samples selected for chemical warfare agent analysis. Identification of these additional sample components could be significant as their identity may indicate possible synthetic pathway information or aid in identifying the source of the chemical warfare agent.

Future plans: Newly characterized compounds of significance to the chemical defence community will be added to the database in a timely manner.

Sommaire

Base de données de spectrométrie de mobilité ionique et de spectrométrie de masse en tandem : caractérisation d'agents de guerre chimique, de produits d'hydrolyse et de composés apparentés

D'Agostino P.A., Chenier C.L.; RDDC Suffield TR 2012-010 ; R & D pour la défense Canada – Suffield, août 2012.

Introduction ou contexte : L'identification non ambiguë d'agents de guerre chimique requiert l'acquisition de données obtenues au moyen d'au moins deux techniques spectrométriques/spectroscopiques, une exigence qui conduit habituellement à plusieurs analyses avec des appareils différents. Il est maintenant possible d'acquérir des données de spectrométrie de mobilité ionique (SMI) et de spectrométrie de masse en tandem (SM^n, avec n = 2 ou 3) lors une seule analyse au moyen d'un nouveau spectromètre de masse à temps de vol commercial nouvellement développé.

Résultats : Nous avons analysé des agents de guerre chimique, leurs produits d'hydrolyse et des composés apparentés en suivant une approche de fragmentation parallèle alignée dans le temps (PAT) qui permet d'obtenir des données de SMI et de SM^n lors d'une même analyse expérimentale. Les composés ont été caractérisés et différenciés en se basant sur les profils de SMI et les données de SM^n haute résolution obtenus, qui comportaient des signatures de l'ion $[M+H]^+$ et, typiquement, de trois ions produits caractéristiques ou plus. Nous donnons des exemples de l'utilité de cette méthode d'identification d'agents de guerre chimique, ainsi que d'une application pratique montrant l'identification non ambiguë de produits d'hydrolyse du sarin, l'acide isopropyl(méthyl)phosphonique et l'acide méthylphosphonique, dans la charge d'une vieille roquette récupérée sur le champ de tir d'entraînement militaire de la BFC Suffield.

Importance : L'utilisation de cette nouvelle méthode analytique devrait permettre de réduire le temps et l'équipement habituellement nécessaires pour une identification non ambiguë d'agents de guerre chimique dans des échantillons collectés par le personnel des Forces canadiennes. Le présent rapport contient aussi une base de données de SMI et de SM^n de 55 entrées, créée suite à la caractérisation des agents de guerre chimique, des produits d'hydrolyse et des composés apparentés disponibles. Cette base de données facilitera l'identification non ambiguë des composés présents dans cette base. De plus, les données collectées en suivant l'approche expérimentale de fragmentation PAT pourraient contribuer à élucider la structure d'agents non traditionnels ou inconnus présents dans des échantillons retenus pour une analyse d'agents de guerre chimique. L'identification de ces éléments additionnels pourrait être importante, leur identité pouvant procurer des renseignements sur de possibles voies de synthèse ou aider à identifier la source de l'agent de guerre chimique.

Perspectives : De nouveaux composés caractérisés ayant une importance pour la communauté de la défense chimique seront ajoutés à cette base de données en temps opportun.

Table of contents

Abstract ……. i
Résumé ……..... i
Executive summary iii
Sommaire iv
Table of contents iv
List of figures vi
List of tables viii
List of Diagrams viii
List of illustrations (illustrative examples in the text) ix
Acknowledgements xii
Introduction 1
Experimental 3
    Instrumental conditions 3
    Samples 3
Results and discussion 4
    Typical DESI-IMS-MS^n and LC-IMS-MS^n data acquisition 5
    Ion mobility profiles of chemical warfare agents 8
    Compounds with the same nominal mass 10
    Compounds with the same exact mass 15
    Application: analysis of an old chemical rocket 18
    IMS and MS^n Database (Figures 3 to 55) 29
Conclusions 85
References 86
Annex A Raw datafiles used to prepare Figures 1 to 55 89

List of figures

Figure 1: Lower collision energy IMS and MS^n data for methylphosphonic acid (96). 30
Figure 2: Higher collision energy IMS and MS^n data for methylphosphonic acid (96). 31
Figure 3: IMS and MS^n data for diisopropylamine (101). 32
Figure 4: Lower collision energy IMS and MS^n data for thiodiglycol (122). 33
Figure 5: Higher collision energy IMS and MS^n data for thiodiglycol (122). 34
Figure 6: IMS and MS^n data for ethyl methylphosphonic acid (124). 35
Figure 7: Lower collision energy IMS and MS^n data for isopropyl methylphosphonic acid (138). 36
Figure 8: Higher collision energy IMS and MS^n data for isopropyl methylphosphonic acid (138). 37
Figure 9: IMS and MS^n data for trimethyl phosphate (140). 38
Figure 10: Lower collision energy IMS and MS^n data for isopropyl methylphosphonofluoridate (sarin, GB) (140). 39
Figure 11: Higher collision energy IMS and MS^n data for isopropyl methylphosphonofluoridate (sarin, GB) (140). 40
Figure 12: IMS and MS^n data for diethyl methylphosphonate (152). 41
Figure 13: IMS and MS^n data for ethyl dimethylphosphoramidic acid (153) 42
Figure 14: Lower collision energy IMS and MS^n data for O-ethyl N,N-dimethylphosphoramidocyanidate (tabun, GA) (162) 43
Figure 15: Moderate collision energy IMS and MS^n data for O-ethyl N,N-dimethylphosphoramidocyanidate (tabun, GA) (162) 44
Figure 16: Higher collision energy IMS and MS^n data for O-ethyl N,N-dimethylphosphoramidocyanidate (tabun, GA) (162) 45
Figure 17: Lower collision energy IMS and MS^n data for cyclohexyl methylphosphonic acid (178). 46
Figure 18: Higher collision energy IMS and MS^n data for cyclohexyl methylphosphonic acid (178). 47
Figure 19: Lower collision energy IMS and MS^n data for cyclohexyl methylphosphonofluoridate (cyclosarin, GF) (180). 48
Figure 20: Higher collision energy IMS and MS^n data for cyclohexyl methylphosphonofluoridate (cyclosarin, GF) (180). 49
Figure 21: Lower collision energy IMS and MS^n data for pinacolyl methylphosphonic acid (180). 50

Figure 22: Higher collision energy IMS and MS^n data for pinacolyl methylphosphonic acid (180). 51
Figure 23: IMS and MS^n data for ethyl tetramethylphosphorodiamidate (180). 52
Figure 24: IMS and MS^n data for diethyl dimethylphosphoramidate (181). 53
Figure 25: IMS and MS^n data for triethyl phosphate (TEP) (182)..... 54
Figure 26: Lower collision energy IMS and MS^n data for pinacolyl methylphosphonofluoridate (soman, GD) (182). 55
Figure 27: Higher collision energy IMS and MS^n data for pinacolyl methylphosphonofluoridate (soman, GD) (182). 56
Figure 28: IMS and MS^n data for 2-(diisopropylamino)ethyl ethyl sulfide (189) 57
Figure 29: IMS and MS^n data for isopropyl tetramethylphosphorodiamidate (194). 58
Figure 30: IMS and MS^n data for ethyl isopropyl dimethylphosphoramidate (195). 59
Figure 31: IMS and MS^n data for diethyl isopropyl phosphate (196)..... 60
Figure 32: Lower collision energy IMS and MS^n data for ethyl pinacolyl methylphosphonate (208). 61
Figure 33: Higher collision energy IMS and MS^n data for ethyl pinacolyl methylphosphonate (208). 62
Figure 34: IMS and MS^n data for diisopropyl dimethylphosphoramidate (209). 63
Figure 35: IMS and MS^n data for diisopropyl ethyl phosphate (210)..... 64
Figure 36: Lower collision energy IMS and MS^n data for tripropyl phosphate (224). 65
Figure 37: Higher collision energy IMS and MS^n data for tripropyl phosphate (224). 66
Figure 38: Lower collision energy IMS and MS^n data for triisopropyl phosphate (224). 67
Figure 39: Higher collision energy IMS and MS^n data for triisopropyl phosphate (224)..... 68
Figure 40: IMS and MS^n data for N,N-dicyclohexylurea (224)..... 69
Figure 41: IMS and MS^n data for diethyl dimethylpyrophosphonate (230). 70
Figure 42: IMS and MS^n data for N,N-dicyclohexylthiourea (240). 71
Figure 43: Lower collision energy IMS and MS^n data for dipinacolyl methylphosphonate (264). 72
Figure 44: Higher collision energy IMS and MS^n data for dipinacolyl methylphosphonate (264). 73
Figure 45: IMS and MS^n data for tributyl phosphate (TBP) (266). 74
Figure 46: IMS and MS^n data for O-ethyl S-[2-(diisopropylamino)ethyl] methylphosphonothiolate (VX) (267). 75
Figure 47: IMS and MS^n data for ethyl dimethylphosphoramidic tetramethylphosphoramidic anhydride (287). 76
Figure 48: IMS and MS^n data for bis(ethyl dimethylphosphoramidic) anhydride (288). 77

Figure 49: IMS and MS^n data for bis[2-(diisopropylamino)ethyl] sulfide (288). 78
Figure 50: IMS and MS^n data for bis[2-diisopropylamino)ethyl] disulfide (320). 79
Figure 51: IMS and MS^n data for O-ethyl-S-[5-diisopropylamino)-3-thiapentyl]methylphonothialate (327). 80
Figure 52: Lower collision energy IMS and MS^n data for 3-quinuclidinyl benzilate (BZ) (337). 81
Figure 53: Moderate collision energy IMS and MS^n data for 3-quinuclidinyl benzilate (BZ) (337). 82
Figure 54: Higher collision energy IMS and MS^n data for 3-quinuclidinyl benzilate (BZ) (337). 83
Figure 55: IMS and MS^n data for 1,9-bis(diisopropylamino)-3,4,7-trithianonane (380). 84

List of tables

Table 1: Instrumental conditions. 3
Table 2: Measured and mass errors for the ions used to characterize ethyl tetramethylphosphorodiamidate. 8

List of Diagrams

Diagram 1: High definition mass spectrometry. 2
Diagram 2: Analysis of the aqueous extract of the rocket fill. 20

List of illustrations (illustrative examples in the text)

Illustration 1: Acquisition of IMS and MS^n data following DESI sample introduction. A total-ion-current chromatogram was acquired for the $[M+H]^+$ ion (m/z 181) of cyclosarin (GF). The IMS profile and MS^n data presented were acquired with trap and transfer collision energies of 3 eV and 3 eV, respectively. 6

Illustration 2: Acquisition of IMS and MS^n data following LC sample introduction. A total-ion-current chromatogram was acquired for the $[M+H]^+$ ion (m/z 181) of ethyl tetramethylphosphorodiamidate. The IMS profile and MS^n data presented were acquired with trap and transfer collision energies of 12 eV and 12 eV, respectively. 7

Illustration 3: Ion mobility profiles obtained for a) sarin (GB), b) tabun (GA), c) cyclosarin (GF), d) soman (GD) and e) VX following DESI-IMS- MS^n analysis of SPME fibers exposed to the headspace above 5 µg each compound. The $[M+H]^+$ ion selected by the quadrupole analyser and one or more product ions (P_1, P_2), generated in the trap region of the collision cell, were separated by IMS (m/z values indicated). Trap and transfer collision energies for a) to e) were 3/3 eV, 7/7 eV, 3/3 eV, 3/3 eV and 15/18 eV, respectively. 9

Illustration 4: MS^2 data obtained for the $[M+H]^+$ ion of a) sarin (GB), b) tabun (GA), c) cyclosarin (GF), d) soman (GD) and e) VX. Trap and transfer collision energies for a) to e) were 3/3 eV, 7/7 eV, 3/3 eV, 3/3 eV and 15/18 eV, respectively. 10

Illustration 5: Ion mobility profiles for three compounds with the same nominal mass (180 Da), a) cyclohexyl methylphosphonofluoridate (GF), b) pinacolyl methylphosphonic acid and c) ethyl tetramethylphosphorodiamidate. The $[M+H]^+$ ion selected by the quadrupole analyser and one or more product ions(P_1, P_2) , generated in the trap region of the collision cell, were separated by IMS (m/z values indicated). Trap and transfer collision energies for a) to c) were 3/3 eV, 3/3 eV, and 12/12 eV, respectively. 11

Illustration 6: MS^2 data obtained for the $[M+H]^+$ ion of a) cyclohexyl methylphosphonofluoridate (GF), b) pinacolyl methylphosphonic acid and c) ethyl tetramethylphosphorodiamidate. Trap and transfer collision energies for a) to c) were 3/3 eV, 3/3 eV, and 12/12 eV, respectively. 12

Illustration 7: MS^3 data obtained for a product ion of a) cyclohexyl methylphosphonofluoridate (GF) – m/z 99, b) pinacolyl methylphosphonic acid – m/z 97 and c) ethyl tetramethylphosphorodiamidate – m/z 153. Trap and transfer collision energies for a) to c) were 3/20 eV, 3/20 eV, and 12/12 eV, respectively. 13

Illustration 8: Ion mobility profiles for two compounds with the same nominal mass (182 Da), a) triethyl phosphate and b) pinacolyl methylphosphonofluoridate (GD). The $[M+H]^+$ ion selected by the quadrupole analyser and one or more product ions(P_1, P_2, P_3), generated in the trap region of the collision cell, were separated by IMS (m/z values indicated). Trap and transfer collision energies for a) to b) were 10/10 eV and 3/3 eV, respectively. 14

Illustration 9: MS^2 data obtained for the $[M+H]^+$ ion of a) triethyl phosphate and b) pinacolyl methylphosphonofluoridate (GD). Trap and transfer collision energies for a) and b) were 10/10 eV, and 3/3 eV, respectively. 14

Illustration 10: MS^3 data obtained for a product ion of a) triethyl phosphate – m/z 155 and b) pinacolyl methylphosphonofluoridate (GD) – m/z 99. Trap and transfer collision energies for a) and b) were 10/10 eV and 3/20 eV, respectively. 15

Illustration 11: Ion mobility profiles for tripropyl phosphate with trap and transfer collision energies of a) 7/7 eV and b) 10/10 eV. Ion mobility profiles for triisopropyl phosphate with trap and transfer collision energies of c) 7/7 eV and d) 10/10 eV. The $[M+H]^+$ ion selected by the quadrupole analyser and three product ions (P_1, P_2, P_3), generated in the trap region of the collision cell, were separated by IMS (m/z values indicated). 16

Illustration 12: MS^2 data for a) m/z 225 and MS^3 data for b) m/z 183, c) 141 and d) m/z 99 acquired for tripropyl phosphate with trap and transfer collision energies of 7/7 eV. MS^2 data for e) m/z 225 and MS^3 data for f) m/z 183, g) 141 and h) m/z 99 acquired for triisopropyl phosphate with trap and transfer collision energies of 7/7 eV. 17

Illustration 13: MS^2 data for a) m/z 225 and MS^3 data for b) m/z 183, c) 141 and d) m/z 99 acquired for tripropyl phosphate with trap and transfer collision energies of 10/10 eV. MS^2 data for e) m/z 225 and MS^3 data for f) m/z 183, g) 141 and h) m/z 99 acquired for triisopropyl phosphate with trap and transfer collision energies of 10/10 eV. 18

Illustration 14: Old rocket found on CFB Suffield Military Training Range. 19

Illustration 15: Gradient programming LC-ESI-MS analysis of aqueous blank. The total-ion-current (TIC) and selected ion traces for sarin and its hydrolysis products are shown. 21

Illustration 16: Gradient programming LC-ESI-MS analysis of aqueous extract of rocket fill. The total-ion-current (TIC) and selected ion traces for sarin and its hydrolysis products are shown. 22

Illustration 17: ESI-MS data acquired at the retention time for methylphosphonic acid. Only the m/z 97 ion could be attributed to methylphosphonic acid. 23

Illustration 18: IMS profiles for aqueous blank and aqueous extract of rocket fill with the m/z 97 ion ($[M+H]^+$ ion for methylphosphonic acid) selected by the quadrupole mass analyser. 24

Illustration 19: IMS profiles for aqueous blank and aqueous extract of rocket fill with the m/z 139 ion ($[M+H]^+$ ion for isopropyl methylphosphonic acid) selected by the quadrupole mass analyser 25

Illustration 20: Isocratic LC-IMS-MS^n data acquired for methylphosphonic acid (50 ng standard) and the aqueous extract of rocket fill (sample) 26

Illustration 21: Isocratic LC-IMS-MS^n data acquired with a lower collision energy for isopropyl methylphosphonic acid (1 ng standard) and the aqueous extract of rocket fill (sample). 27

Illustration 22: Isocratic LC-IMS-MS^n data acquired with a higher collision energy for isopropyl methylphosphonic acid (1 ng standard) and the aqueous extract of rocket fill (sample). 28

Acknowledgements

The authors would like to thank C. R. Jackson Lepage and S. D. Huelin for providing the fill sample from the chemical rocket that was used as an application of the IMS-MS^n methodology.

Introduction

Detection and identification methods for the determination of chemical warfare agents, their degradation products and related compounds have been thoroughly reviewed over the past decade [1-10]. Aqueous samples or extracts, containing organophosphorus chemical warfare agents, their hydrolysis products and related compounds may be analysed directly by liquid chromatography electrospray ionization mass spectrometry (LC-ESI-MS) [3, 7-10] without the need for additional sample handling and derivatization steps [6]. DRDC Suffield has completed a number of LC-ESI-MS investigations, including the analysis of tabun and related compounds in synthetic and munitions grade samples [11-13], the analysis of sarin in snow samples [14, 15] and the analysis of VX and its degradation products in an aged sample [16, 17]. More recently DRDC Suffield demonstrated the application of desorption electrospray ionization mass spectrometry (DESI-MS) for the direct analysis of solid phase micro-extraction (SPME) fibers for chemical warfare agents [18-22]. Analysis was rapid and acquired data were identical to data obtained during LC-ESI-MS. A large number of sample components were characterized following LC-ESI-MS and DESI-MS analysis of chemical warfare agent containing samples at DRDC Suffield and these techniques now form a cornerstone in the overall detection and identification strategy employed at DRDC Suffield.

Ion mobility spectrometry (IMS) has been used successfully within the defence and public security communities for the detection of explosives and chemical warfare agents, with the hand-held Chemical Agent Monitor (CAM) being a well-recognized IMS device [23]. IMS has been interfaced prior to the mass analyser on a variety of mass spectrometers, resulting in rapid separation and identification of chemical warfare agent simulants and degradation products [24-29]. High field asymmetric waveform IMS-MS was utilized for the analysis of chemical warfare agents spiked into food products [30] and most recently DRDC Suffield reported DESI-MS applications using a Waters Synapt HDMS [20, 21], illustrated in the following schematic. Incorporation of the IMS cell within the Triwave collision cell of the Synapt HDMS allowed acquisition of both IMS data and MS^n (typically n=2 or 3) data following DESI sample introduction. Data acquired in this manner, referred to as time-aligned parallel (TAP) fragmentation data, were used for the first time for the rapid confirmation of chemical warfare agents [26]. Individual chemical warfare agents were differentiated on the basis of their IMS profiles and acquired full scanning, high resolution MS^n data. MS^n data contained evidence of the $[M+H]^+$ ion and three or more characteristic product ions (acquired with one or more collision energy settings). A screening approach was also developed for the analysis of sarin, soman, tabun and cyclosarin. Individual chemical warfare agents were spiked onto Dacron sampling swabs, office furniture fabric or cardboard and successfully screened for the presence of all four chemical warfare agents during a single DESI-IMS-MS^n analysis [21].

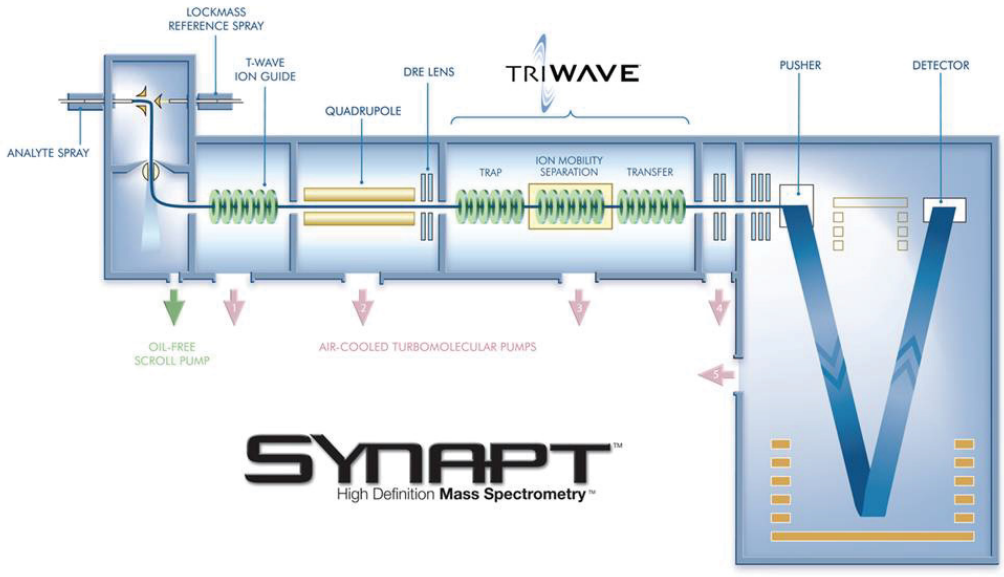

Diagram 1: High definition mass spectrometry.

As the number of sample components requiring characterization increases, the usefulness of batch introduction techniques such as DESI decreases. Chromatographic sample introduction techniques, including liquid chromatography, would typically be employed to enable separation of sample components prior to spectrometric characterization. A Synapt HDMS instrument was used for the first time to acquire both IMS and MS^n (n = 2 or 3) data for chemical defence compounds following LC sample introduction. Samples were initially screened by LC-MS under low collision energy conditions that resulted in formation of significant $[M+H]^+$ ions for the sample components. Retention time windows, associated with observed $[M+H]^+$ ions during LC-MS screening, were established for the acquisition of LC-IMS-MS^n data for individual sample components in a simulant mixture and two chemical warfare agent hydrolysis products [31].

The results of the DESI-IMS-MS^n and LC-IMS-MS^n investigations [20, 21, 31] suggested that the acquisition of both IMS and MS^n data for chemical warfare agents and related compounds, using the TAP approach, may be sufficient for unambiguous identification purposes. However to be useful in the larger community, a chemical warfare agent database of IMS and MS^n data, similar to DRDC Suffield's electrospray database of chemical warfare agents and related compounds [32], would be required for comparative purposes. IMS and MS^n data were acquired following either DESI or LC sample introduction for a large number of available chemical warfare agents, hydrolysis products and related compounds. Data have been summarized for each compound on a single page that illustrates typical IMS and MS^n data, at a given collision energy, as well as possible ion structures (or elemental assignments) consistent with the masses of the observed ions. Higher collision energy settings were also employed to enhance product ion formation for some compounds, resulting in the generation of additional characteristic product ions that may be used for confirmation purposes.

Experimental

Instrumental conditions

Instrumental conditions typically used for data acquisition are listed below.

Table 1: Instrumental conditions.

Parameter	Setting
Mass spectrometer	Waters Synapt HDMS
Source	Z-spray electrospray source
Capillary voltage	Typically 3 kV
Source temperature	80 ^{o}C
Desolvation temperature	100 ^{o}C
Nitrogen cone gas	50 L/min
Nitrogen desolvation gas	300 L/Min
Sampling cone	15 V (typically)
Trap collision energy	3 to 25 eV
Transfer collision energy	3 to 25 eV
Argon trap gas	4.5 mL/min
Helium ion mobility gas	35 mL/min
Resolution	8000 (50% valley definition)
Mass range	From m/z 40 to as high as m/z 400
Scan time	0.5 to 1 sec/scan
DESI sample introduction	Performed using solid phase microextraction fibers. The mobile phase was 1:1 acetonitrile/water (0.1% trifluoroacetic acid) flowing at 10 µL/min.
LC sample introduction	Isocratic and gradient (typically 5 to 75% B in 15 min) LC separations were performed with an Agilent 1100 capillary LC with a flow rate of 10 µL/min. The following solvent compositions were prepared for the mobile phase: Solvent A (0.1% trifluoroacetic acid in water) and Solvent B (acetonitrile). All LC separations were performed with Agilent 50 mm x 0.3 mm i.d. fused-silica capillary columns packed with Zorbax SB C18 (1.8 µm particle size).

Samples

Chemical warfare agents and many related reference standards were provided by the DRDC Suffield CNSSSF laboratory or purchased commercially. Additional compounds were characterized during analysis of deliberately hydrolysed chemical warfare agent samples, aged chemical warfare agent samples or munitions grade chemical agents.

Results and discussion

Unambiguous identification of chemical warfare agents requires the acquisition of data from two spectrometric/spectroscopic techniques that agrees with that acquired for a authentic reference compound (NATO definition) or authentic reference compound data (OPCW definition). Ideally this data should come from two completely different spectrometric/spectroscopic techniques, including, but not limited to mass spectrometry, nuclear magnetic resonance spectrometry and infrared spectroscopy. In some situations, where component separation or sensitivity limits the choice of techniques, two different mass spectrometric techniques, including electron impact ionization, chemical ionization, electrospray ionization (ESI) or another atmospheric pressure ionization technique, may be used. Comparison of chromatographic retention time (or retention index) would also typically be performed during confirmation using only mass spectrometric techniques.

Ion mobility spectrometry (IMS), while used extensively for field detection with devices such as the CAM, has not typically been associated with chemical warfare agent confirmation in a laboratory setting. New instrumentation now enables the rapid acquisition of both MS^n (typically n = 2 or 3) and ion mobility data during a single instrumental analysis. Recent reports have demonstrated differences in the ion mobility spectra of chemical warfare agents and related compounds [20, 21, 31] and combined with multiple MS^n data present a compelling case for compound confirmation. Typically this MS^n data would be acquired with a resolution of 8000-9000 (10% valley definition) resulting in mass measurements errors of less than 2 mDa. For chemical warfare agents and other lower mass compounds this often enables assignment of elemental composition(s), a particularly helpful tool for the identification of previously uncharacterized compounds or unknowns [31].

The unique collision cell in the Synapt HDMS mass spectrometer used in recent studies [20, 21,31] enables analysts to perform a variety of MS^n (typically n = 2 or 3) experiments by making use of the ESI source region and Triwave collision cell. Organophosphorus chemical warfare agents and related compounds typically ionize in the ESI source giving rise to abundant $[M+H]^+$ ions (and other adduct ions) at lower sampling cone voltages. If desired, product ions may be produced by increasing the sampling cone voltage. Ions formed in the ESI source may be passed through the quadrupole mass analyser or a particular ion may be selected by the quadrupole mass analyser for subsequent investigation. The quadrupole mass analyser can mass select with varying window widths and a one m/z window was used to reduce chemical noise during all data acquisition at DRDC Suffield. Mass selected $[M+H]^+$ ions (or product ions formed in the ESI source) may then undergo fragmentation in the trap collision region prior to the IMS cell in the Triwave collision cell. During a typical experiment, moderate trap collision energy settings that maintained significant $[M+H]^+$ intensity but also resulted in the formation of the one or more product ions were typically used. The $[M+H]^+$ ion and product ions exiting the trap collision region were rapidly separated (9 msec) in the IMS cell on the basis of their ion mobility, resulting in the acquisition of a characteristic ion mobility profile for each compound. Finally, the ion mobility separated ions were fragmented in the transfer collision region, using moderate energy setting that resulted in the acquisition of MS^n data for the $[M+H]^+$ ion and product ions separated in the IMS cell. Acquisition of IMS and MS^n data in this manner has been referred to as time-aligned parallel (TAP) fragmentation.

IMS and MS^n data were initially acquired for five organophosphorus chemical warfare agents [20, 21], two simulants [31] and thirteen compounds identified in hydrolysed tabun and VX [31]. In the current study additional compounds of chemical defence interest were characterized in an attempt to create the first database of IMS and MS^n data. In all cases an ion mobility profile was acquired along with multiple MS^n high resolution mass spectra. Conditions were selected that preserved the $[M+H]^+$ ion for all compounds, yet yielded a number of characteristic product ions that could be used for confirmation purposes. MS^2 data were acquired for the $[M+H]^+$ ion selected by the quadrupole mass analyser, for all the chemical warfare agents, hydrolysis products and related compounds. Additional MS^3 data for characteristic product ions that were formed in the trap collision region, separated in the IMS cell and fragmented in the transfer collision region were acquired in the TAP experiment. For some compounds the number (and abundance) of product ions formed in the trap collision region under conditions that maintained a significant population of $[M+H]^+$ was limited. Supplementary TAP data were therefore also acquired under higher collision energy conditions that favoured product ion formation. Acquisition of IMS and MS^n data at both lower collision energies that favoured the presence of the $[M+H]^+$ ion and at higher collision energies that enhanced the formation of characteristic product ions, while not necessary for many of the compounds characterized, should be considered to increase the number the ions available for identification purposes.

Available chemical warfare agents, hydrolysis products and related compounds (often found in crude or munitions grade samples) were analysed using the TAP experimental approach. The acquired IMS and MS^n data has been compiled into a database organized by increasing molecular mass in much the same manner as the DRDC electrospray mass spectrometric database for chemical warfare agents and related compounds [32]. Data were acquired for common organophosphorus chemical warfare agents, hydrolysis products and related compounds typically found in hydrolysed, crude or munitions grade samples. The IMS and MS^n database, containing compounds over a wide molecular mass range, is contained in Figures 1 to 55. Archived raw data file information used to generate each Figure resides in Annex A.

During the generation of the database, a number of examples of the usefulness of IMS-MS^n data acquisition became apparent. These examples and illustrations associated with each example are presented below.

Typical DESI-IMS-MS^n and LC-IMS-MS^n data acquisition

Mass spectrometric data acquired using DESI or ESI techniques were indistinguishable for the chemical defence compounds analysed. Both DESI (Illustration 1) and ESI (following LC sample introduction, Illustration 2) were used to acquire IMS and MS^n data for the chemical defence compounds contained in the database, with LC being preferred for multi-component samples. A typical total-ion-current chromatogram acquired for the selected $[M+H]^+$ ion for each compound in Illustrations 1 and 2 is presented in the lower section of each Illustration. A unique IMS profile and MS^n data were acquired during each LC-IMS-MS^n or DESI-IMS-MS^n analysis, which would enable unambiguous identification of the chemical warfare agent under investigation.

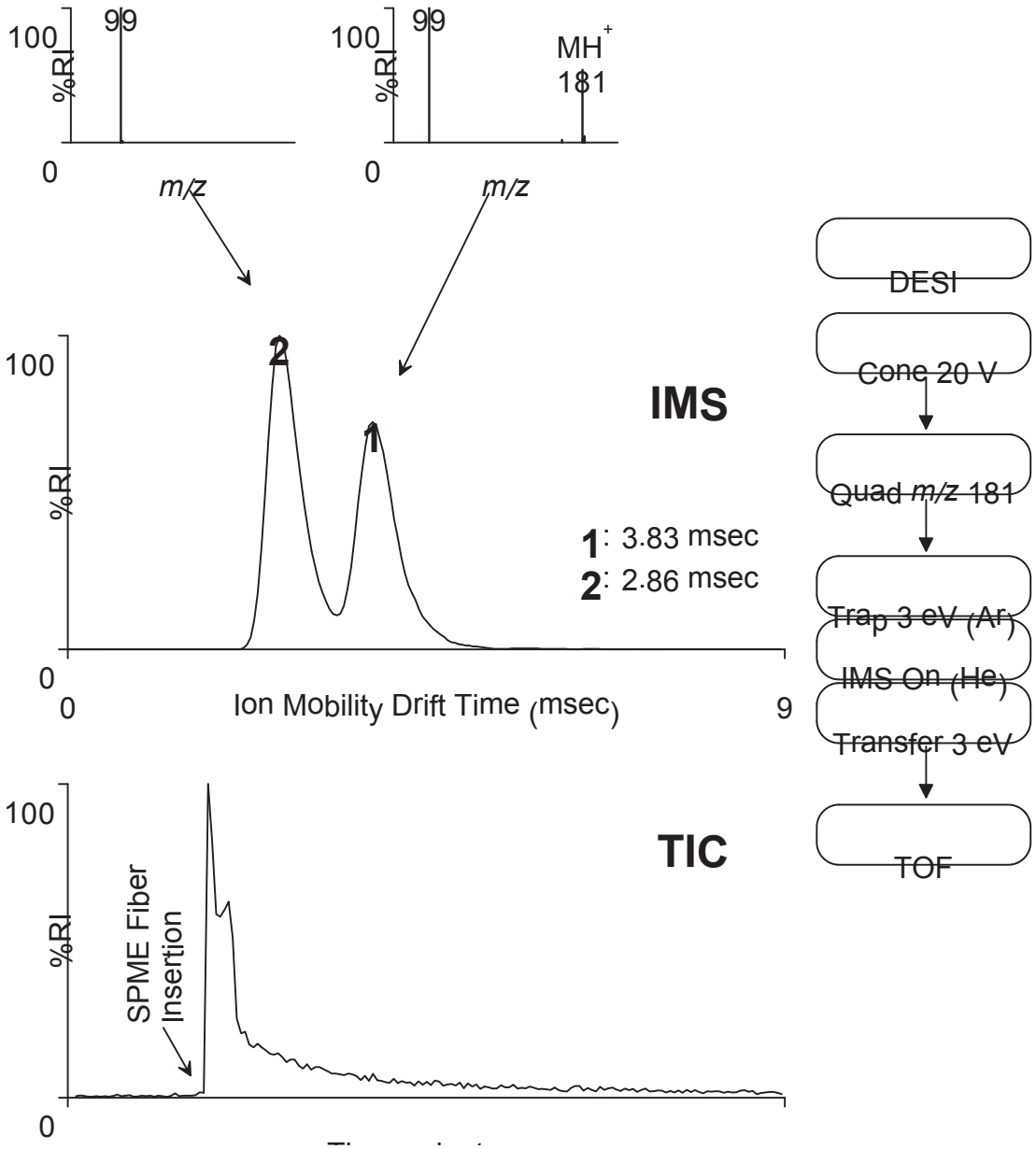

Illustration 1: Acquisition of IMS and MS^n data following DESI sample introduction. A total-ion-current chromatogram was acquired for the $[M+H]^+$ ion (m/z 181) of cyclosarin (GF). The IMS profile and MS^n data presented were acquired with trap and transfer collision energies of 3 eV and 3 eV, respectively.

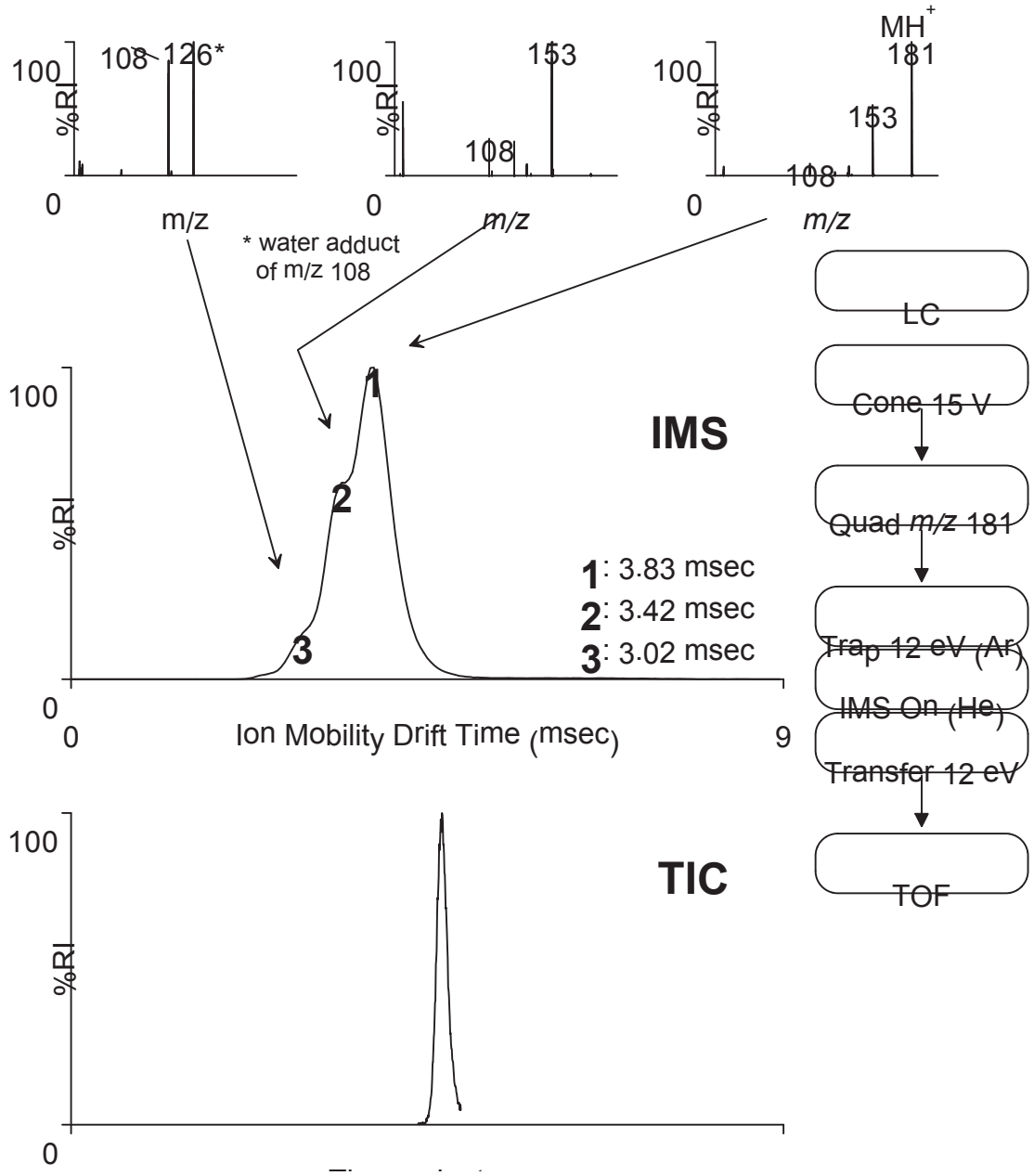

Illustration 2: Acquisition of IMS and MS^n data following LC sample introduction. A total-ion-current chromatogram was acquired for the $[M+H]^+$ ion (m/z 181) of ethyl tetramethylphosphorodiamidate. The IMS profile and MS^n data presented were acquired with trap and transfer collision energies of 12 eV and 12 eV, respectively.

MS^n data were acquired with a resolution of 8000-9000 (50% valley definition). Accurate mass measurement for chemical warfare agents and other lower molecular mass compounds can be quite helpful both for confirming the elemental composition of an ion and for the assignment of possible elemental compositions during the identification of previously uncharacterized compounds. Mass measurement errors were typically less than 2 mDa [20, 21], with the best results being achieved with a lock mass reference ion. The list below illustrates the measured, theoretical and mass errors for the ions used to characterize ethyl tetramethylphosphorodiamidate (Illustration 2), an impurity in tabun.

Table 2: Measured, theoretical and mass errors for the ions used to characterize ethyl tetramethylphosphorodiamidate

Measured Mass (Da)	Theoretical Mass (Da)	Error (Da)
181.1074	181.1106	0.0032
153.0787	153.0793	0.0006
136.0526	136.0527	0.0001
126.0313	126.0320	0.0007
108.0232	108.0214	0.0018
46.0645	46.0657	0.0012

Ion mobility profiles of chemical warfare agents

The ion mobility profiles of five common chemical warfare agents [20, 21] were initially acquired to demonstrate the potential usefulness of this technique for identification purposes. Illustration 3 presents the unique ion mobility profiles that can be used to differentiate the five chemical warfare agents, sarin, tabun, cyclosarin, soman and VX. Errors associated with the ion mobility measurements were typically less than 0.03 msec [20]. Differences were also readily observed in the acquired MS^n data provided in Illustration 4. Product ions due to the loss of an alkene related to the alkoxy group were significant at lower energies for sarin, tabun, cyclosarin and soman. At higher collision energies, the $[M+H]^+$ ion was generally not observed. However, additional lower mass product ions that could be used for identification were detected and have been reported for these chemical warfare agents in the IMS and MS^n database created during this study.

The m/z 85 ion for soman has a drift time that was longer than the m/z 99 ion, likely due to it having a larger volume than the m/z 99 ion. This was confirmed by geometry optimization done at UHF/6-31G, which indicated that the m/z 85 ion would occupy approximately a 12% larger tumbling volume than the m/z 99 ion in the IMS cell [20].

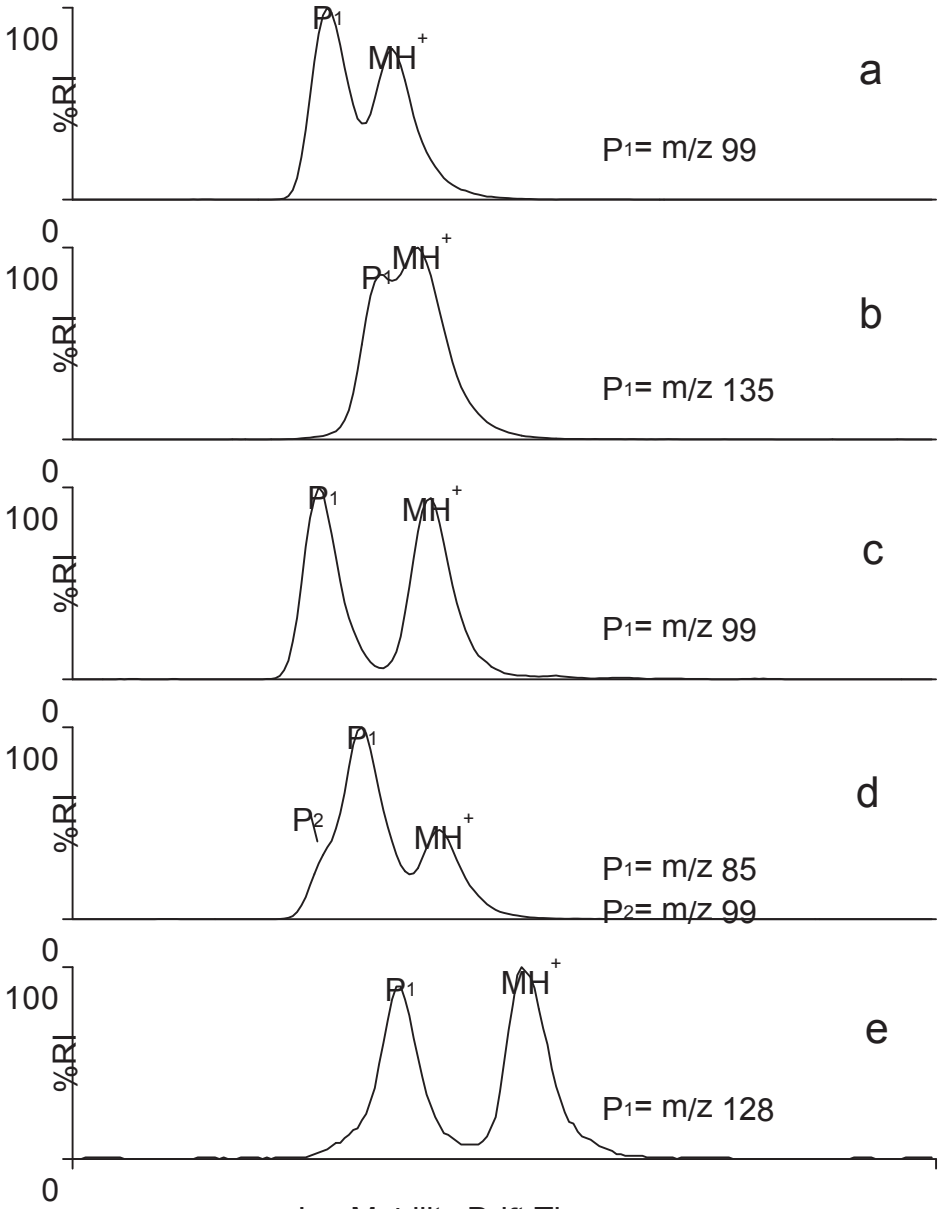

Illustration 3: Ion mobility profiles obtained for a) sarin (GB), b) tabun (GA), c) cyclosarin (GF), d) soman (GD) and e) VX following DESI-IMS- MS^n analysis of SPME fibers exposed to the headspace above 5 µg each compound. The $[M+H]^+$ ion selected by the quadrupole analyser and one or more product ions (P_1, P_2), generated in the trap region of the collision cell, were separated by IMS (m/z values indicated). Trap and transfer collision energies for a) to e) were 3/3 eV, 7/7 eV, 3/3 eV, 3/3 eV and 15/18 eV, respectively.

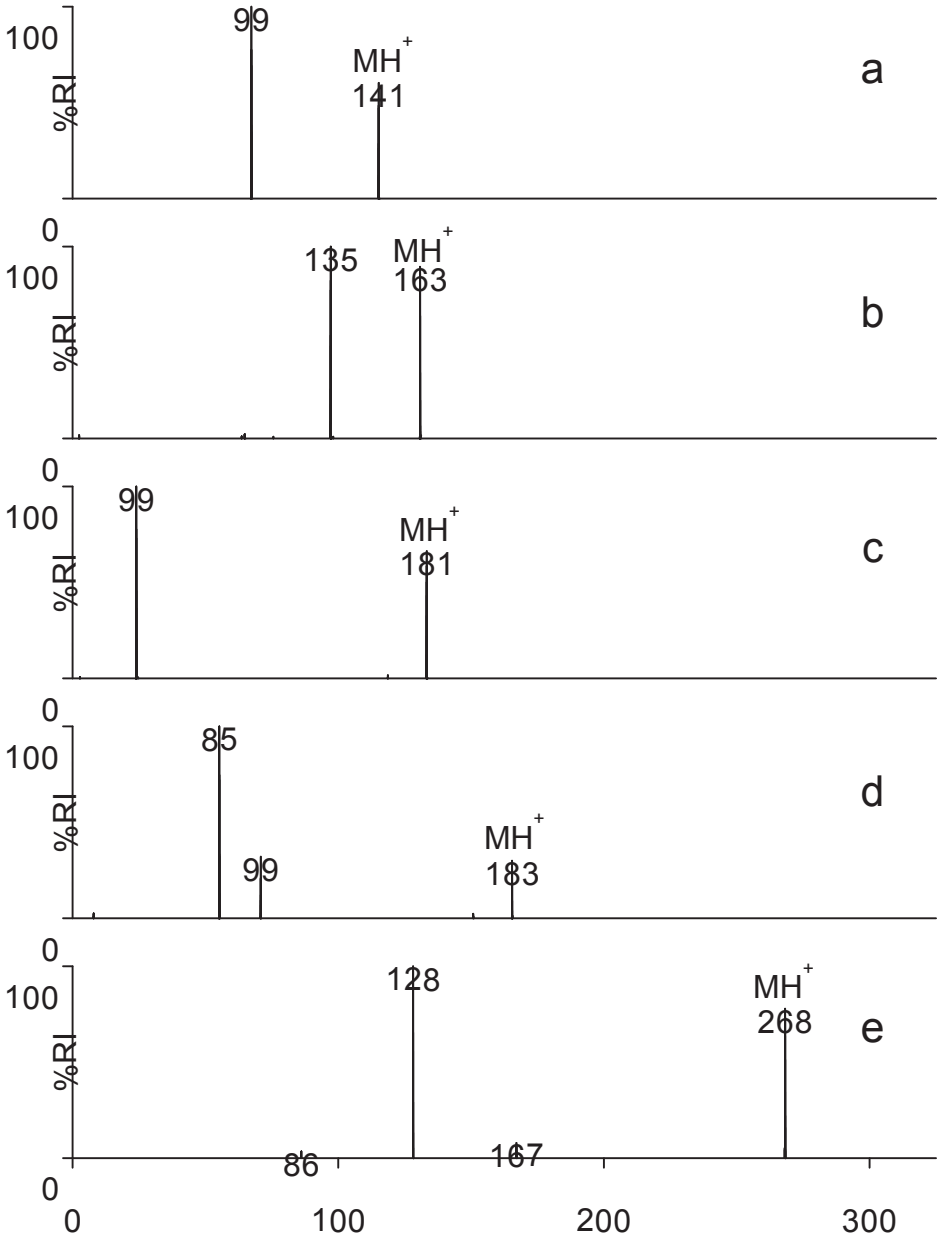

Illustration 4: MS^2 data obtained for the $[M+H]^+$ ion of a) sarin (GB), b) tabun (GA), c) cyclosarin (GF), d) soman (GD) and e) VX. Trap and transfer collision energies for a) to e) were 3/3 eV, 7/7 eV, 3/3 eV, 3/3 eV and 15/18 eV, respectively.

Compounds with the same nominal mass

Several examples of compounds with the same nominal mass exist in the database. Illustration 5 demonstrates the differences in ion mobility profiles for three compounds with the same nominal mass (180 Da), cyclohexyl methylphosphonofluoridate (GF), pinacolyl methylphosphonic acid and ethyl tetramethylphosphorodiamidate. The acquired MS^n data in Illustrations 6 and 7 were

also markedly different. The most abundant product ions observed in Illustration 6 resulted from the loss of an alkene from the alkoxy group of each compound. Observation of the product ions at m/z 99 and m/z 97 during the analysis of suspect samples suggests the presence of methylphosphonofluoridates (or phosphates) and alkyl methylphosphonic acids, respectively. Alkyl fragments related to the alkoxy groups(s) were also observed at higher collision energies in the MS^2 data (contained in the database). At higher collision energies the MS^3 data for the principal product ions at m/z 99, m/z 97 and m/z 153 (Illustration 7) exhibited structurally informative low mass ions at m/z 47 (indicative of phosphorus content) and m/z 46 (indicative of dimethylamine substitution), cyclosarin (and other alkyl methylphosphonofluoridates) also exhibited product ions at both m/z 81 and m/z 79 due to loss of H_2O and HF, respectively, from the diagnostic m/z 99 ion, while pinacolyl methylphosphonic acid (and other alkyl methylphosphonic acids) exhibited an additional product ion at m/z 79 due to loss of H_2O from the diagnostic m/z 97 ion (Illustration 7).

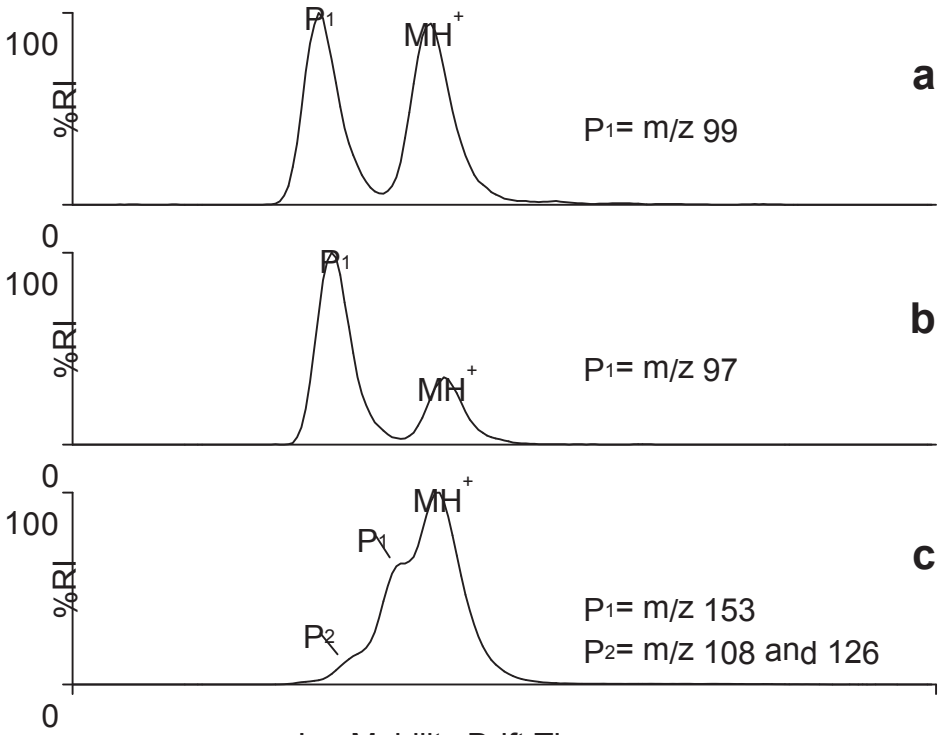

Illustration 5: Ion mobility profiles for three compounds with the same nominal mass (180 Da), a) cyclohexyl methylphosphonofluoridate (GF), b) pinacolyl methylphosphonic acid and c) ethyl tetramethylphosphorodiamidate. The $[M+H]^+$ ion selected by the quadrupole analyser and one or more product ions(P_1, P_2) , generated in the trap region of the collision cell, were separated by IMS (m/z values indicated). Trap and transfer collision energies for a) to c) were 3/3 eV, 3/3 eV, and 12/12 eV, respectively.

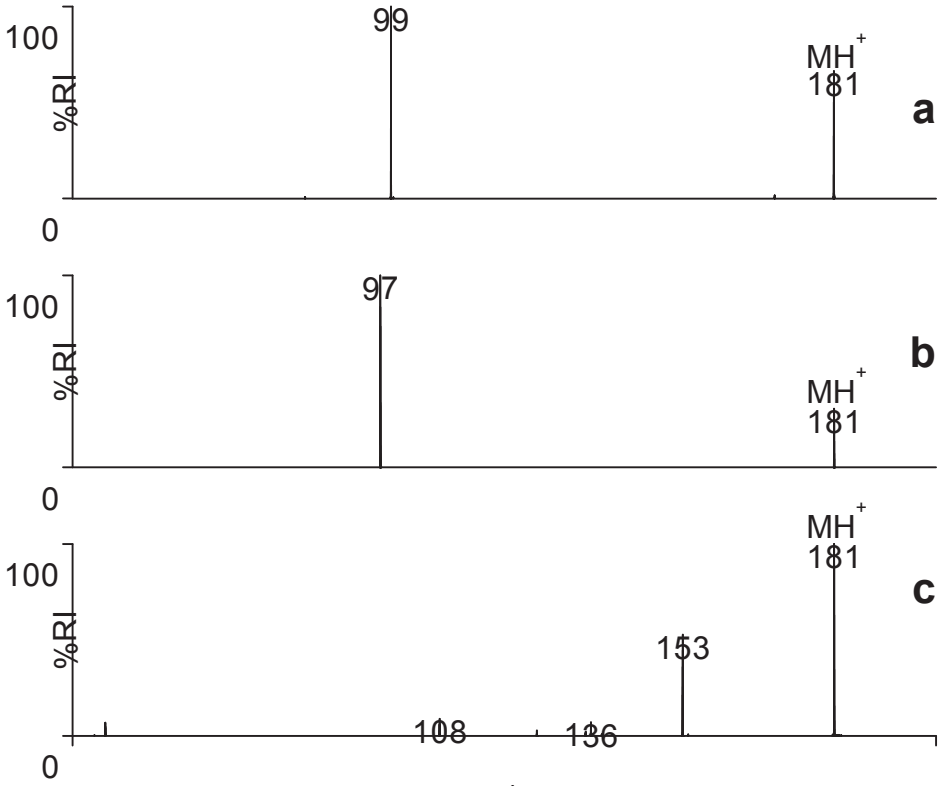

Illustration 6: MS^2 data obtained for the $[M+H]^+$ ion of a) cyclohexyl methylphosphonofluoridate (GF), b) pinacolyl methylphosphonic acid and c) ethyl tetramethylphosphorodiamidate. Trap and transfer collision energies for a) to c) were 3/3 eV, 3/3 eV, and 12/12 eV, respectively.

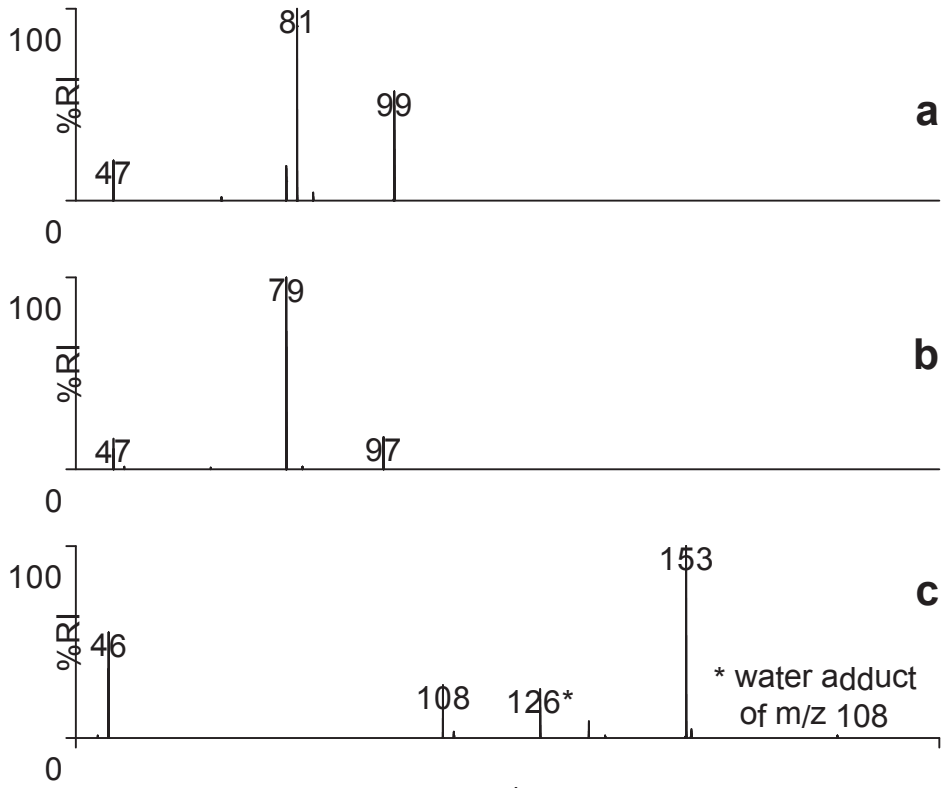

Illustration 7: MS^3 data obtained for a product ion of a) cyclohexyl methylphosphonofluoridate (GF) – m/z 99, b) pinacolyl methylphosphonic acid – m/z 97 and c) ethyl tetramethylphosphorodiamidate – m/z 153. Trap and transfer collision energies for a) to c) were 3/20 eV, 3/20 eV, and 12/12 eV, respectively.

Both the simulant triethyl phosphate and pinacolyl methylphosphonofluoridate have the same nominal mass. Their ion mobility profiles differ significantly (Illustration 8) as does their MS^n data shown in Illustrations 9 and 10. Triethyl phosphate exhibits ions at m/z 155, m/z 127 and m/z 99 due to sequential loss of the ethylene and a weak ion at m/z 81 due to loss of H_2O from the m/z 99 ion in the MS^3 data. Soman fragments relatively easily giving rise to ions related to the alkoxy group, m/z 99 due to loss of the alkene from the alkoxy group and m/z 85 due to the alkyl portion of the alkoxy group ($C_6H_{13}^+$). The MS^3 data for the m/z 99 ion of soman resulted in a number of lower mass product ions at m/z 81 (loss of H_2O), m/z 79 (loss of HF) and m/z 47 (PO^+). All are typically observed for alkyl methylphosphonofluoridates.

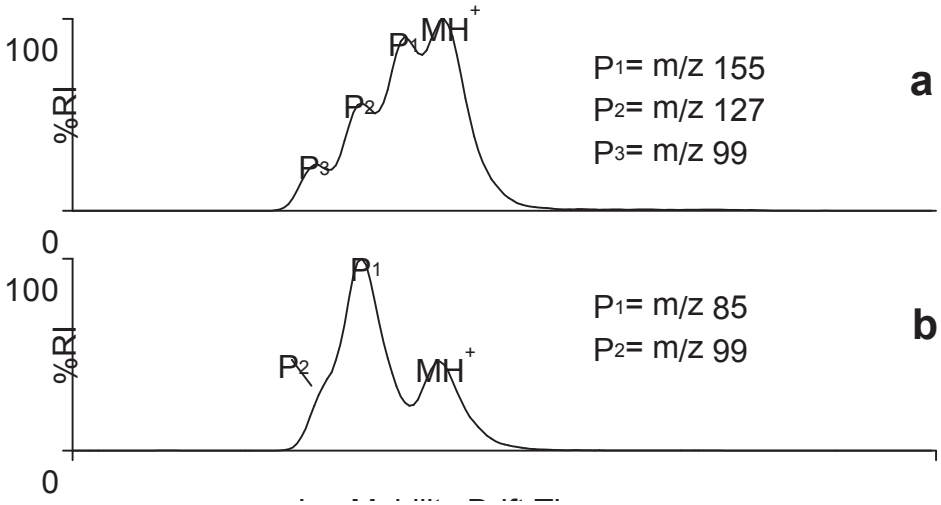

Illustration 8: Ion mobility profiles for two compounds with the same nominal mass (182 Da), a) triethyl phosphate and b) pinacolyl methylphosphonofluoridate (GD). The $[M+H]^+$ ion selected by the quadrupole analyser and one or more product ions(P_1, P_2, P_3), generated in the trap region of the collision cell, were separated by IMS (m/z values indicated). Trap and transfer collision energies for a) to b) were 10/10 eV and 3/3 eV, respectively.

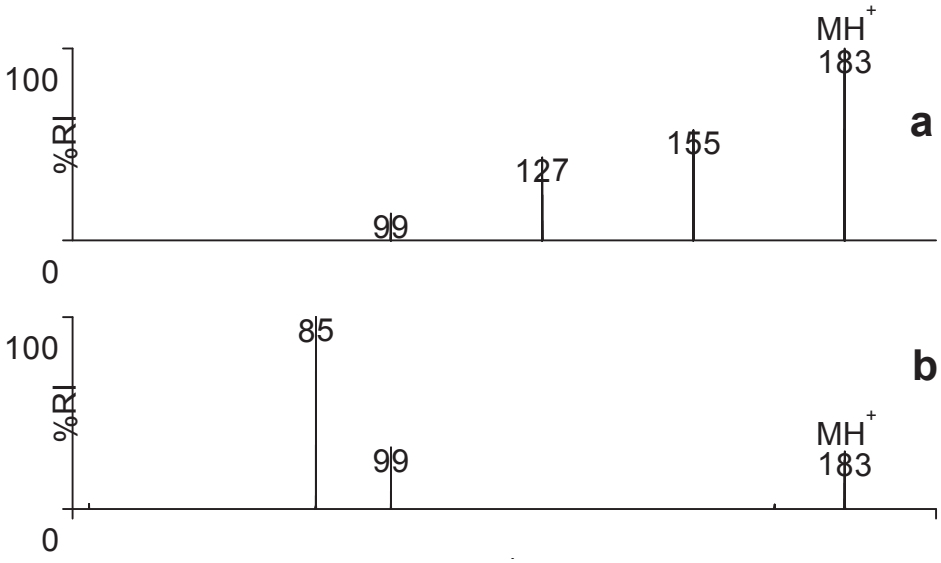

Illustration 9: MS^2 data obtained for the $[M+H]^+$ ion of a) triethyl phosphate and b) pinacolyl methylphosphonofluoridate (GD). Trap and transfer collision energies for a) and b) were 10/10 eV, and 3/3 eV, respectively.

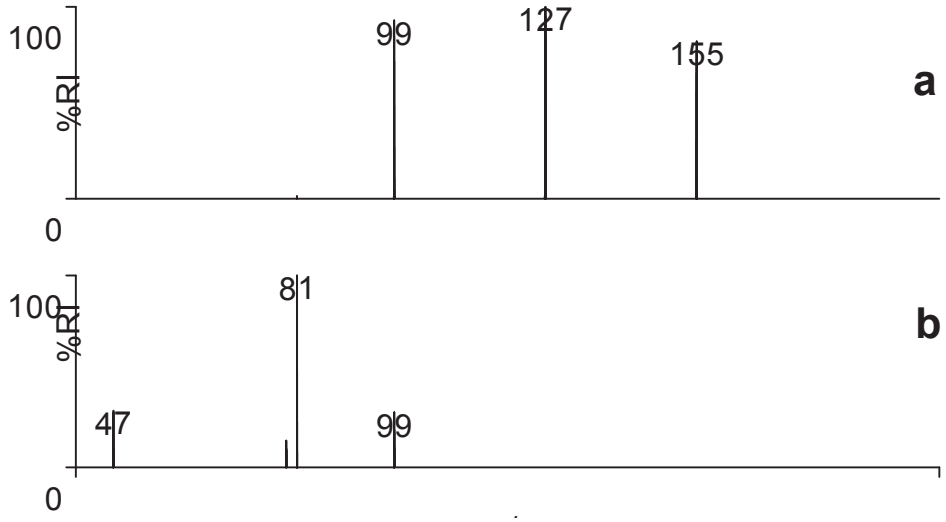

Illustration 10: MS^3 data obtained for a product ion of a) triethyl phosphate – m/z 155 and b) pinacolyl methylphosphonofluoridate (GD) – m/z 99. Trap and transfer collision energies for a) and b) were 10/10 eV and 3/20 eV, respectively.

Compounds with the same exact mass

The ion mobility profiles of two isomers, tripropyl phosphate and triisopropyl phosphate, were different at both lower and higher collision energies (Illustration 11). The MS^n data acquired for these two isomers were also marked different in relative intensity at both collision energy settings (Illustrations 12 and 13). Product ions were due to sequential loss of the alkene (C_3H_6) from the alkoxyl groups of tripropyl phosphate and triisopropyl phosphate.

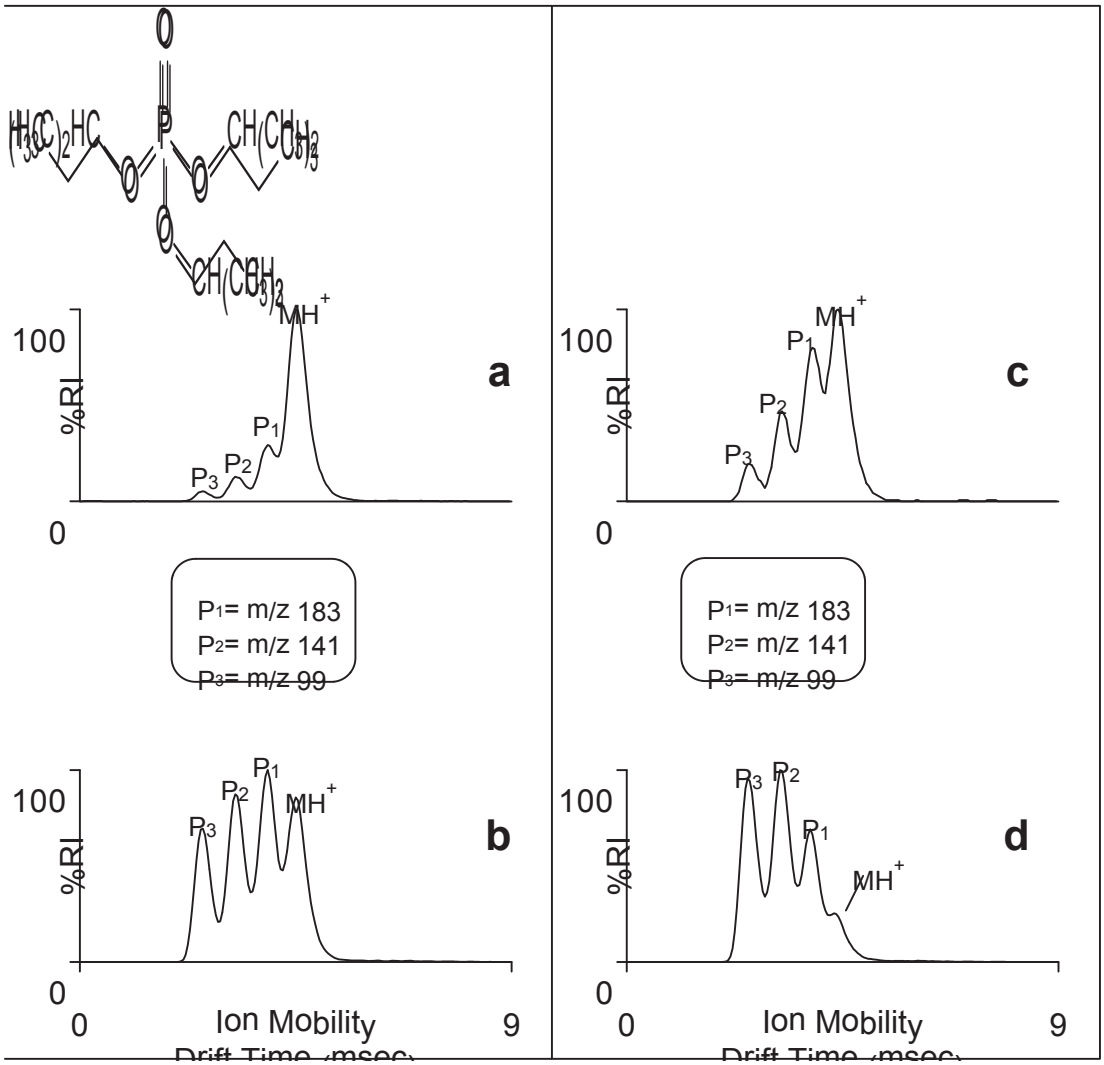

Illustration 11: Ion mobility profiles for tripropyl phosphate with trap and transfer collision energies of a) 7/7 eV and b) 10/10 eV. Ion mobility profiles for triisopropyl phosphate with trap and transfer collision energies of c) 7/7 eV and d) 10/10 eV. The $[M+H]^+$ ion selected by the quadrupole analyser and three product ions (P_1, P_2, P_3), generated in the trap region of the collision cell, were separated by IMS (m/z values indicated).

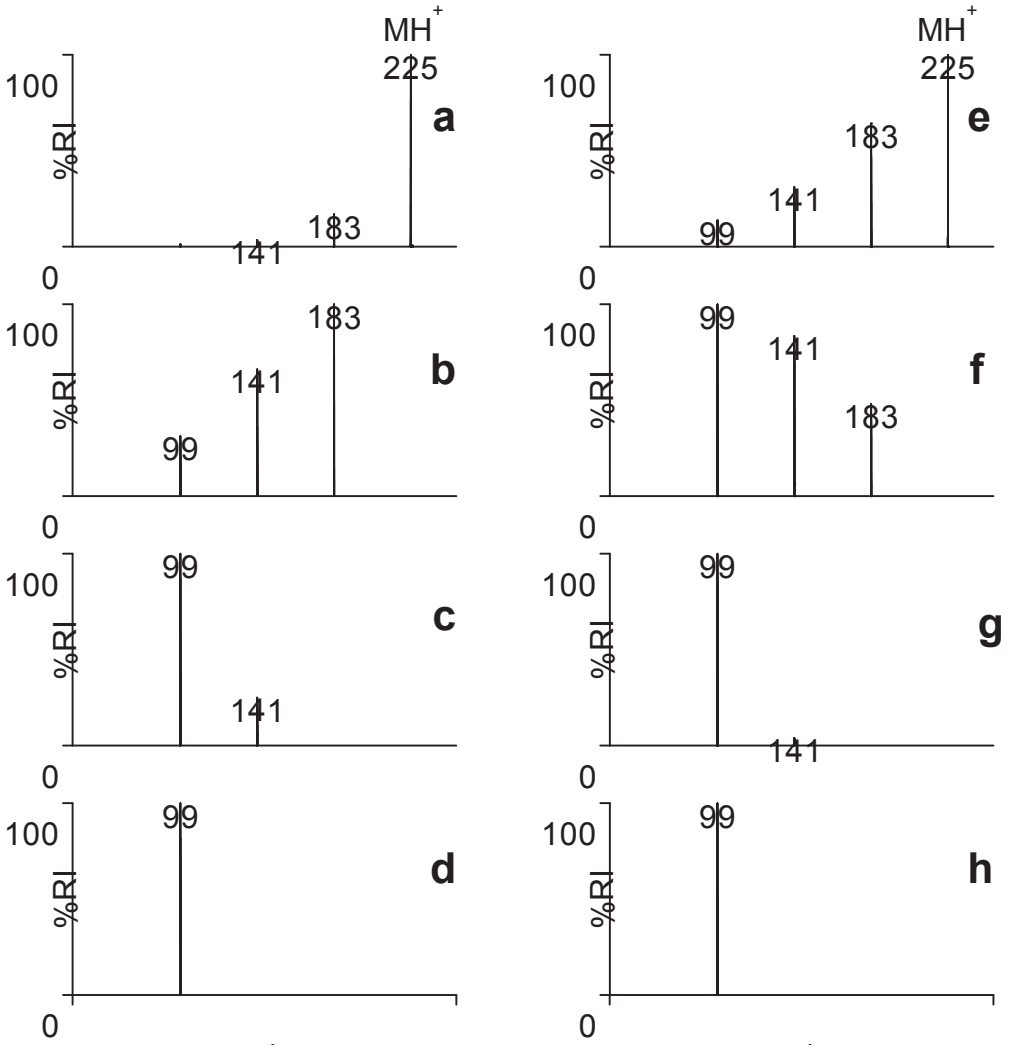

Illustration 12: MS^2 data for a) m/z 225 and MS^3 data for b) m/z 183, c) 141 and d) m/z 99 acquired for tripropyl phosphate with trap and transfer collision energies of 7/7 eV. MS^2 data for e) m/z 225 and MS^3 data for f) m/z 183, g) 141 and h) m/z 99 acquired for triisopropyl phosphate with trap and transfer collision energies of 7/7 eV.

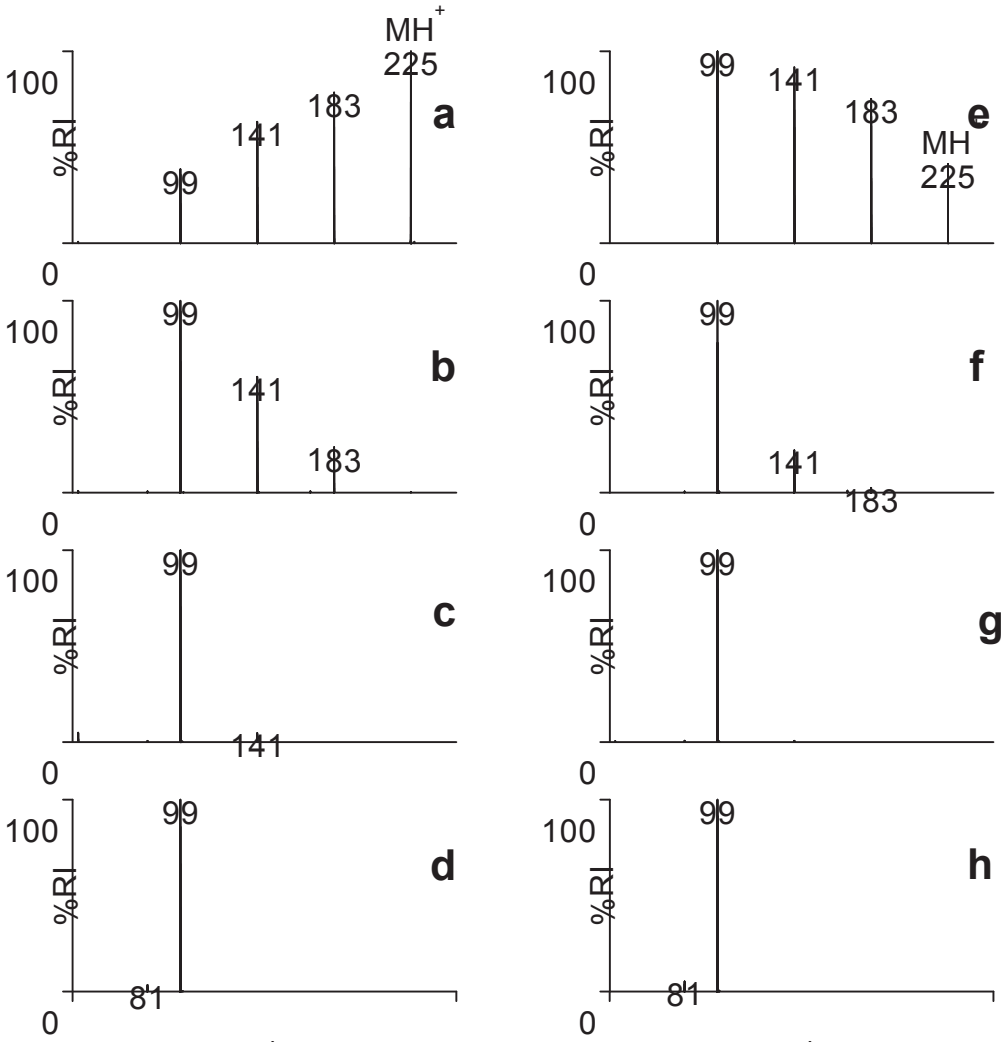

Illustration 13: MS^2 data for a) m/z 225 and MS^3 data for b) m/z 183, c) 141 and d) m/z 99 acquired for tripropyl phosphate with trap and transfer collision energies of 10/10 eV. MS^2 data for e) m/z 225 and MS^3 data for f) m/z 183, g) 141 and h) m/z 99 acquired for triisopropyl phosphate with trap and transfer collision energies of 10/10 eV.

Application: analysis of an old chemical rocket

In 2011 an old chemical rocket was found on the CFB Suffield Military Training Range and the fill sampled for chemical warfare agent content (Illustration 14). The rocket contained a peat moss like fill and was thought to have originally contained sarin (based on historical records). Headspace GC-MS analysis provided no evidence of chemical warfare agents in the fill. A portion of the peat moss like fill was then provided to the mass spectrometry laboratory for LC-MS analysis. Aqueous extracts of the fill were analysed for the presence of sarin hydrolysis products using this technique.

Illustration 14: Old rocket found on CFB Suffield Military Training Range.

The aqueous extract of the rocket fill was analysed by LC-MS for the presence of isopropyl methylphosphonic acid and methylphosphonic acid, the hydrolysis products of sarin shown below.

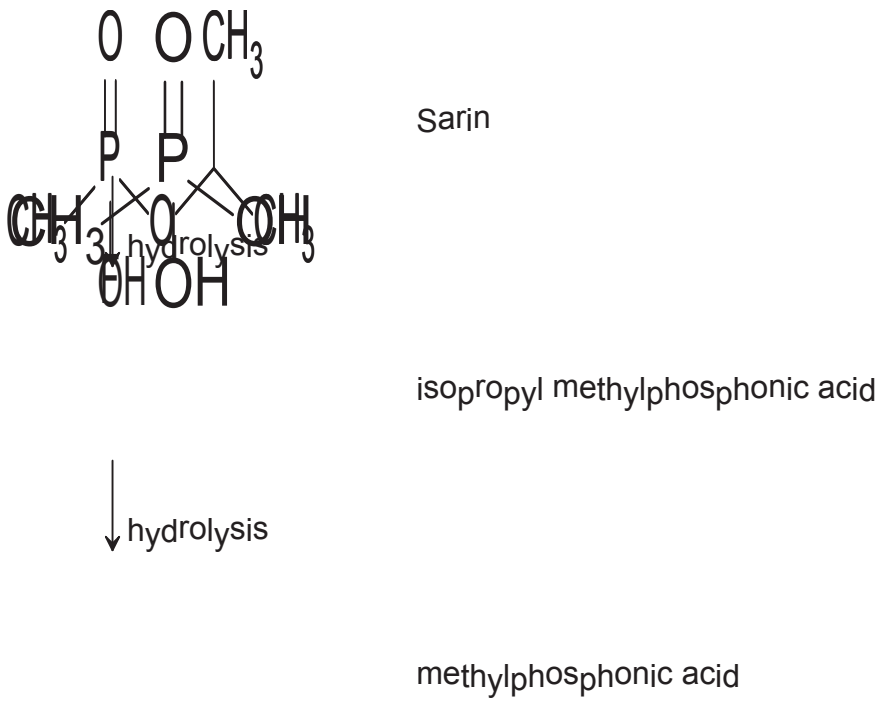

Diagram 2: Analysis of the aqueous extract of the rocket fill.

An aqueous blank (Illustration 15) and an aqueous extract of the rocket fill (Illustration 16) were initially analysed by LC-ESI-MS. No appreciable signal was recorded in the total-ion-current of the blank or for the selected ions at m/z 141 and 99 (indicative of sarin), or m/z 139 and 97 (indicative of sarin hydrolysis products). However, in the aqueous extract of the rocket fill there was signal detected for m/z 97 and m/z 139 (low level). Both methyl phosphonic acid and isopropyl methylphosphonic acid eluted near the beginning of the LC gradient program and considerable chemical interference was noted even after background enhancement (Illustration 17). A considerable number of ions not related to the hydrolysis product(s) were acquired in the m/z 150 to 300 range.

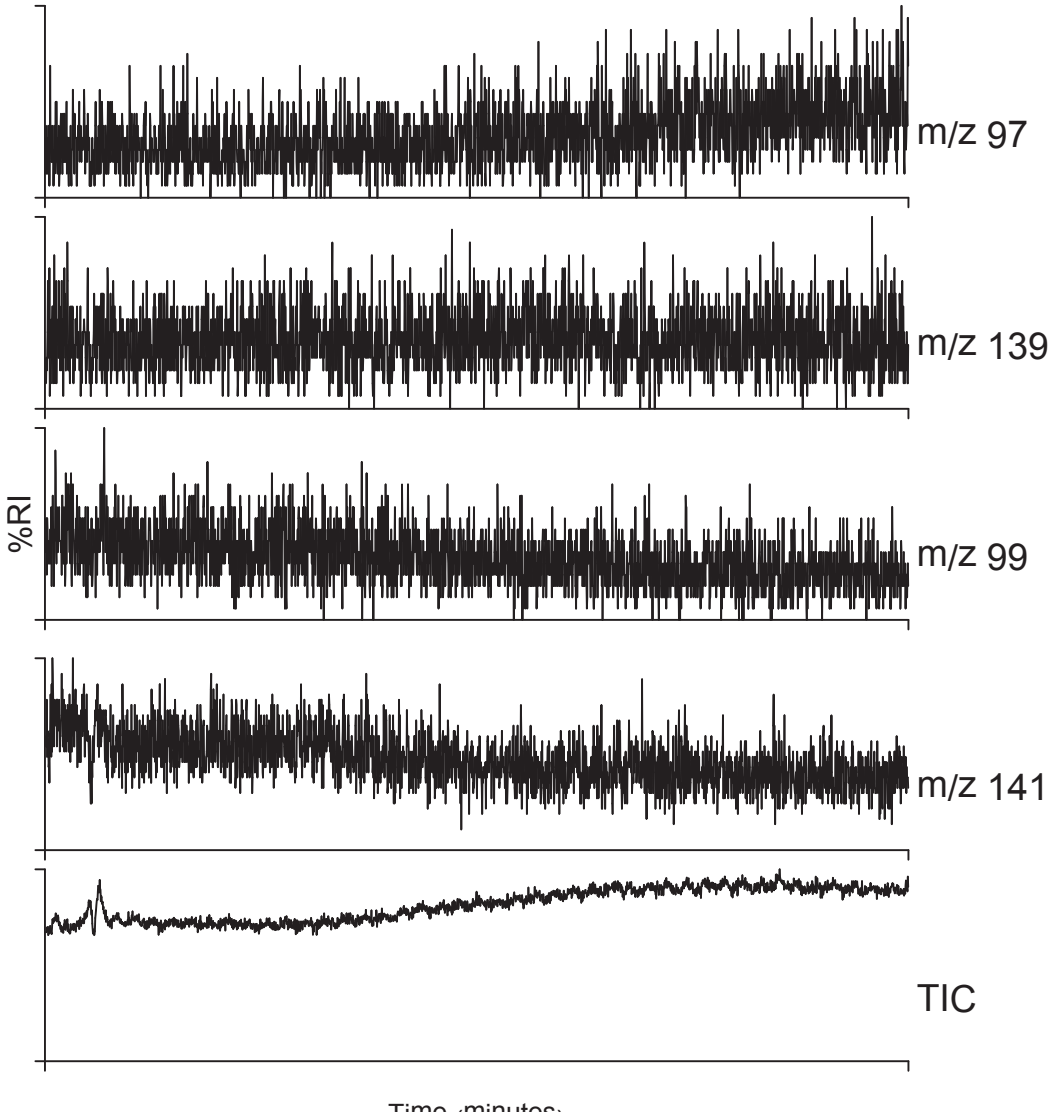

Illustration 15: Gradient programming LC-ESI-MS analysis of aqueous blank. The total-ion-current (TIC) and selected ion traces for sarin and its hydrolysis products are shown.

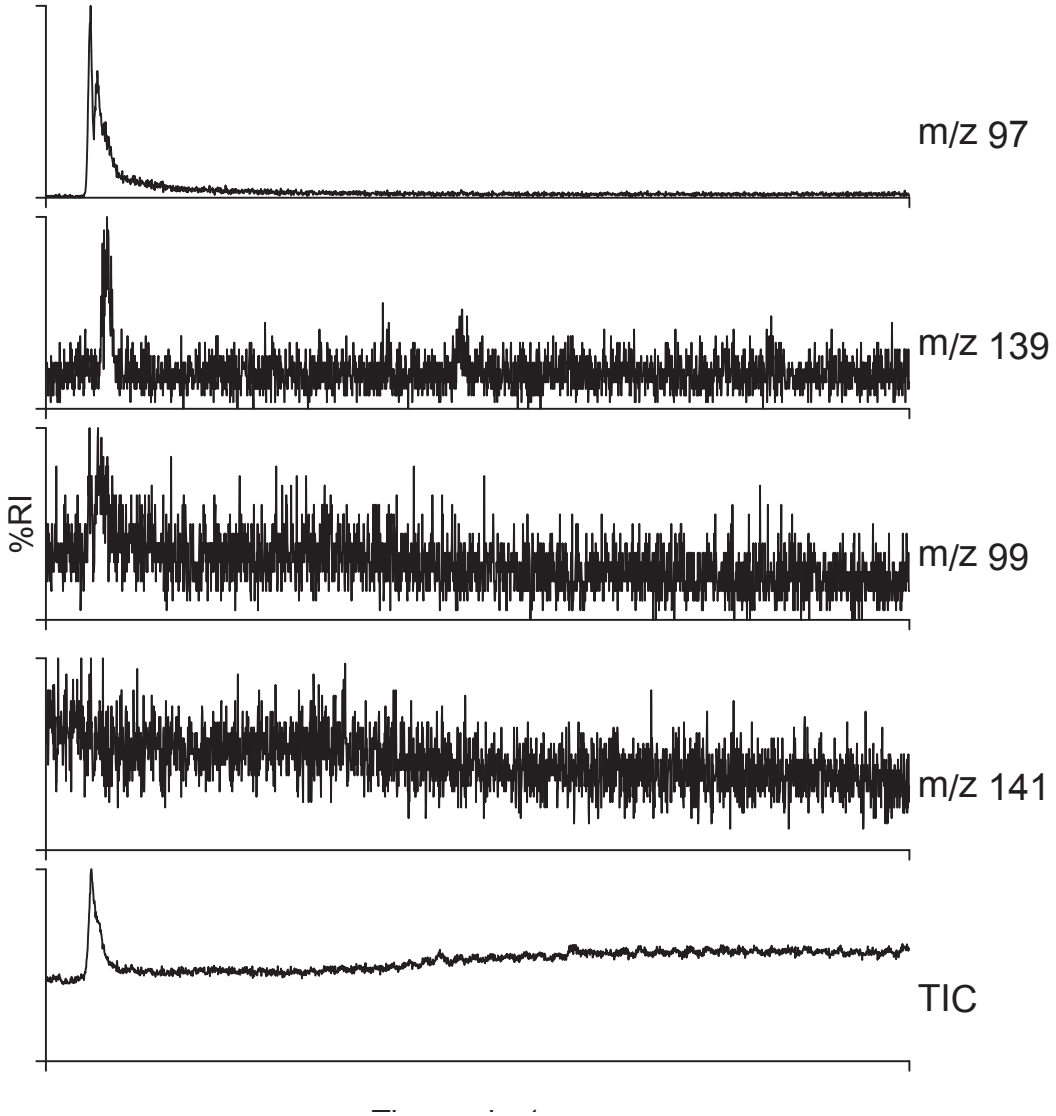

Illustration 16: Gradient programming LC-ESI-MS analysis of aqueous extract of rocket fill. The total-ion-current (TIC) and selected ion traces for sarin and its hydrolysis products are shown.

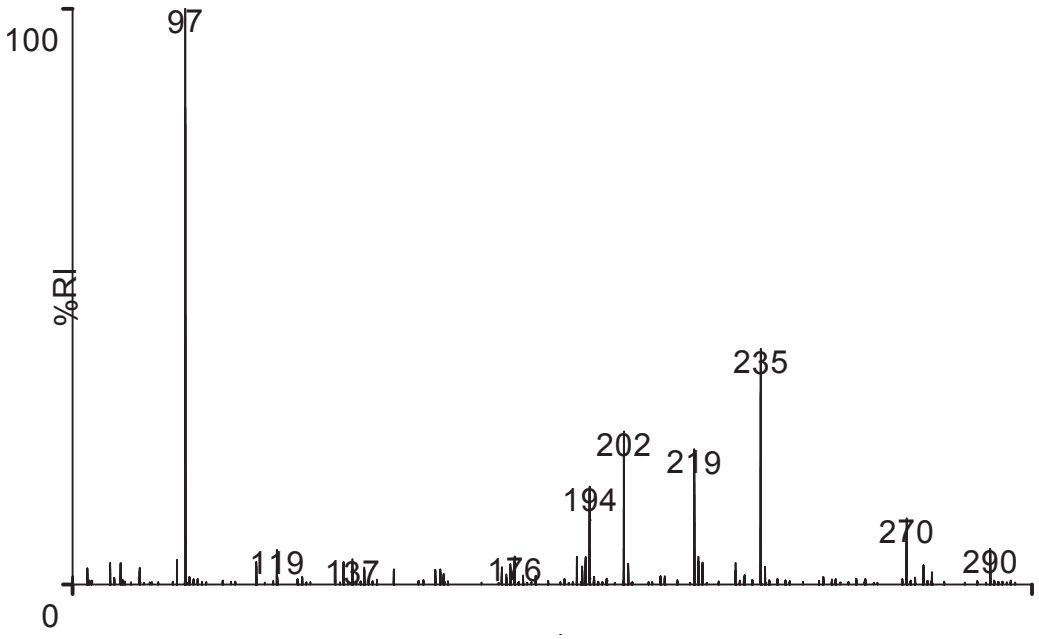

Illustration 17: ESI-MS data acquired at the retention time for methylphosphonic acid. Only the m/z 97 ion could be attributed to methylphosphonic acid.

Specificity should be improved with the use of IMS-MS^n. The lack of sample components with longer retention times enabled the use of isocratic LC separation [5% acetonitrile and 95% water (with 0.1% trifluoroacetic acid)] and a flow rate of 10 µL/min.

The IMS profiles for the aqueous blank and aqueous extract of the rocket fill were acquired at the isocratic retention times of methylphosphonic acid (Illustration 18) and isopropyl methylphosphonic acid (Illustration 19). The acquired IMS profiles (and drift times) for the aqueous extracts of the rocket fill were consistent with the data acquired for methylphosphonic acid and isopropyl methylphosphonic acid reference standards and data compiled in the IMS and MS^n database.

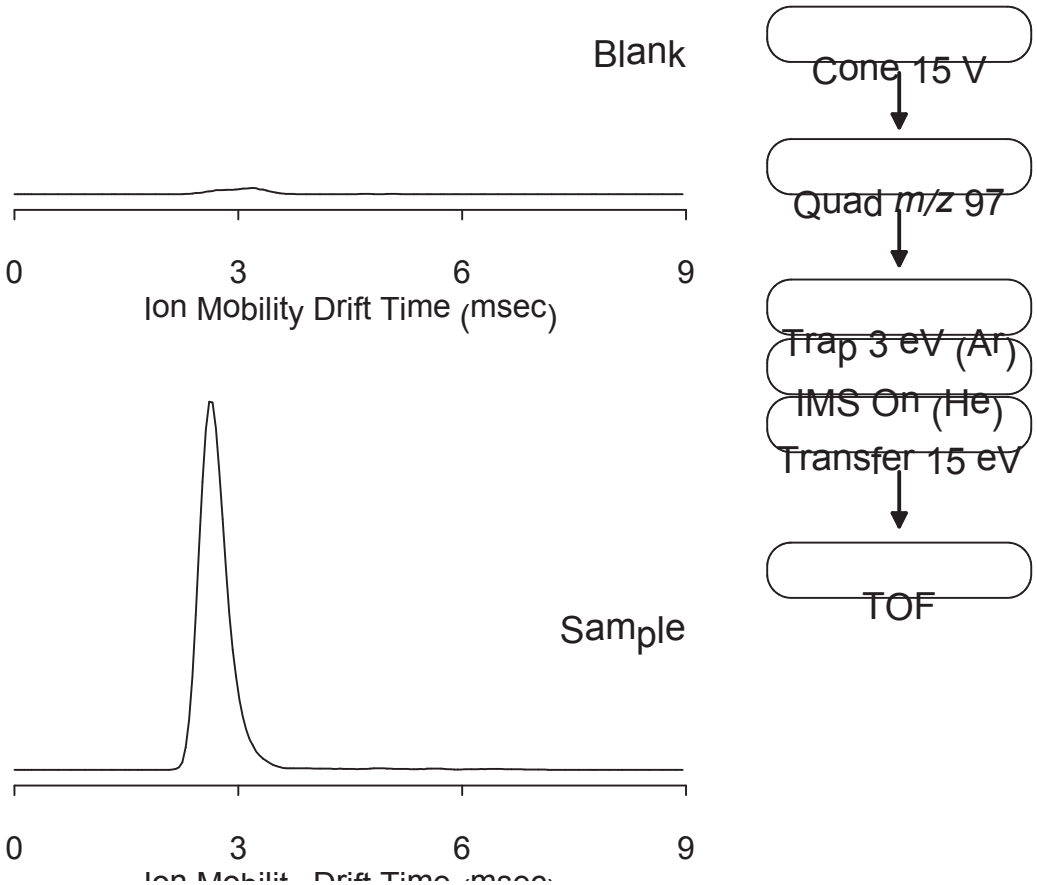

Illustration 18: IMS profiles for aqueous blank and aqueous extract of rocket fill with the m/z 97 ion ($[M+H]^+$ ion for methylphosphonic acid) selected by the quadrupole mass analyser.

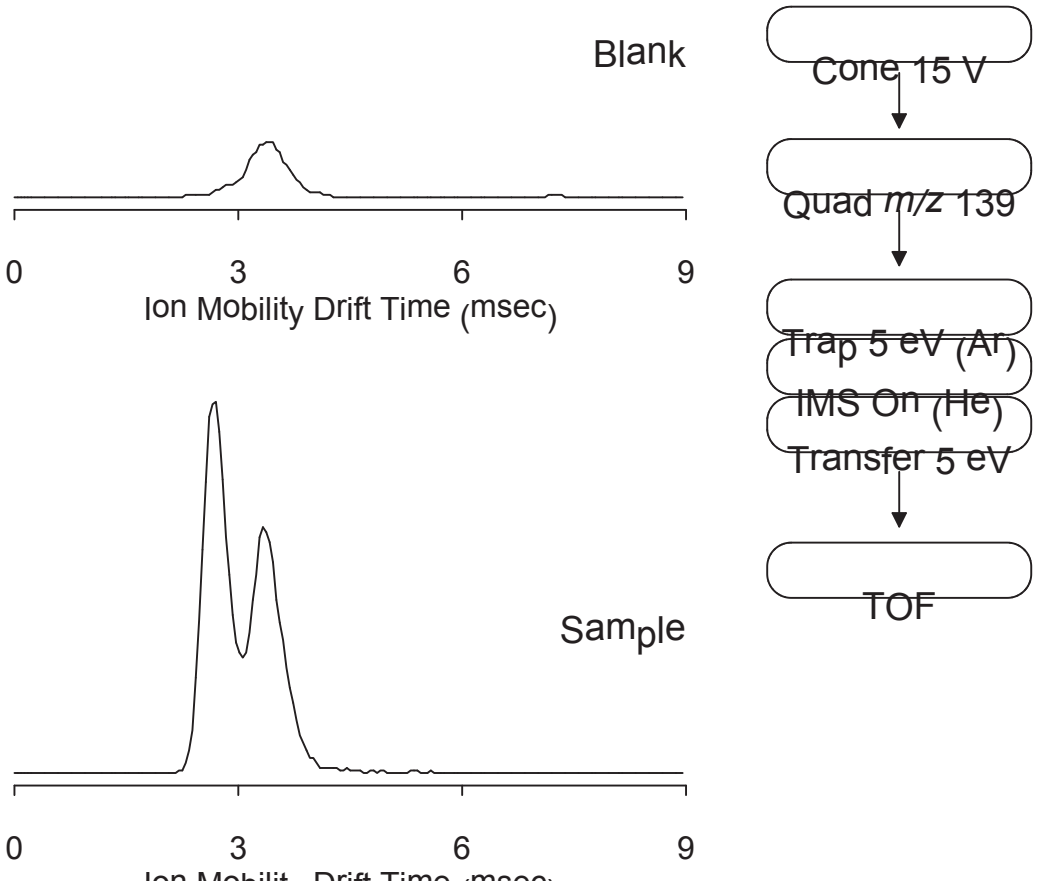

Illustration 19: IMS profiles for aqueous blank and aqueous extract of rocket fill with the m/z 139 ion ($[M+H]^+$ ion for isopropyl methylphosphonic acid) selected by the quadrupole mass analyser.

LC-IMS-MS^n data for the aqueous extract of the rocket were acquired and compared to reference standard data for methylphosphonic acid (Illustration 20) and isopropyl methylphosphonic acid at lower (Illustration 21) and higher (Illustration 22) collision energy. Essentially identical IMS and MS^n data were acquired allowing for the unambiguous identification of both sarin hydrolysis products. Methylphosphonic acid and isopropyl methylphosphonic acid were found to be present in the rocket fill at approximately 400 µg/g and 2 µg/g, respectively.

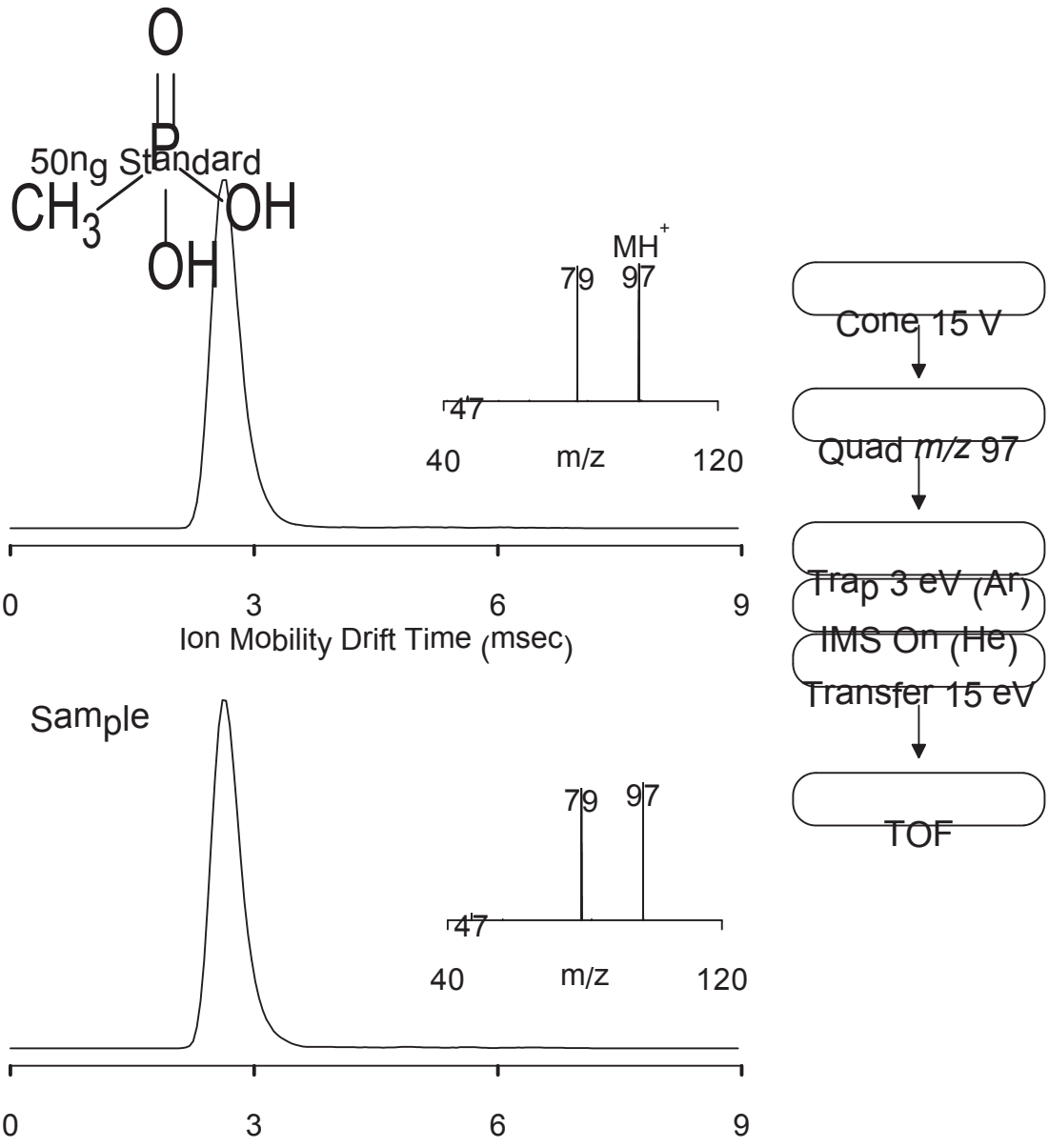

Illustration 20: Isocratic LC-IMS-MS^n data acquired for methylphosphonic acid (50 ng standard) and the aqueous extract of rocket fill (sample).

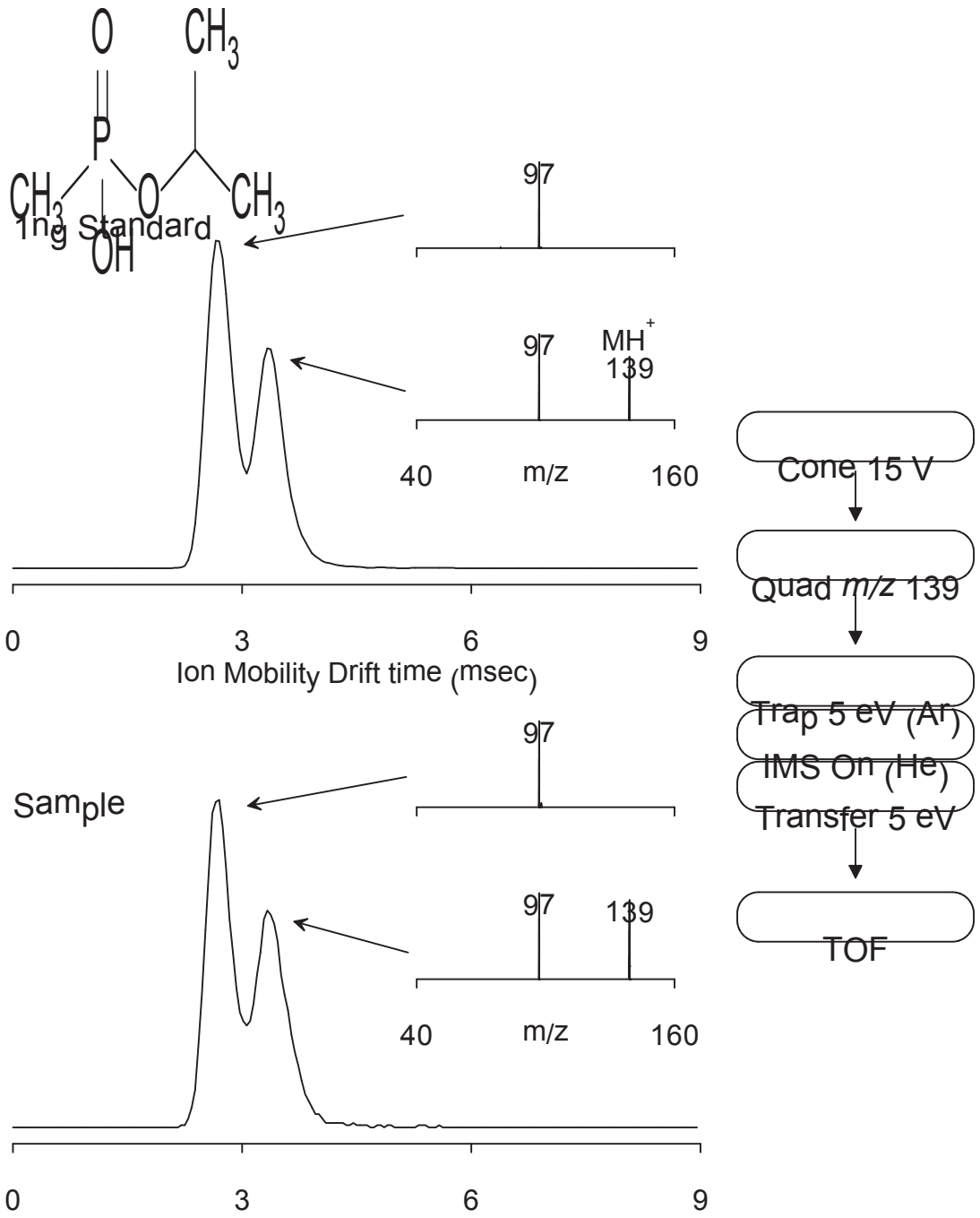

Illustration 21: Isocratic LC-IMS-MS^n data acquired with a lower collision energy for isopropyl methylphosphonic acid (1 ng standard) and the aqueous extract of rocket fill (sample).

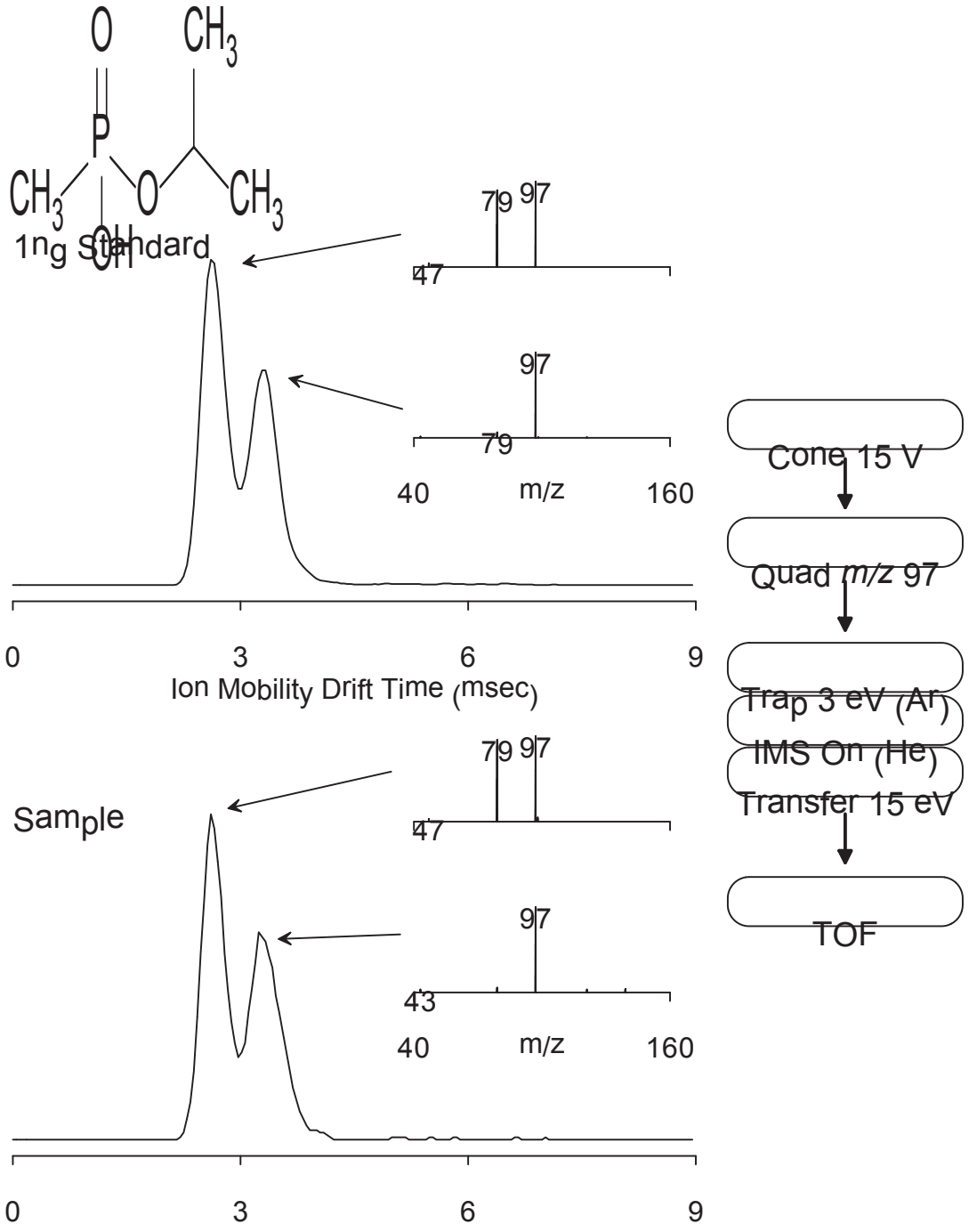

Illustration 22: Isocratic LC-IMS-MS^n data acquired with a higher collision energy for isopropyl methylphosphonic acid (1 ng standard) and the aqueous extract of rocket fill (sample).

IMS and MS^n Database (Figures 1 to 55)

Figures 1to 55 list the IMS and MS^n database entries by increasing molecular mass. Each entry contains the IMS profile and MS^n data acquired under a specified trap/transfer collision energy and ion structures consistent with the acquired high resolution mass spectrometric data.

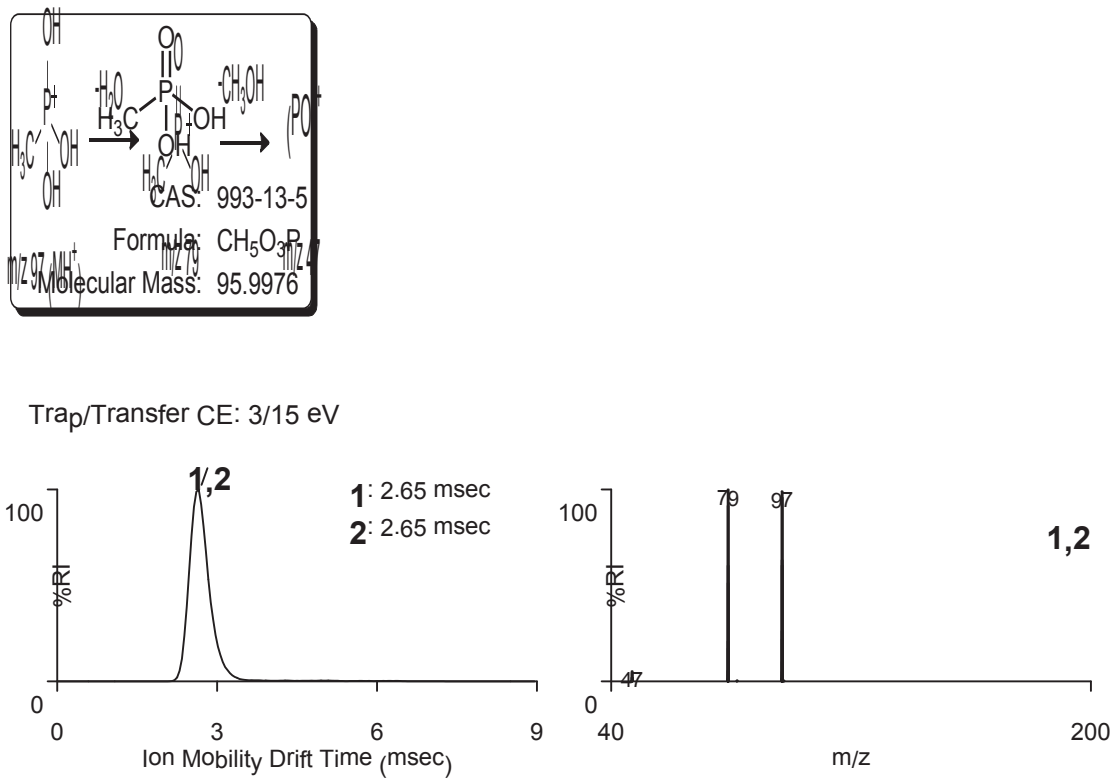

Figure 1: Lower collision energy IMS and MS^n data for methylphosphonic acid (96).

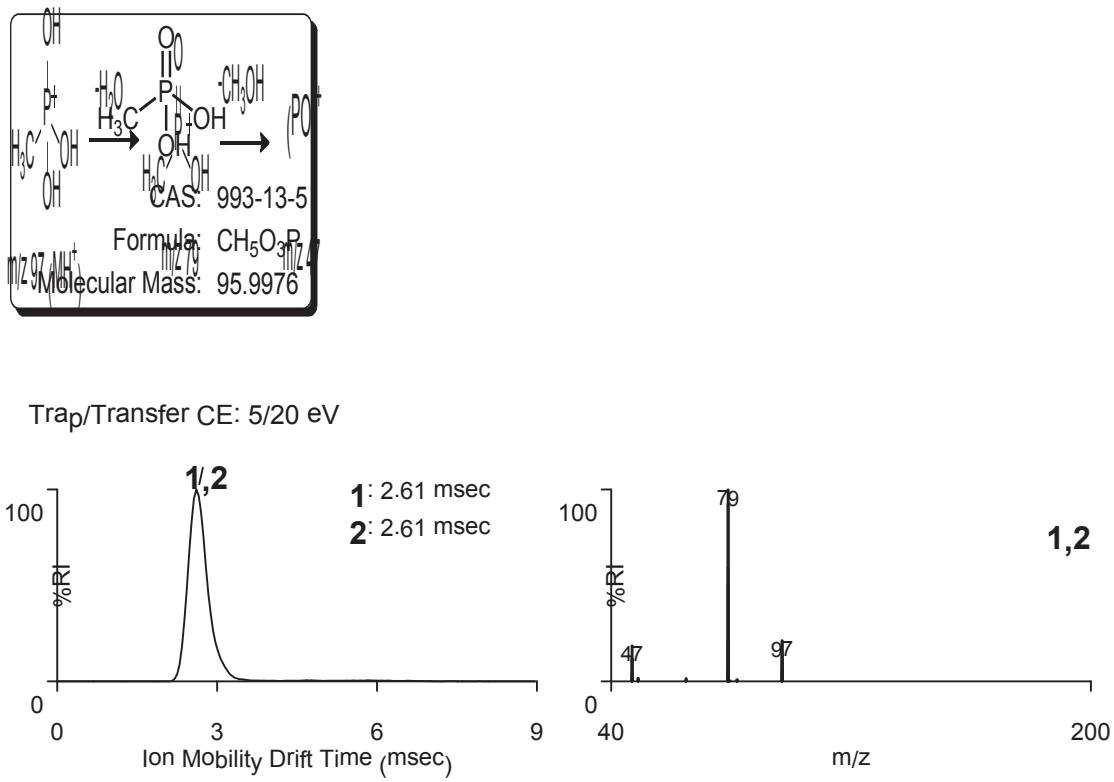

Figure 2: Higher collision energy IMS and MS^n data for methylphosphonic acid (96).

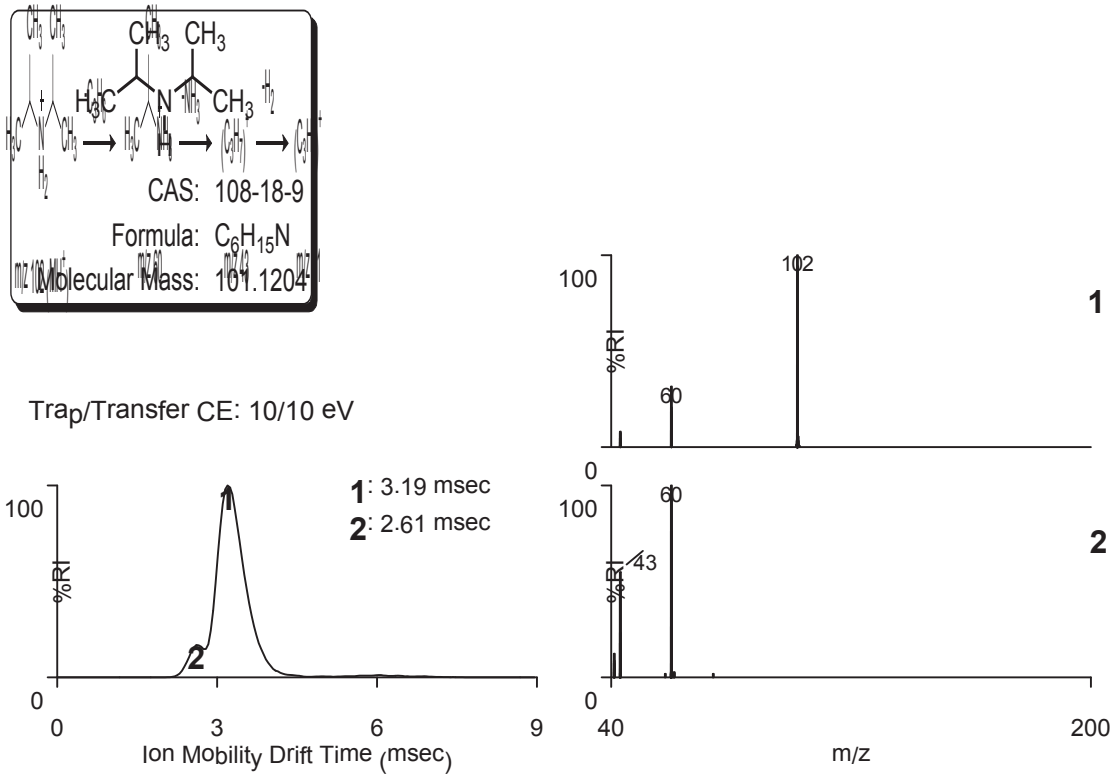

Figure 3: IMS and MS^n data for diisopropylamine (101).

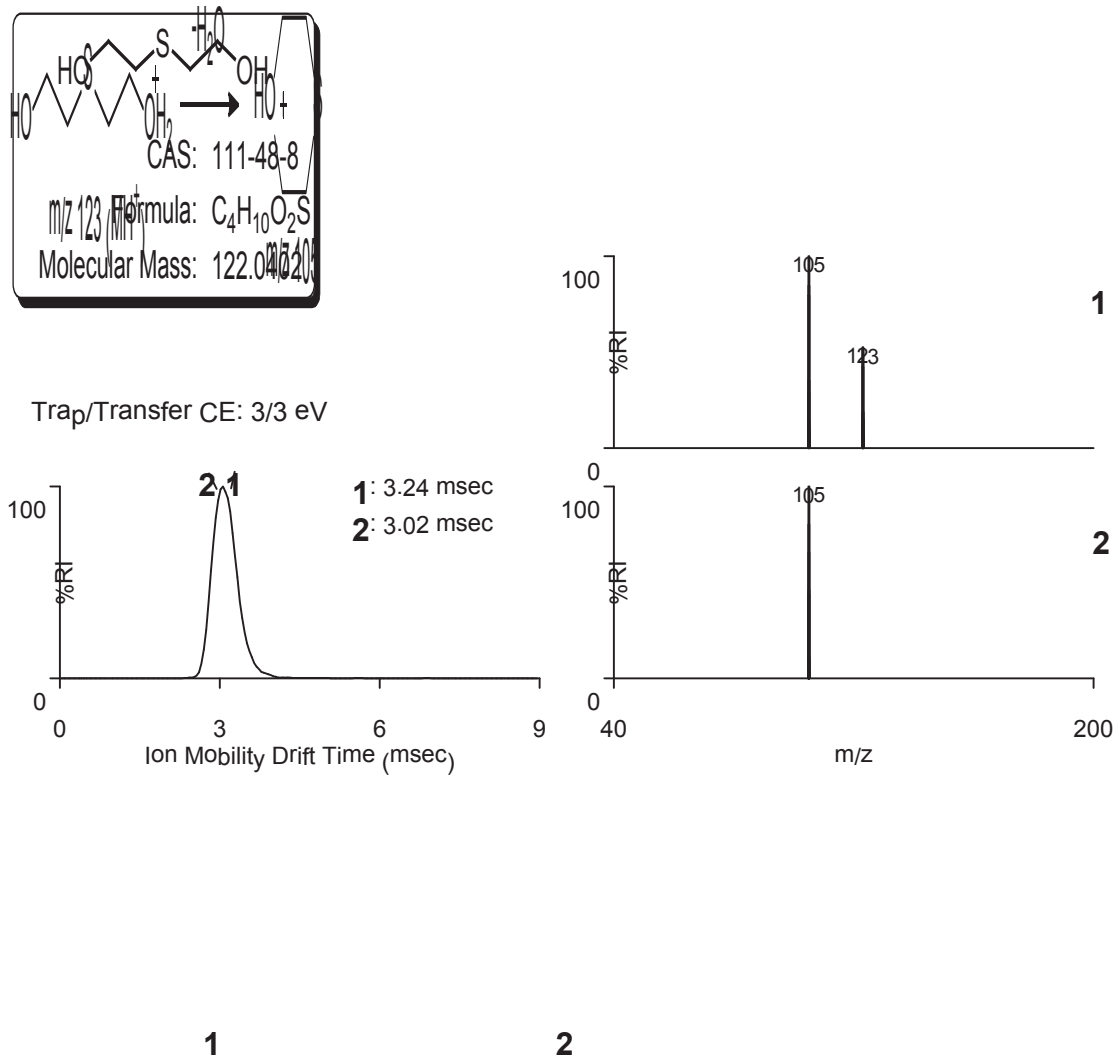

Figure 4: Lower collision energy IMS and MS^n data for thiodiglycol (122).

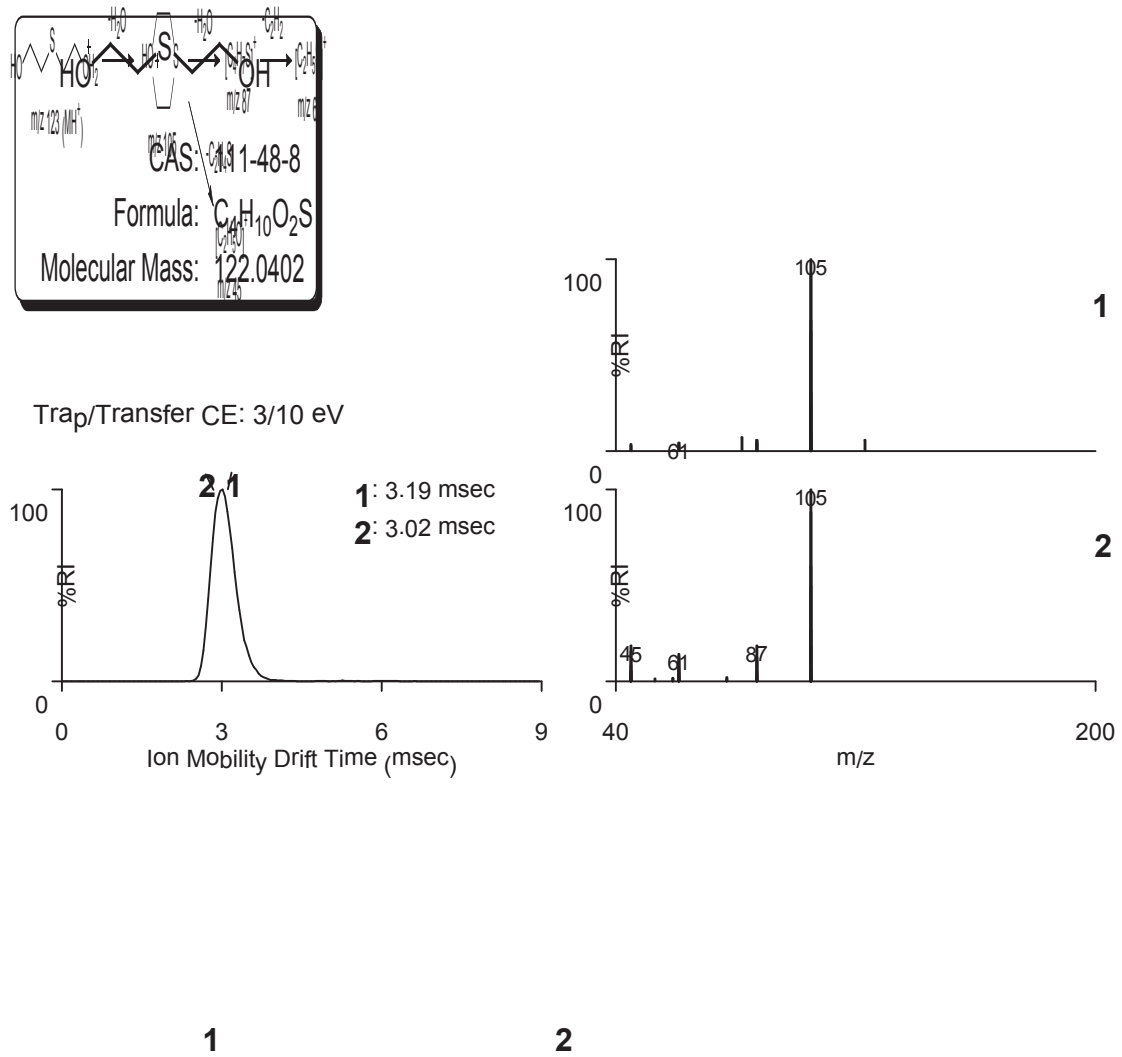

Figure 5: Higher collision energy IMS and MS^n data for thiodiglycol (122).

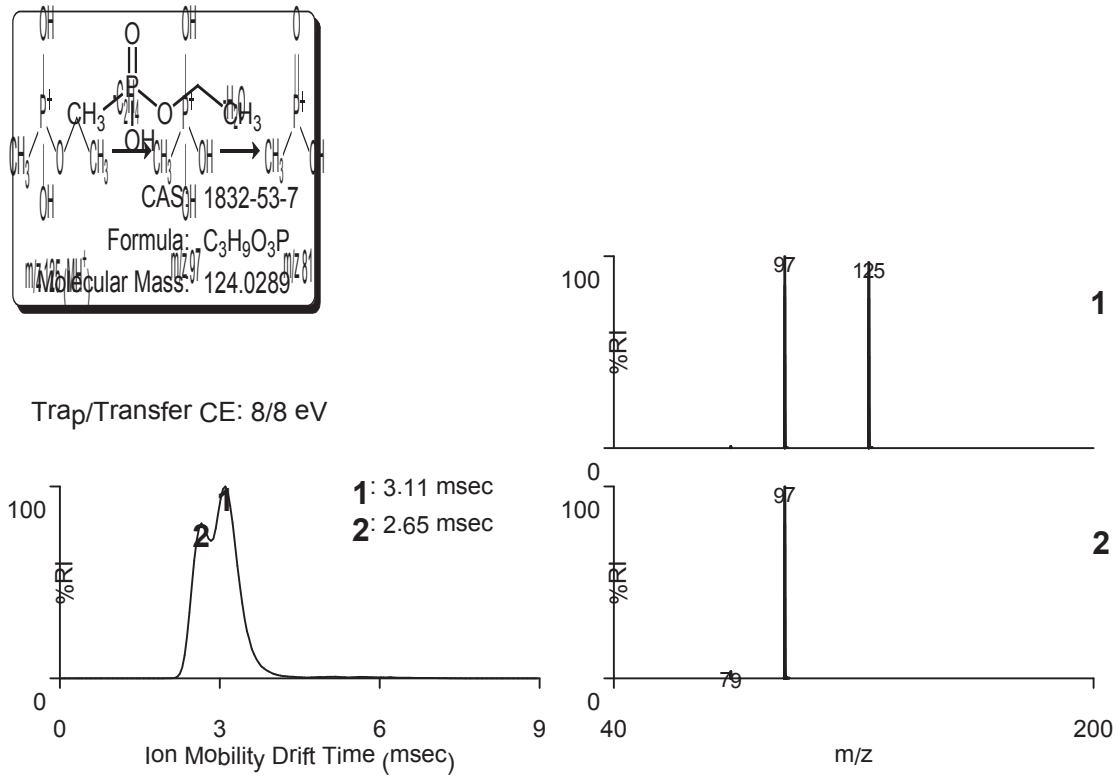

Figure 6: IMS and MS^n data for ethyl methylphosphonic acid (124).

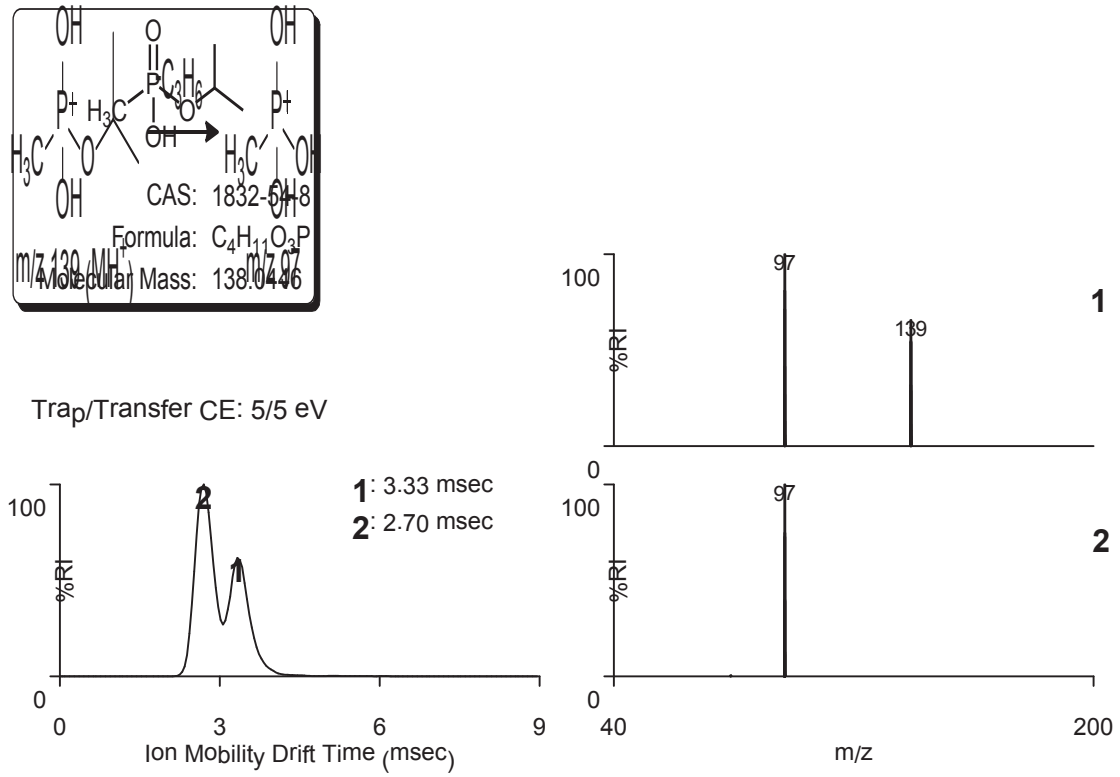

Figure 7: Lower collision energy IMS and MS^n data for isopropyl methylphosphonic acid (138).

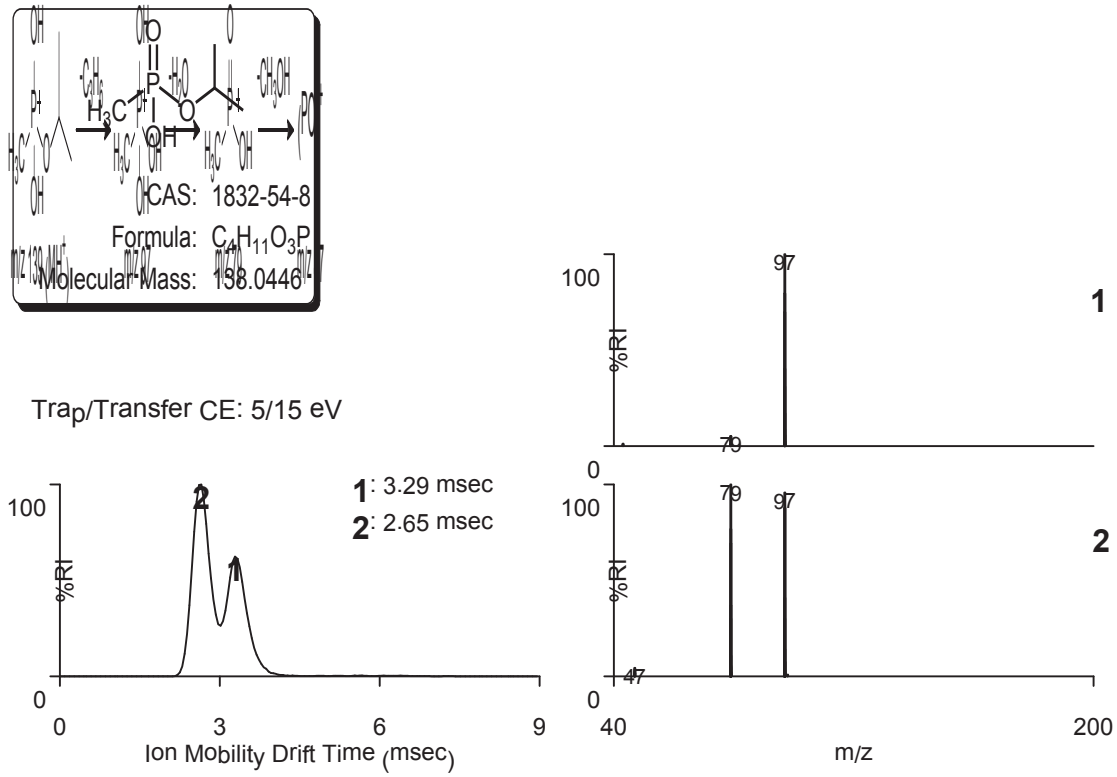

Figure 8: Higher collision energy IMS and MS^n data for isopropyl methylphosphonic acid (138).

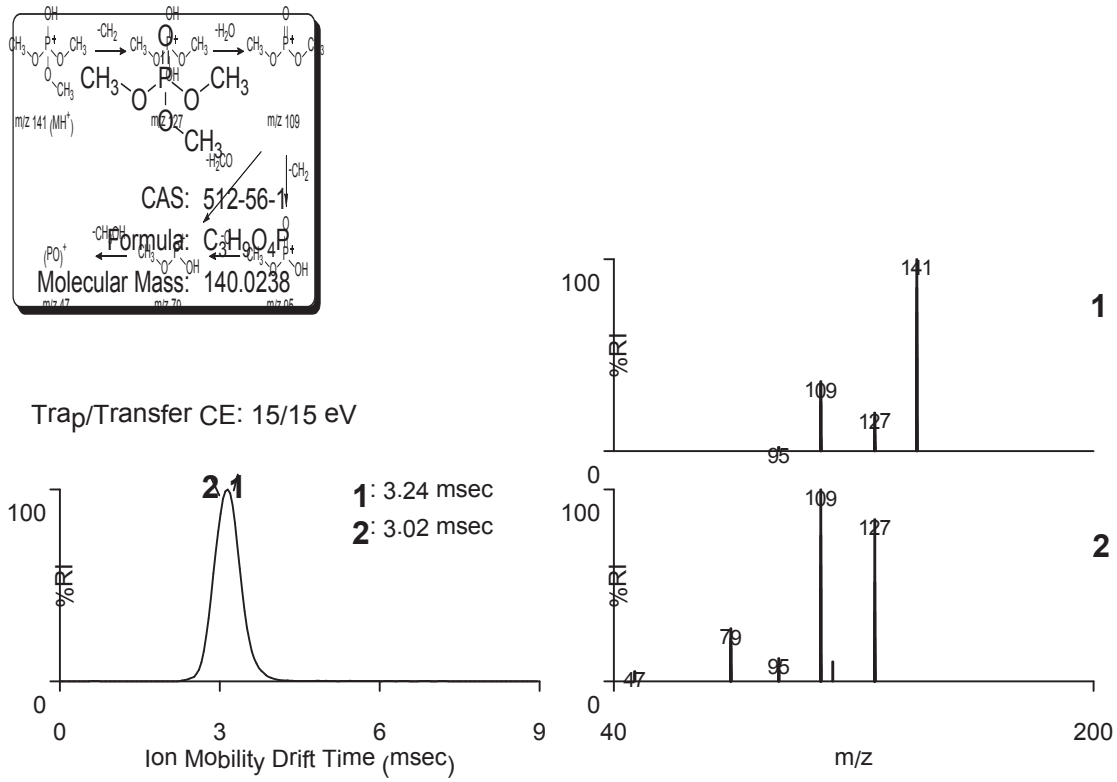

Figure 9: IMS and MS^n data for trimethyl phosphate (140).

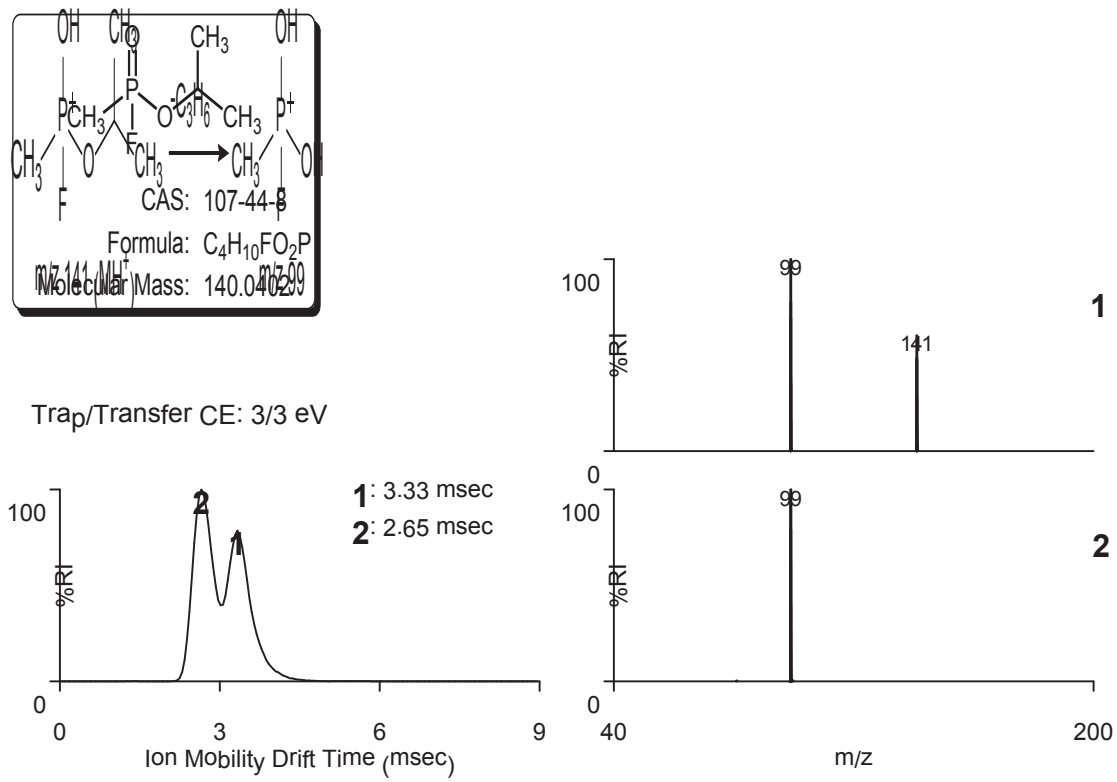

Figure 10: Lower collision energy IMS and MS^n data for isopropyl methylphosphonofluoridate (sarin, GB) (140).

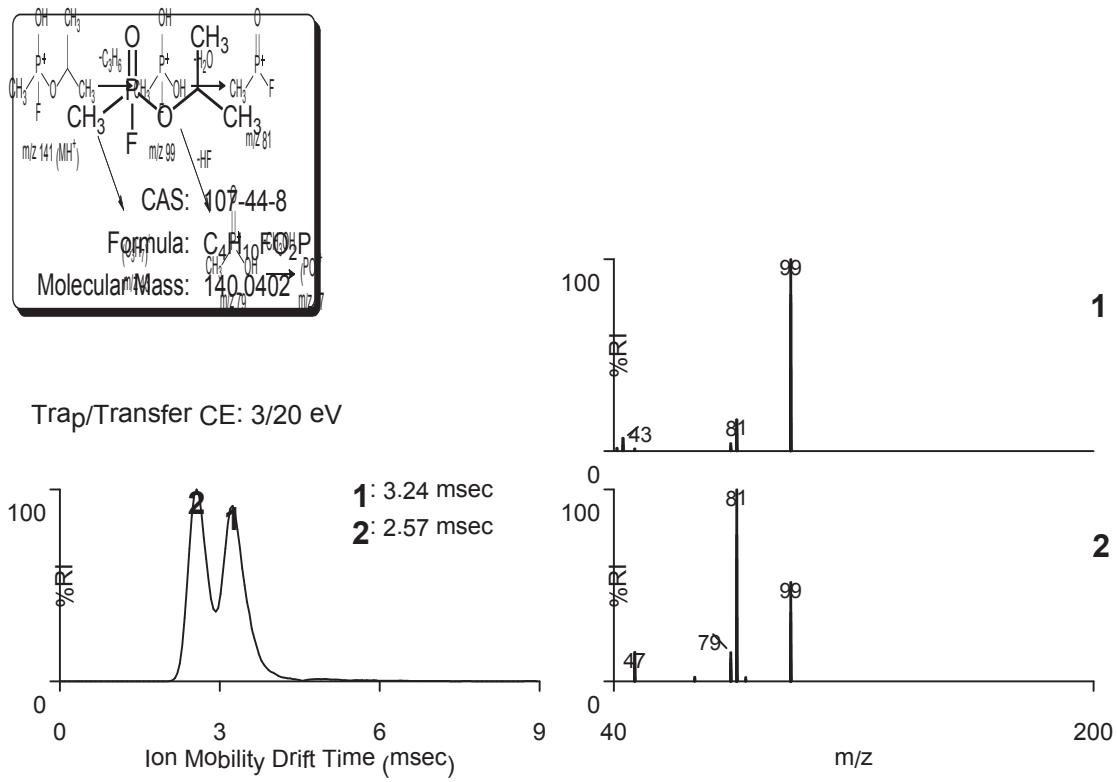

Figure 11: Higher collision energy IMS and MS^n data for isopropyl methylphosphonofluoridate (sarin, GB) (140).

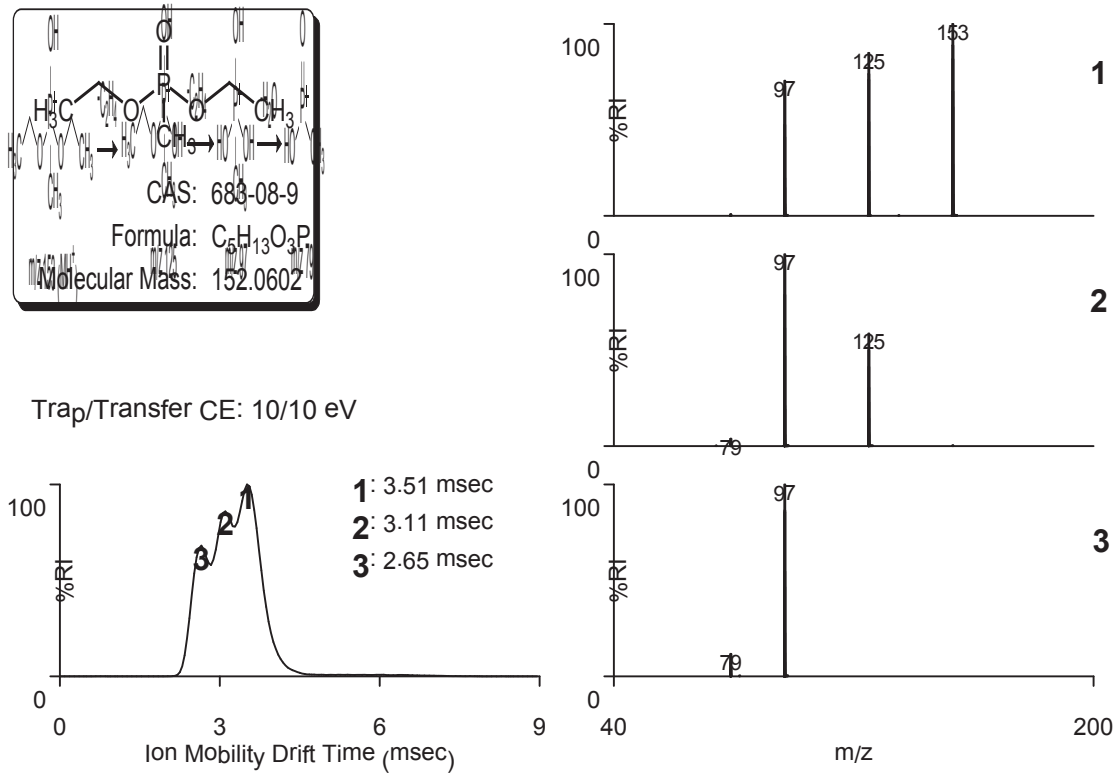

Figure 12: IMS and MS^n data for diethyl methylphosphonate (152).

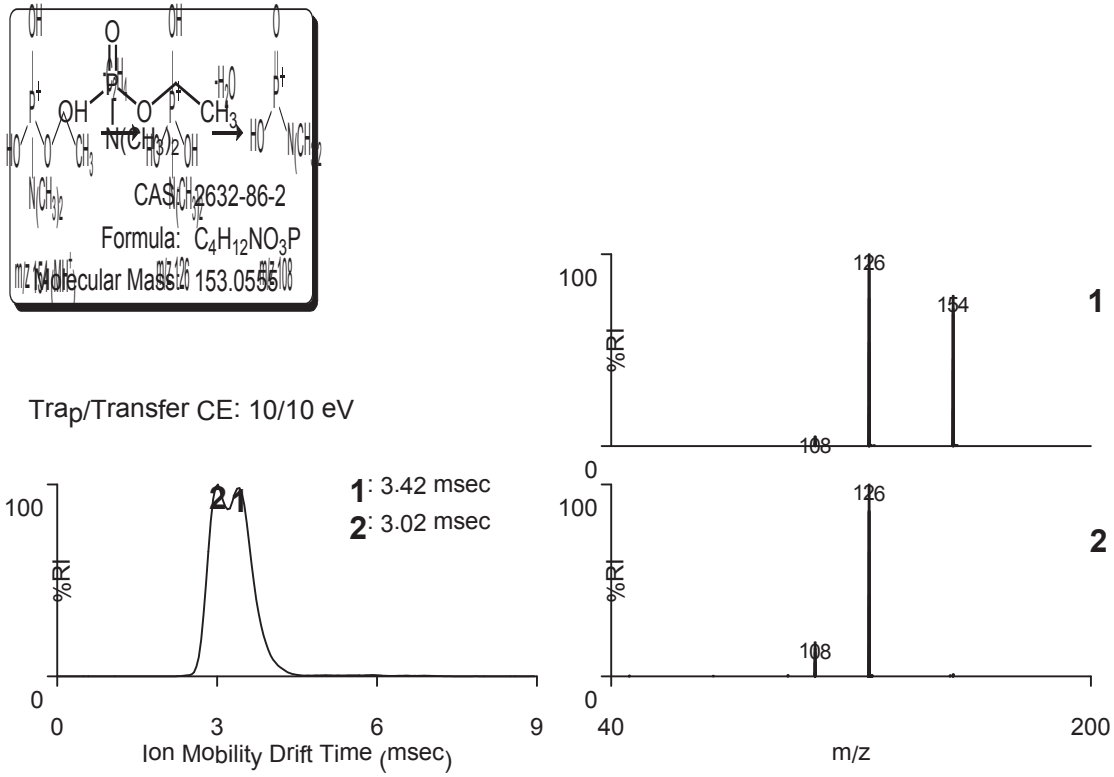

Figure 13: IMS and MS^n data for ethyl dimethylphosphoramidic acid (153).

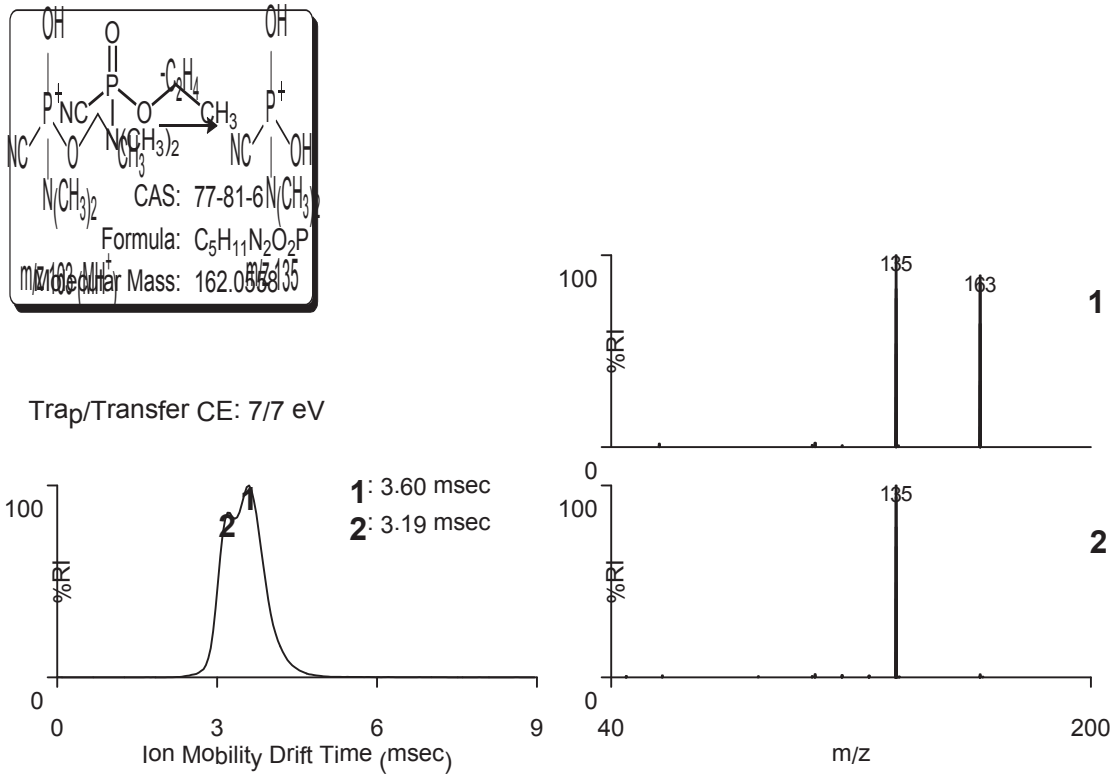

1 **2**

Figure 14: Lower collision energy IMS and MS^n data for O-ethyl N,N-dimethylphosphoramidocyanidate (tabun, GA) (162).

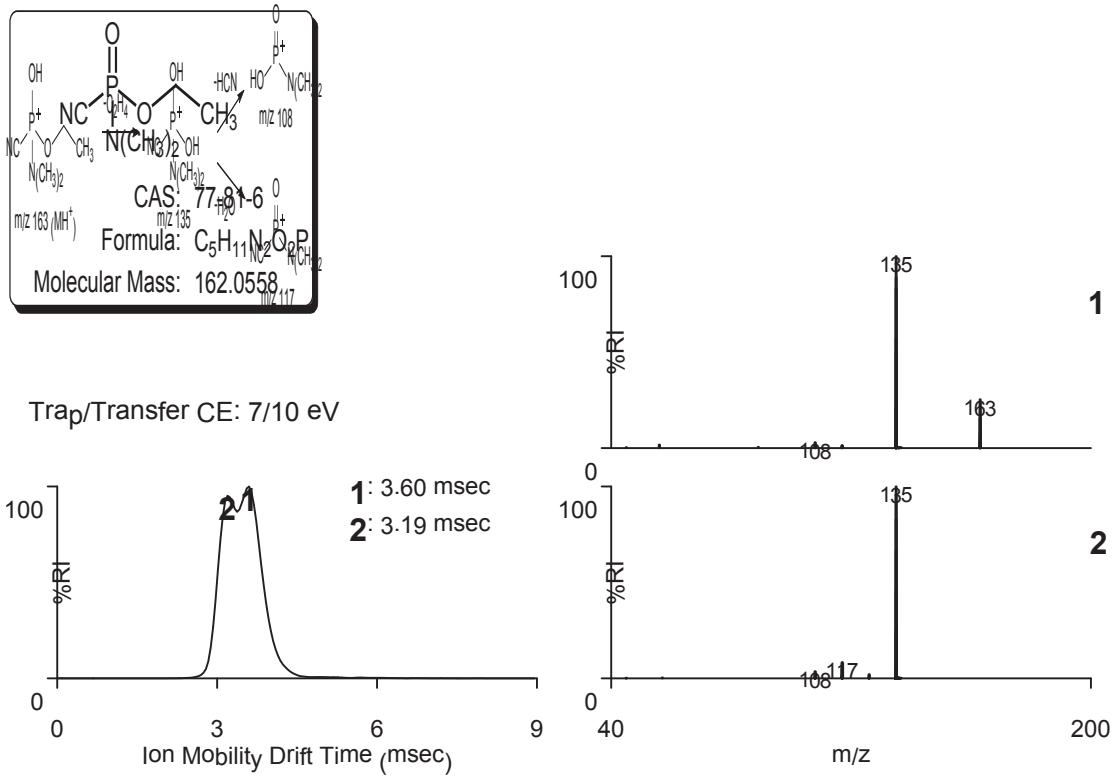

Figure 15: Moderate collision energy IMS and MS^n data for O-ethyl N,N-dimethylphosphoramidocyanidate (tabun, GA) (162).

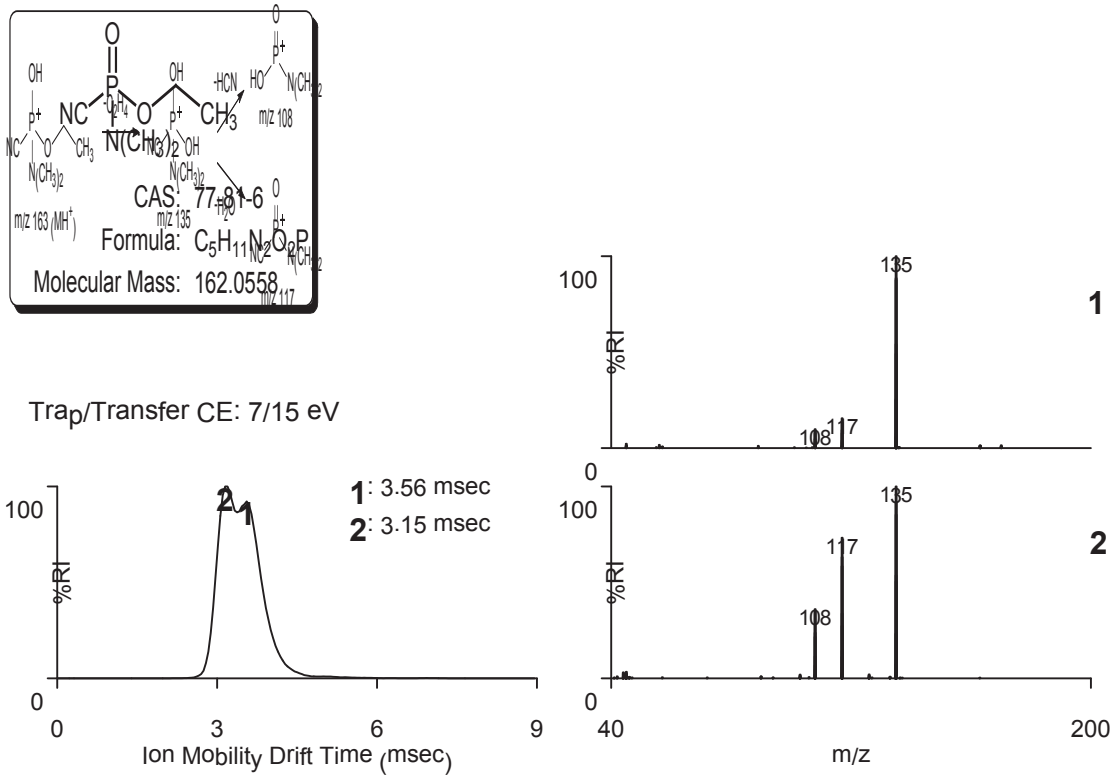

Figure 16: Higher collision energy IMS and MS^n data for O-ethyl N,N-dimethylphosphoramidocyanidate (tabun, GA) (162).

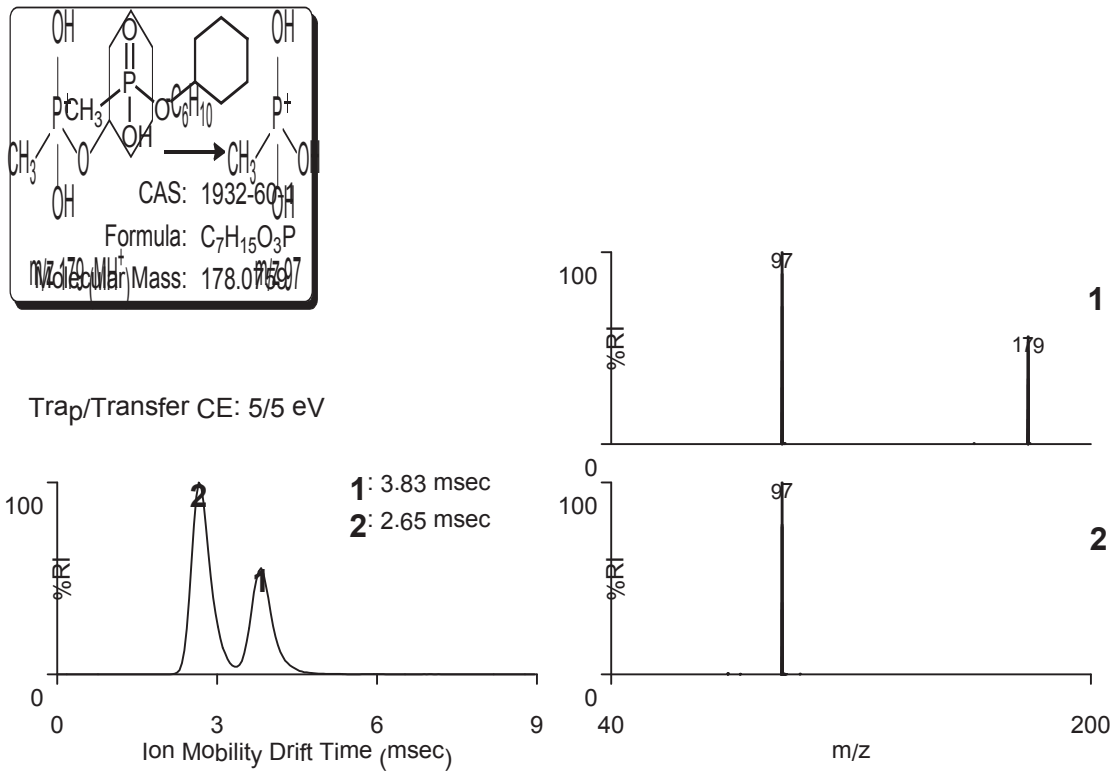

Figure 17: Lower collision energy IMS and MS^n data for cyclohexyl methylphosphonic acid (178).

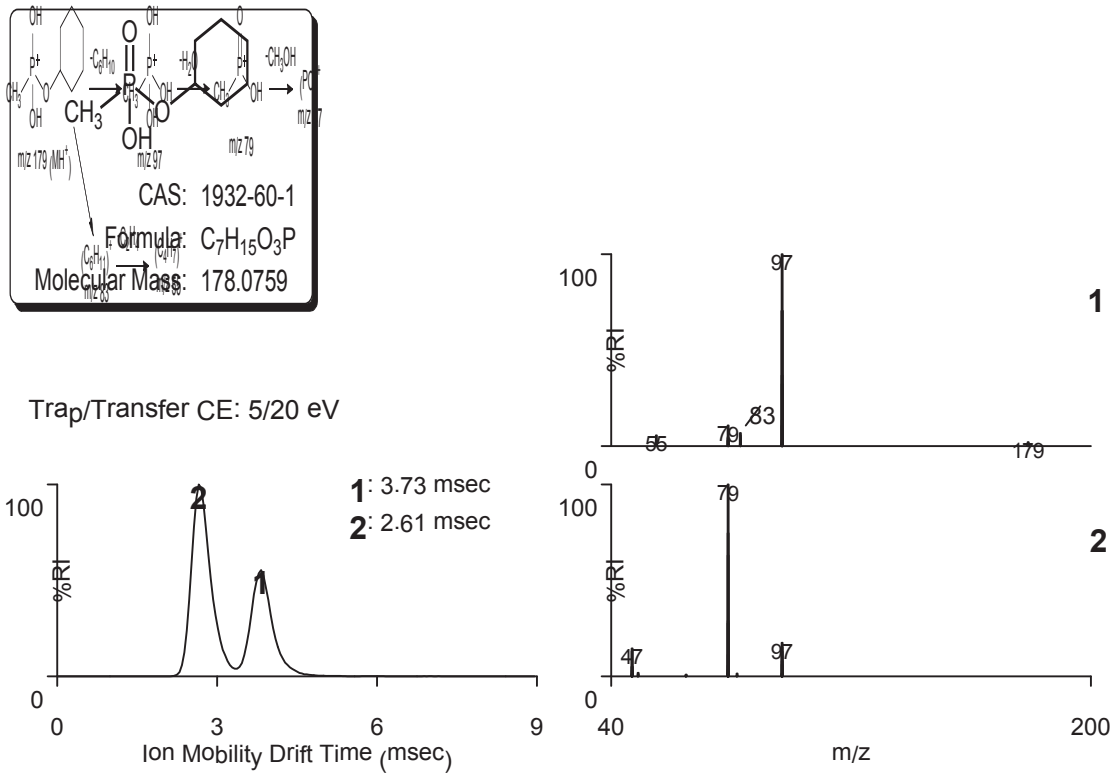

Figure 18: Higher collision energy IMS and MS^n data for cyclohexyl methylphosphonic acid (178).

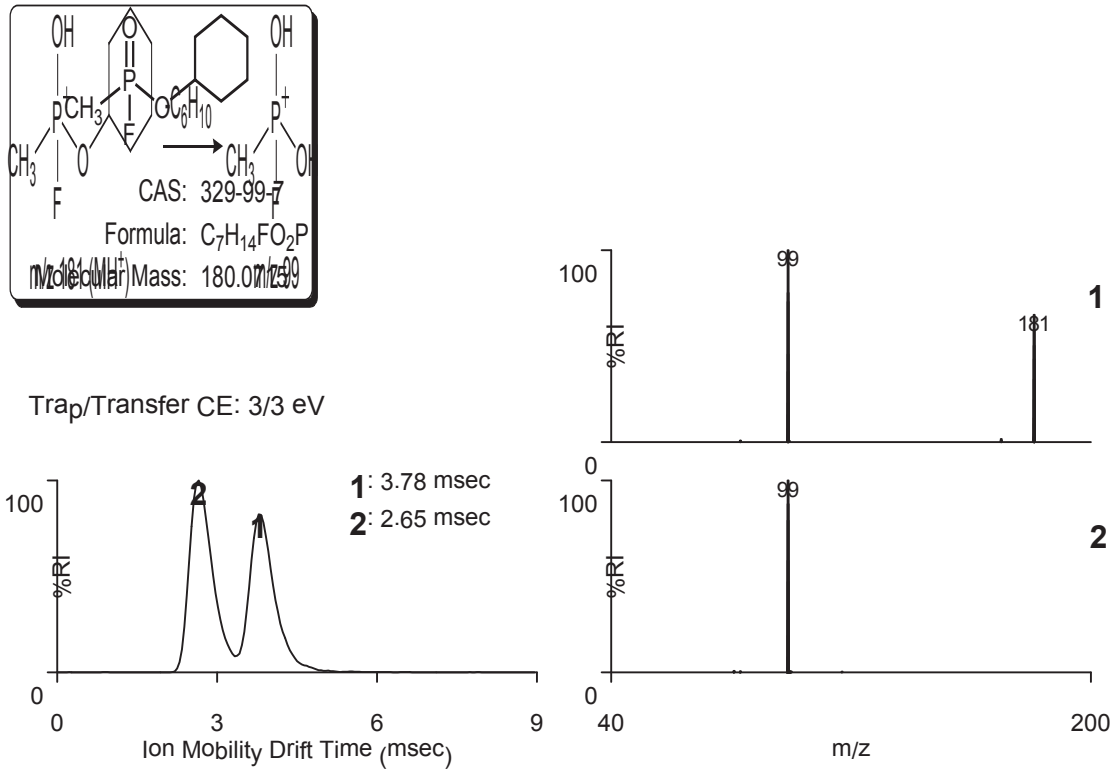

Figure 19: Lower collision energy IMS and MS^n data for cyclohexyl methylphosphonofluoridate (cyclosarin, GF) (180).

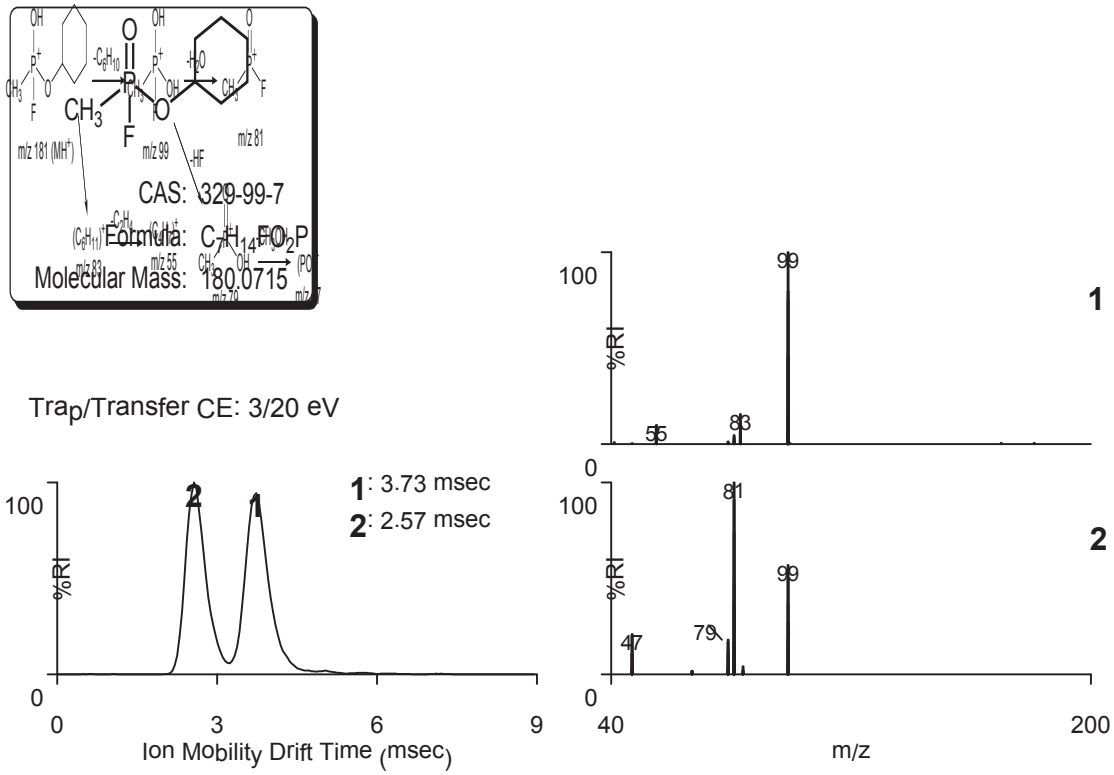

Figure 20: Higher collision energy IMS and MS^n data for cyclohexyl methylphosphonofluoridate (cyclosarin, GF) (180).

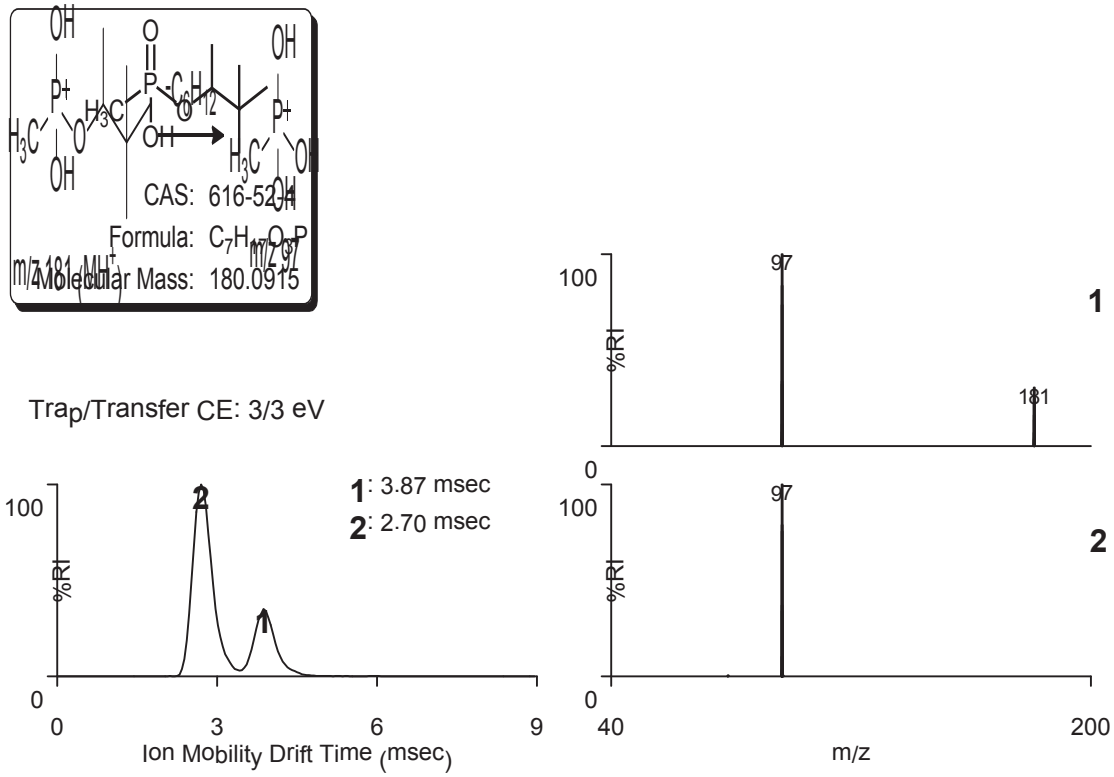

Figure 21: Lower collision energy IMS and MS^n data for pinacolyl methylphosphonic acid (180).

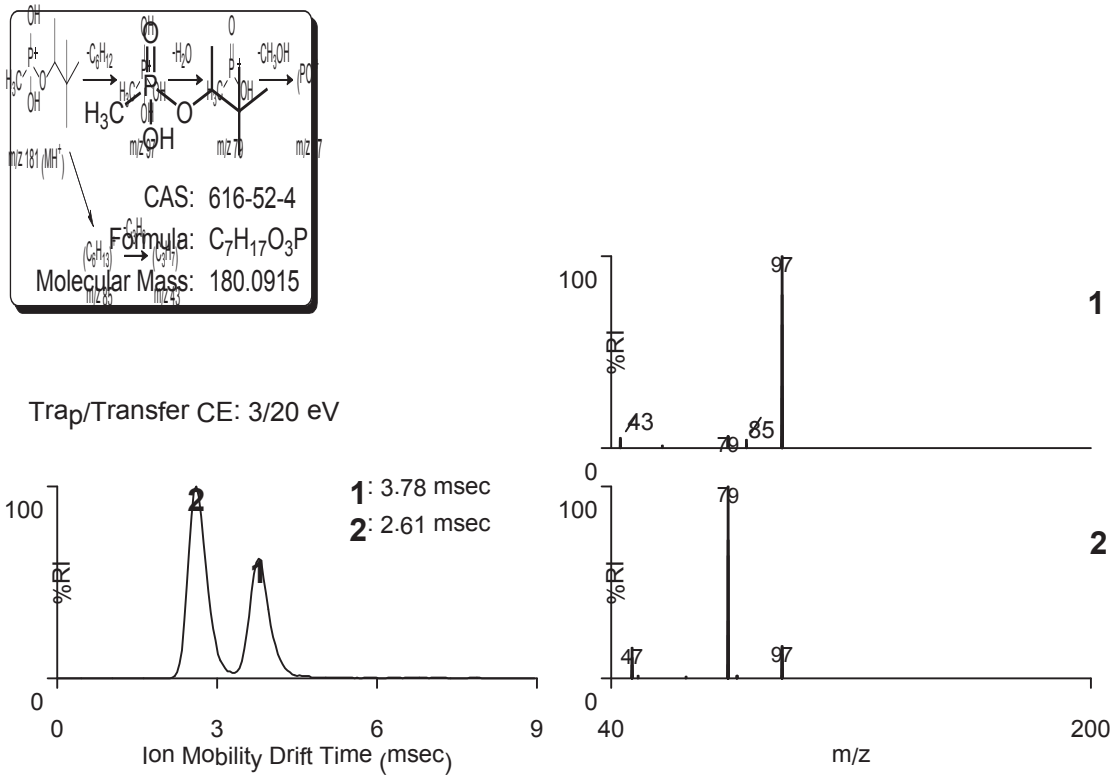

Figure 22: Higher collision energy IMS and MS^n data for pinacolyl methylphosphonic acid (180).

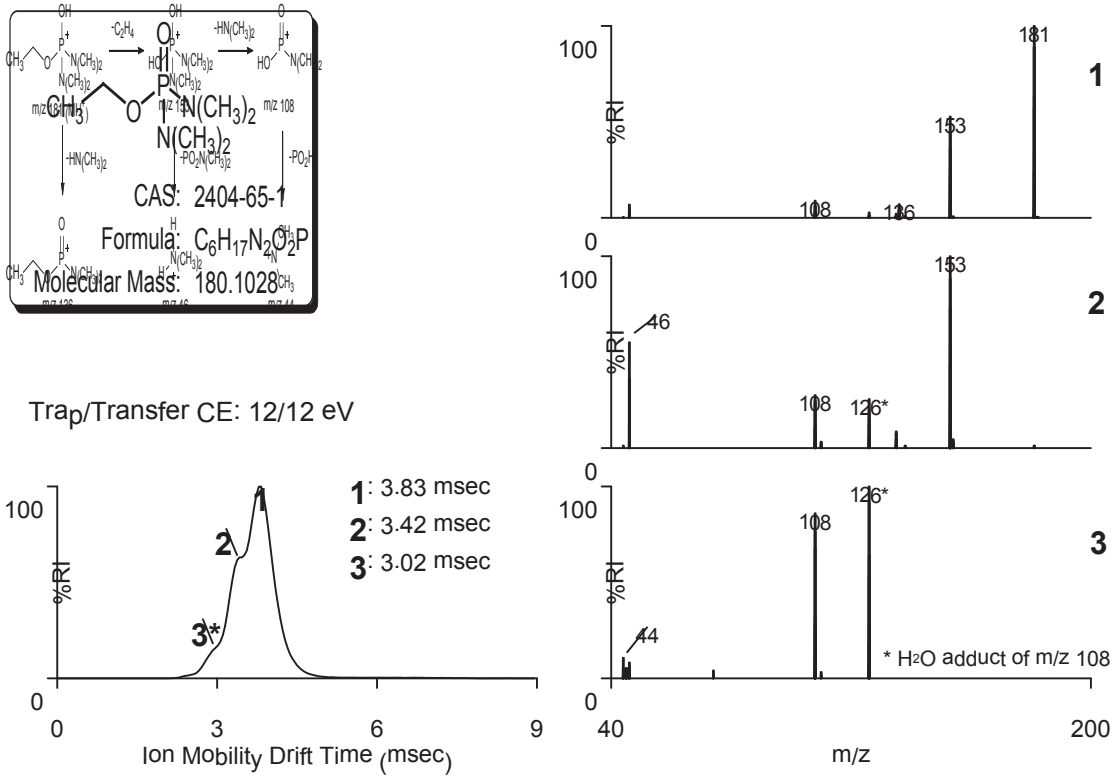

1 **2** **3**

3* - m/z 108 + m/z 126

Figure 23: IMS and MS^n data for ethyl tetramethylphosphorodiamidate (180).

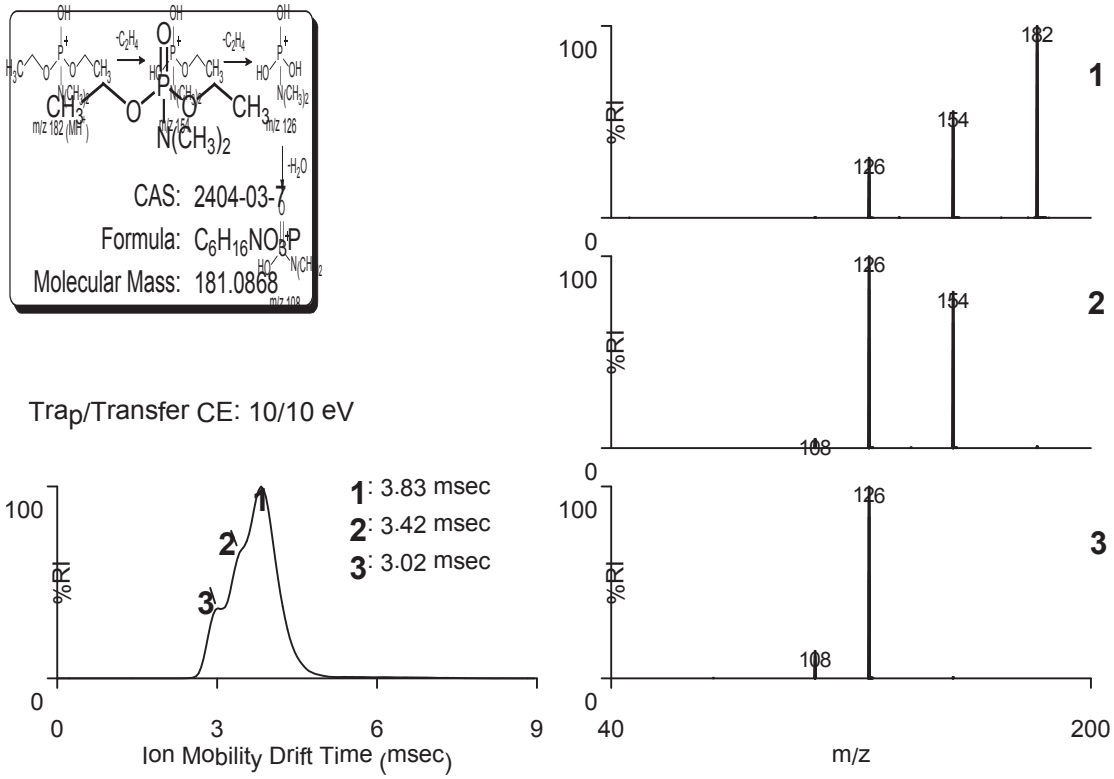

Figure 24: IMS and MS^n data for diethyl dimethylphosphoramidate (181).

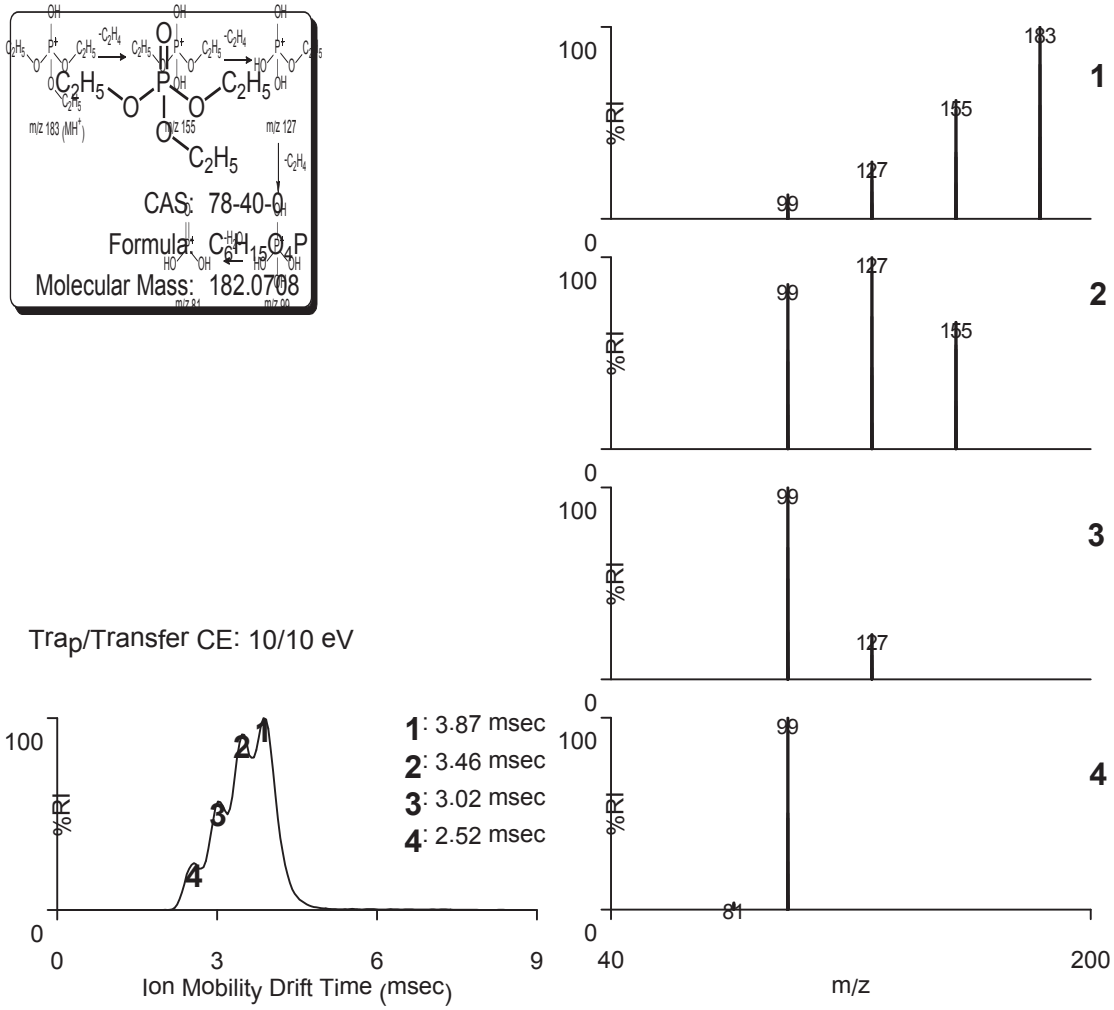

Figure 25: IMS and MS^n data for triethyl phosphate (TEP) (182)

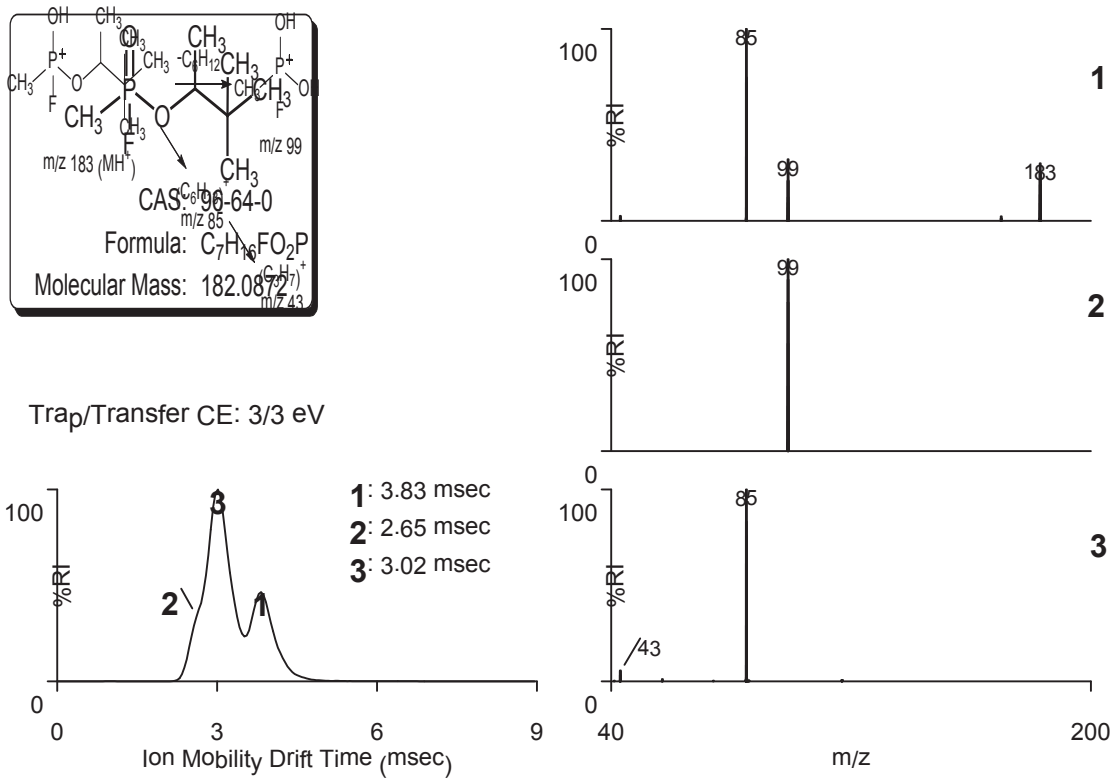

Figure 26: Lower collision energy IMS and MS^n data for pinacolyl methylphosphonofluoridate (soman, GD) (182).

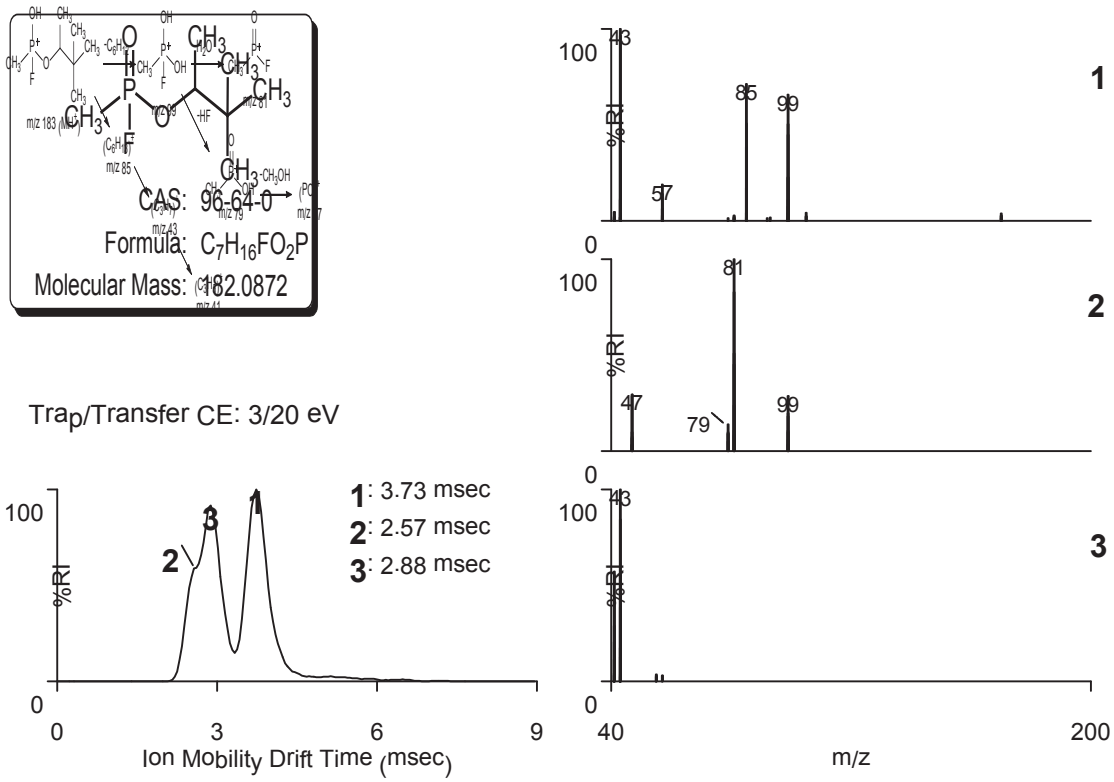

Figure 27: Higher collision energy IMS and MS^n data for pinacolyl methylphosphonofluoridate (soman, GD) (182).

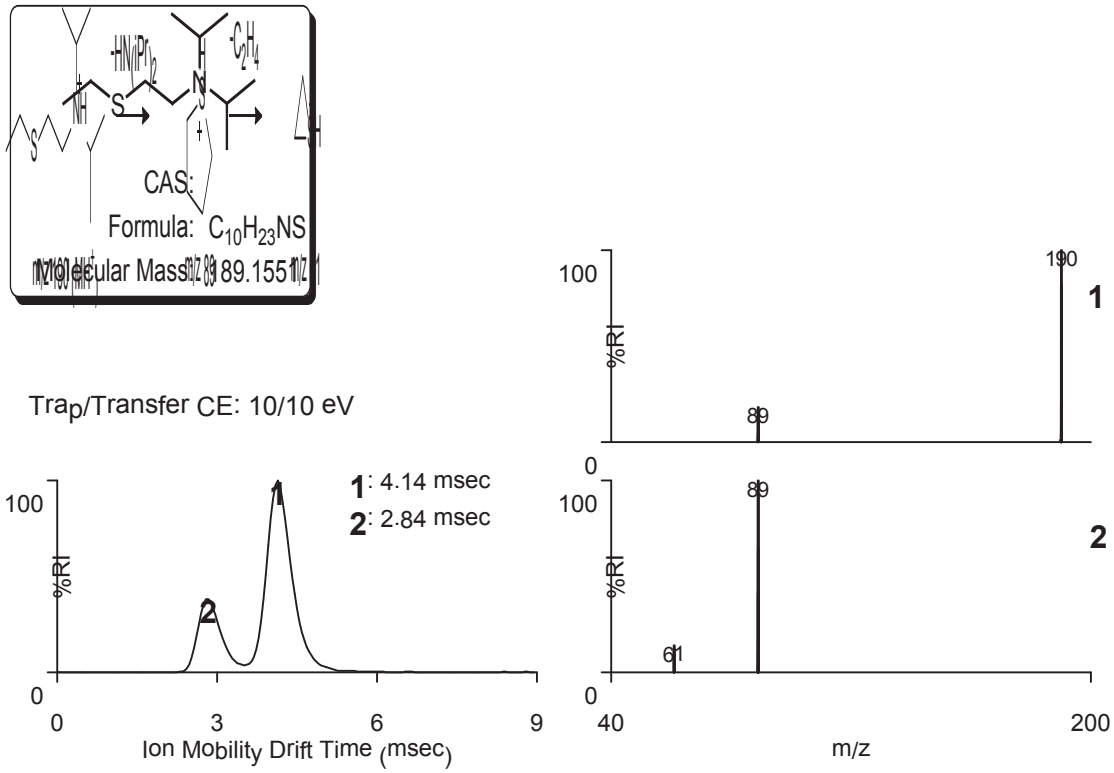

Figure 28: IMS and MS^n data for 2-(diisopropylamino)ethyl ethyl sulfide (189)

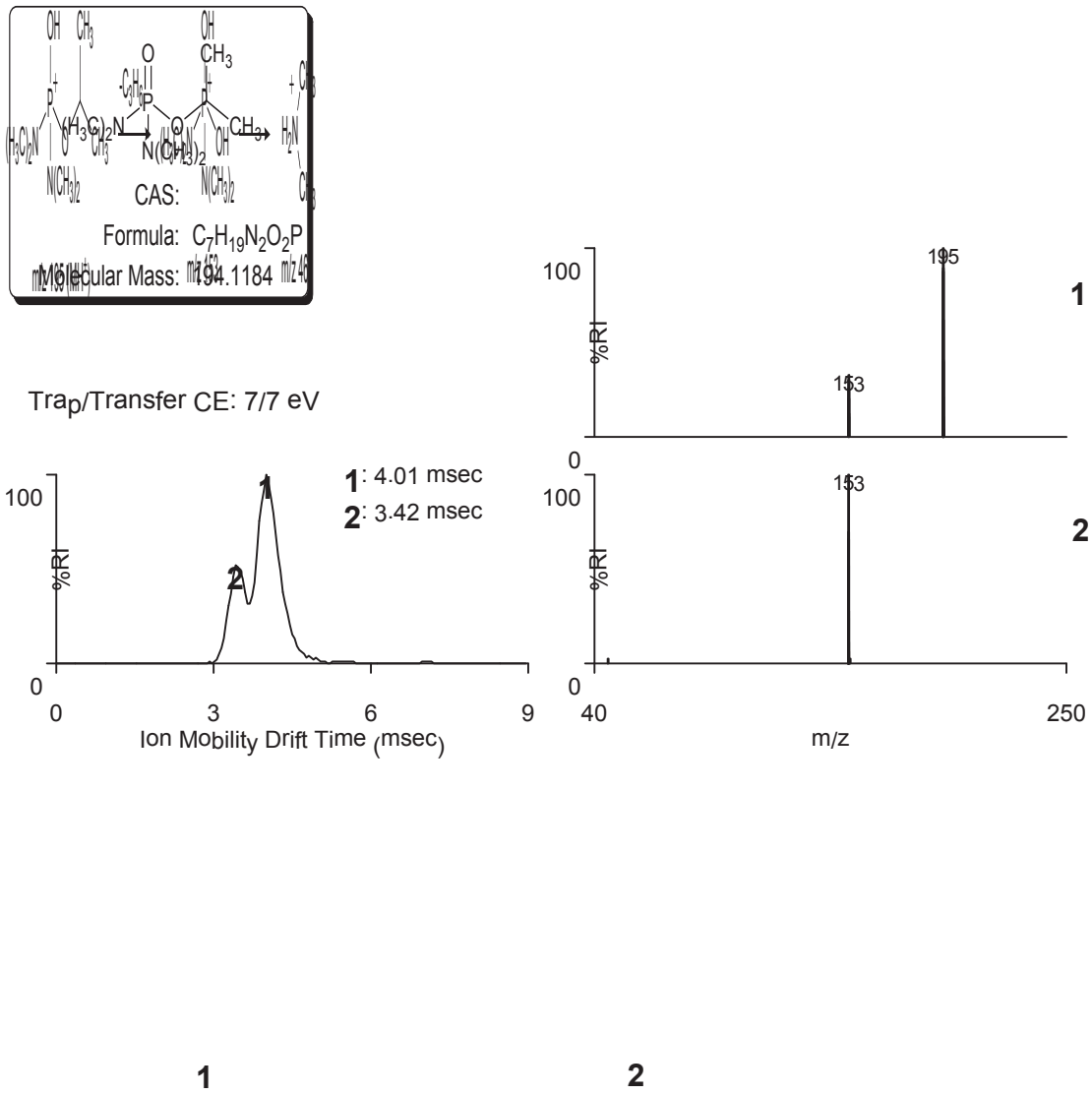

Figure 29: IMS and MS^n data for isopropyl tetramethylphosphorodiamidate (194).

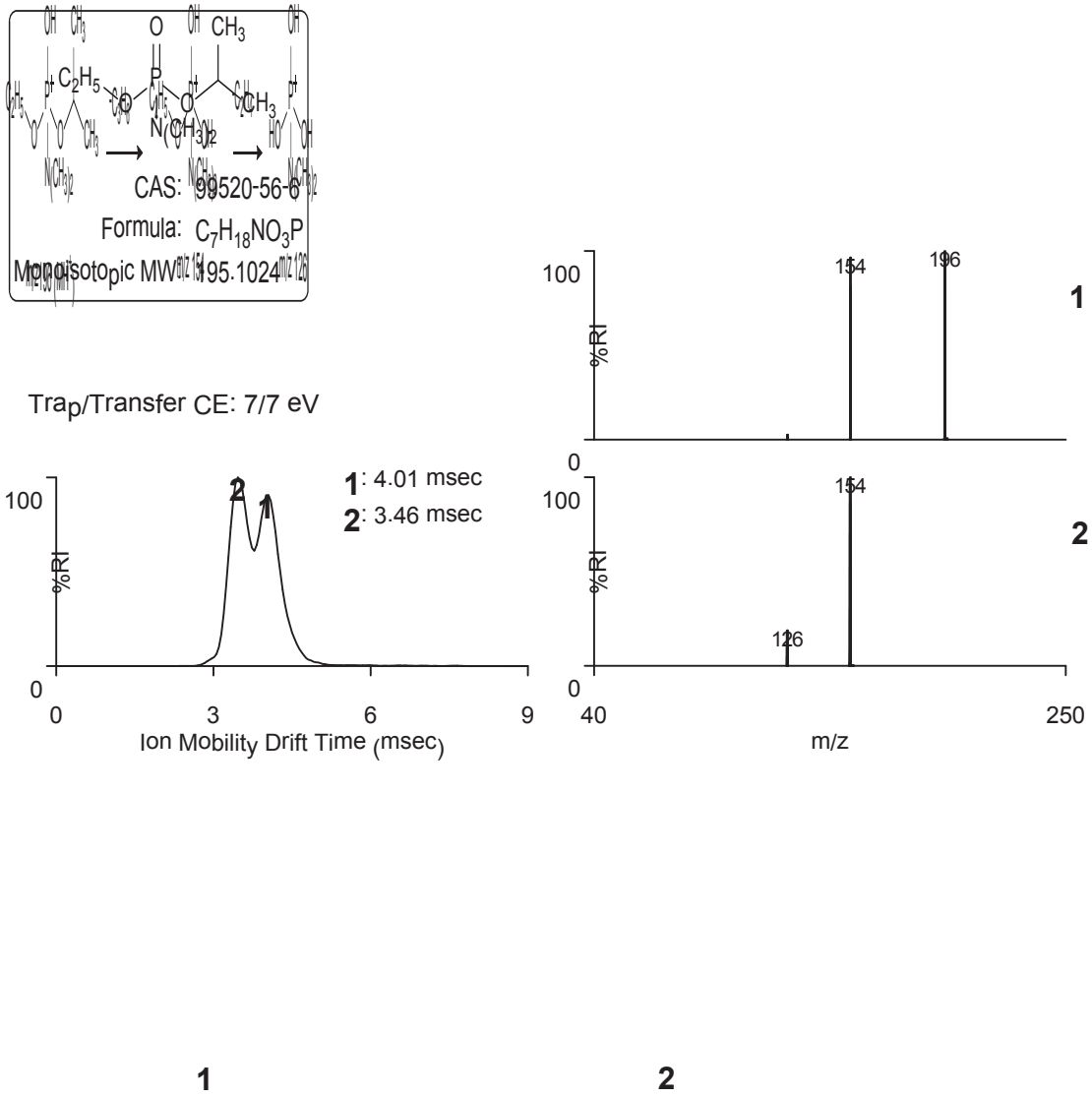

Figure 30: IMS and MS^n data for ethyl isopropyl dimethylphosphoramidate (195).

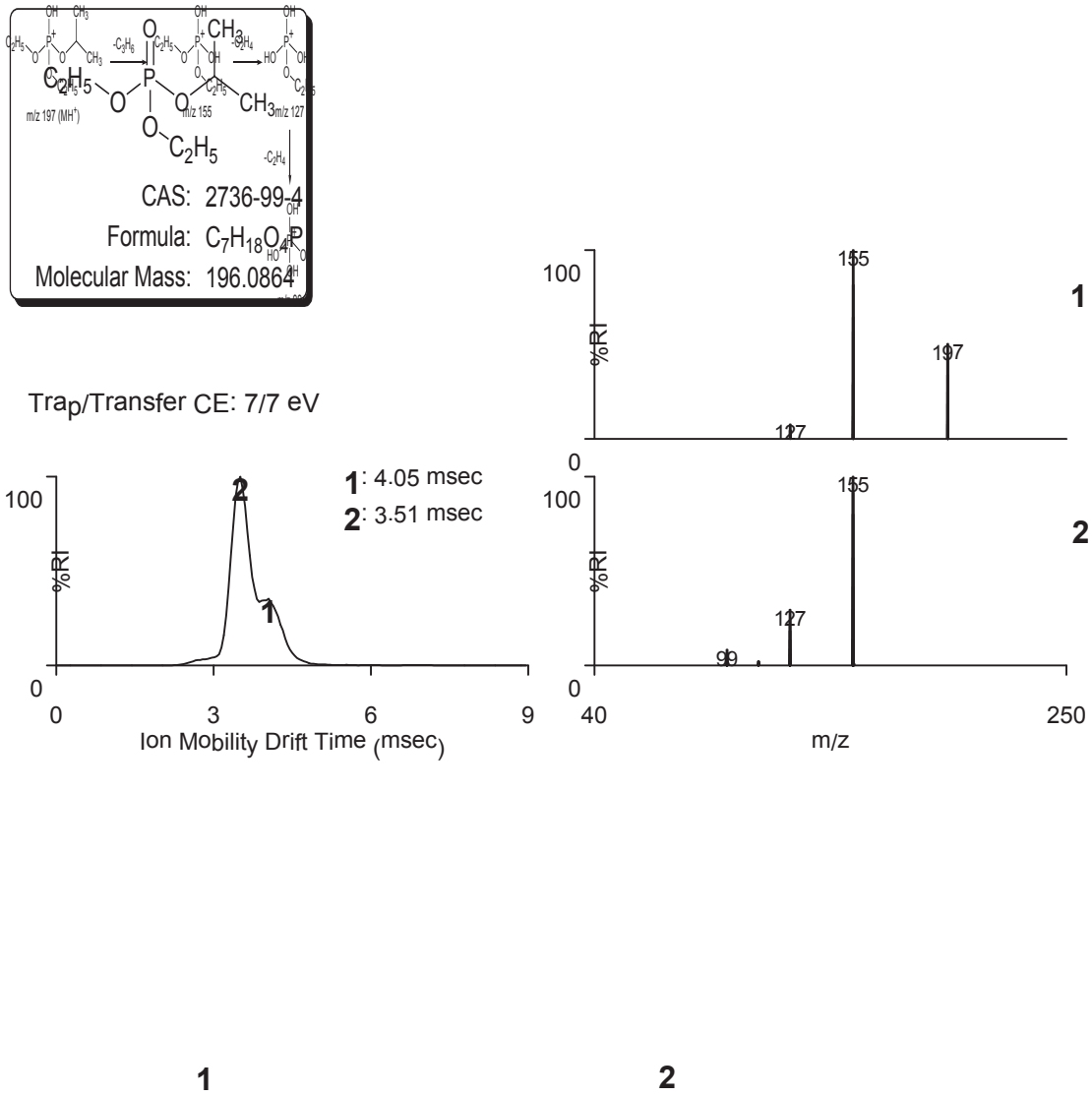

Figure 31: IMS and MS^n data for diethyl isopropyl phosphate (196).

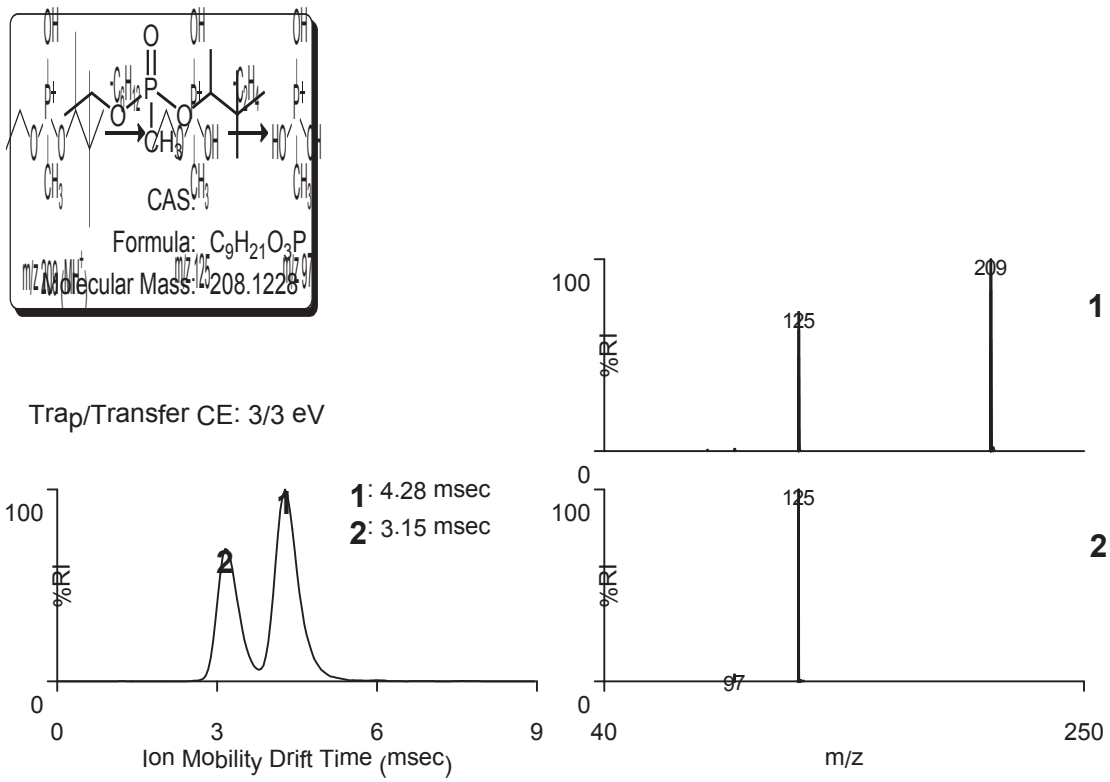

Figure 32: Lower collision energy IMS and MS^n data for ethyl pinacolyl methylphosphonate (208).

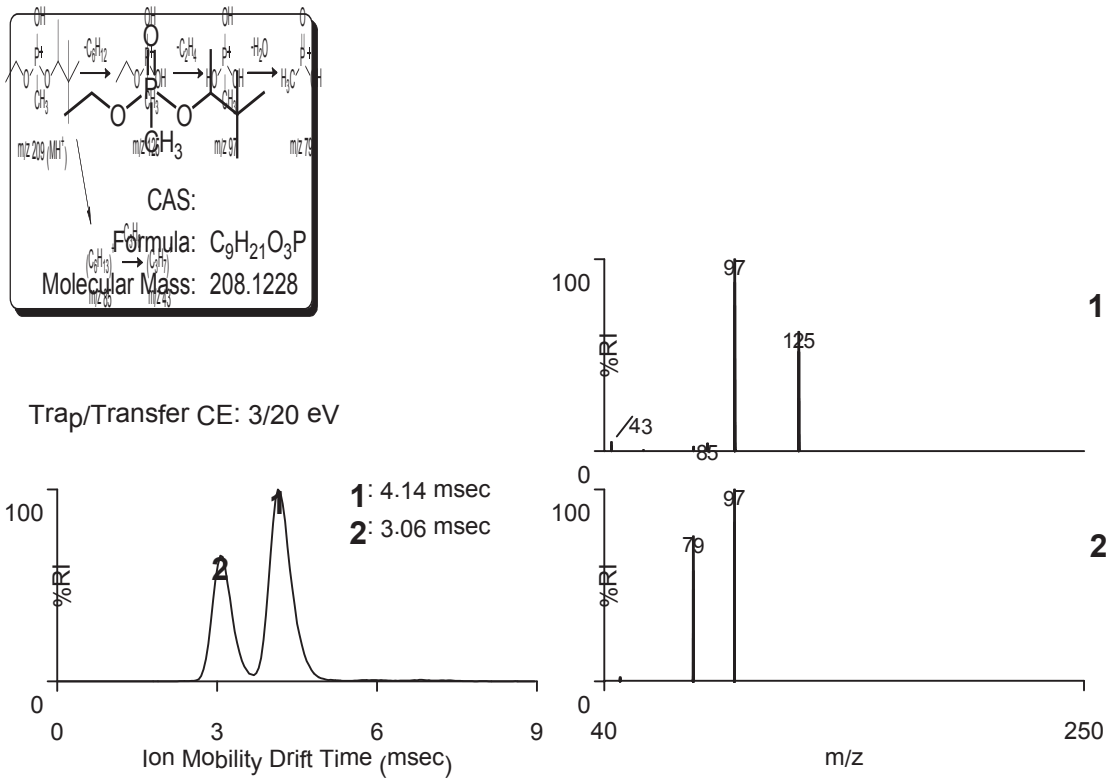

1 **2**

Figure 33: Higher collision energy IMS and MS^n data for ethyl pinacolyl methylphosphonate (208).

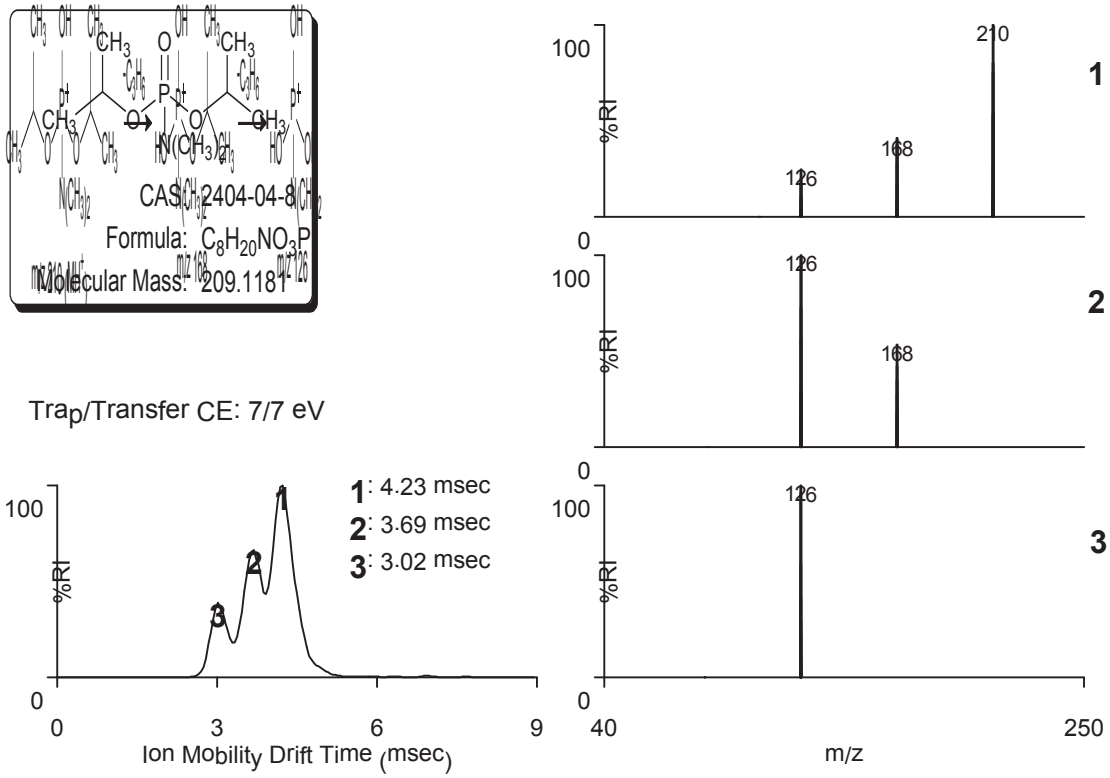

Figure 34: IMS and MS^n data for diisopropyl dimethylphosphoramidate (209).

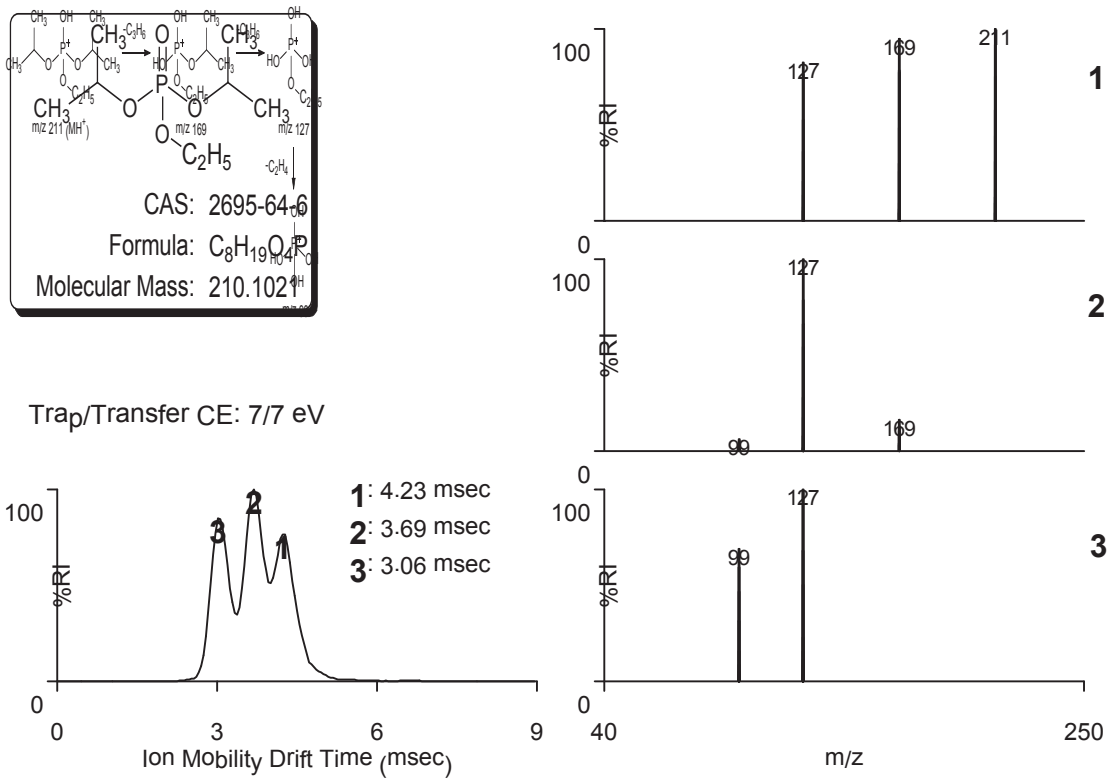

Figure 35: IMS and MS^n data for diisopropyl ethyl phosphate (210).

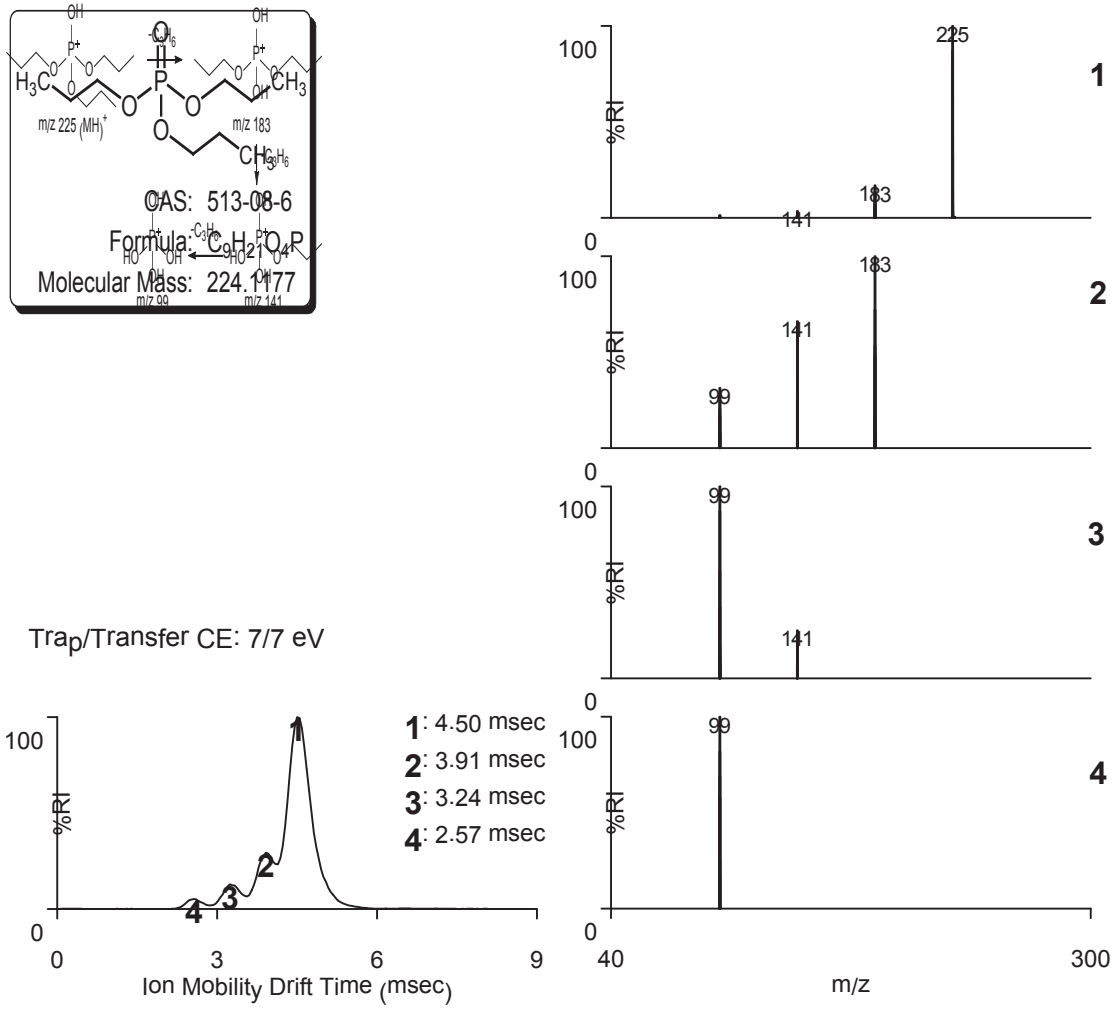

Figure 36: Lower collision energy IMS and MS^n data for tripropyl phosphate (224).

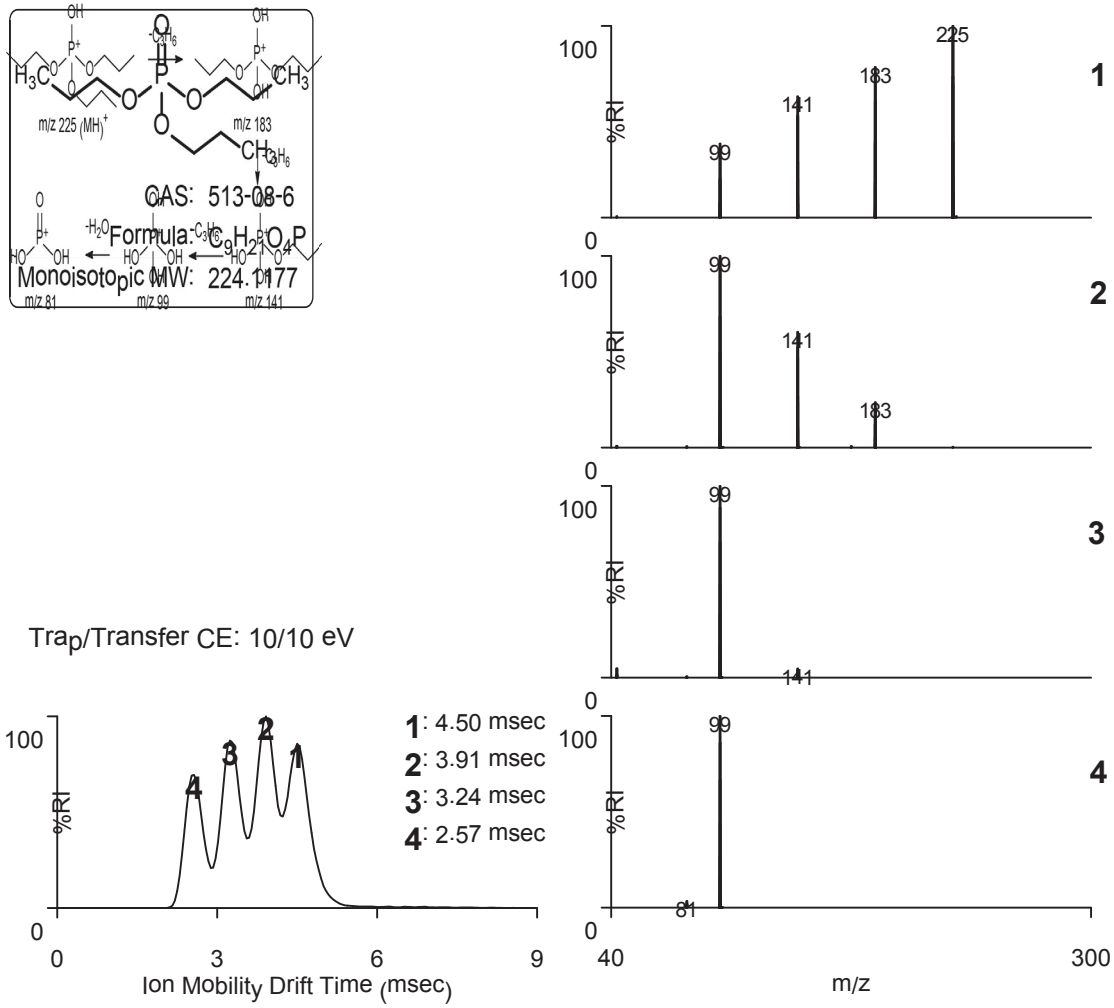

Figure 37: Higher collision energy IMS and MS^n data for tripropyl phosphate (224).

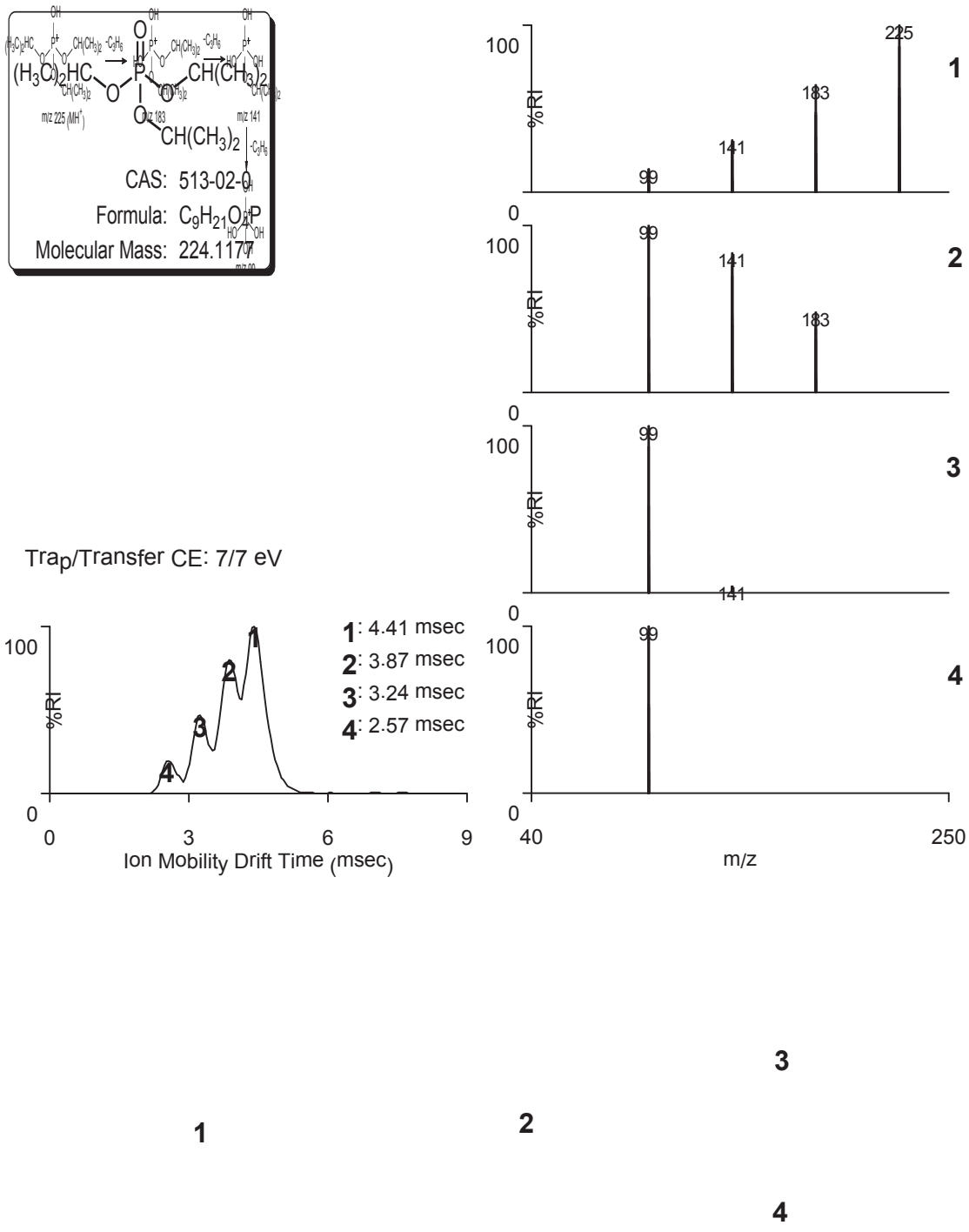

Figure 38: Lower collision energy IMS and MS^n data for triisopropyl phosphate (224).

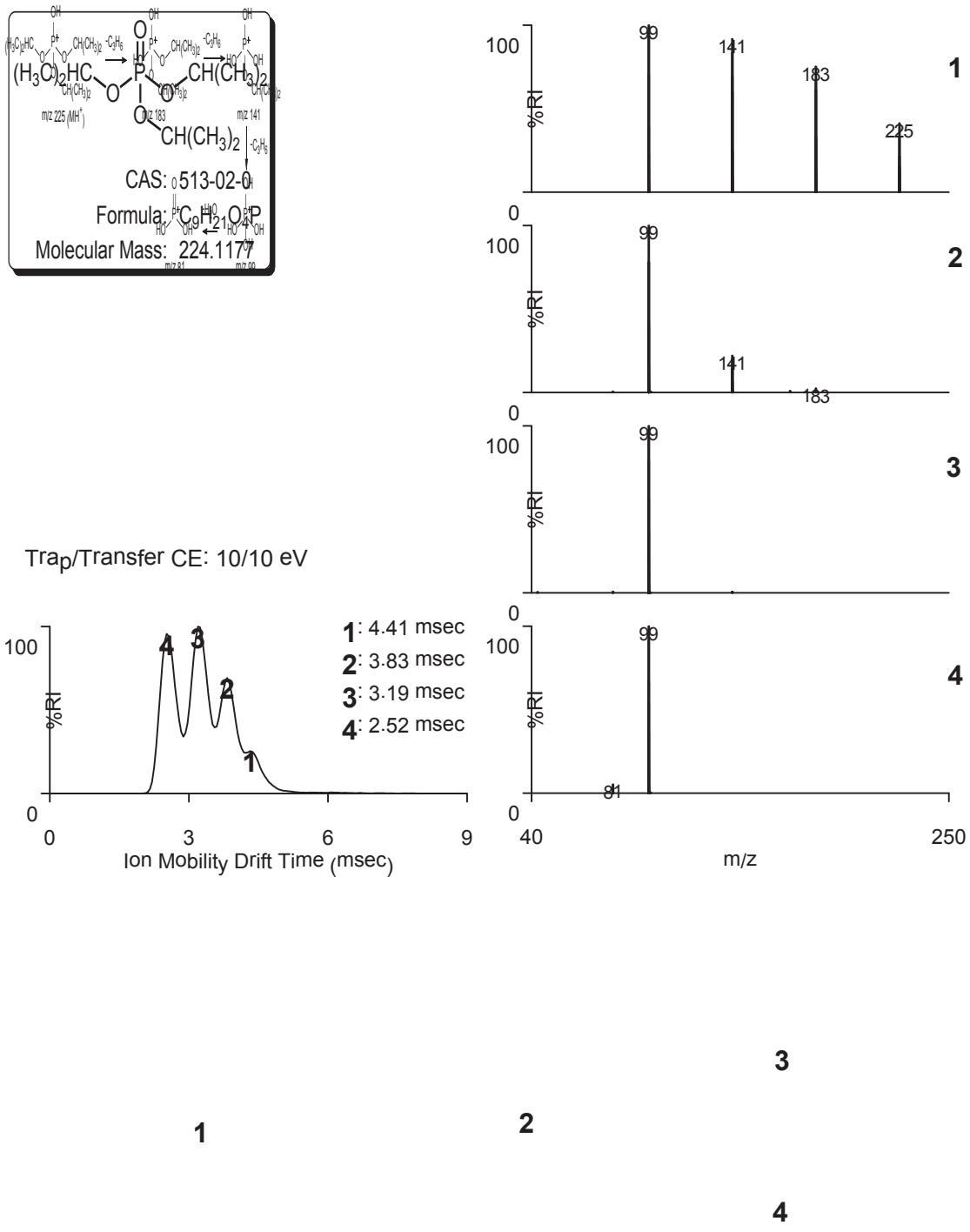

Figure 39: Higher collision energy IMS and MS^n data for triisopropyl phosphate (224).

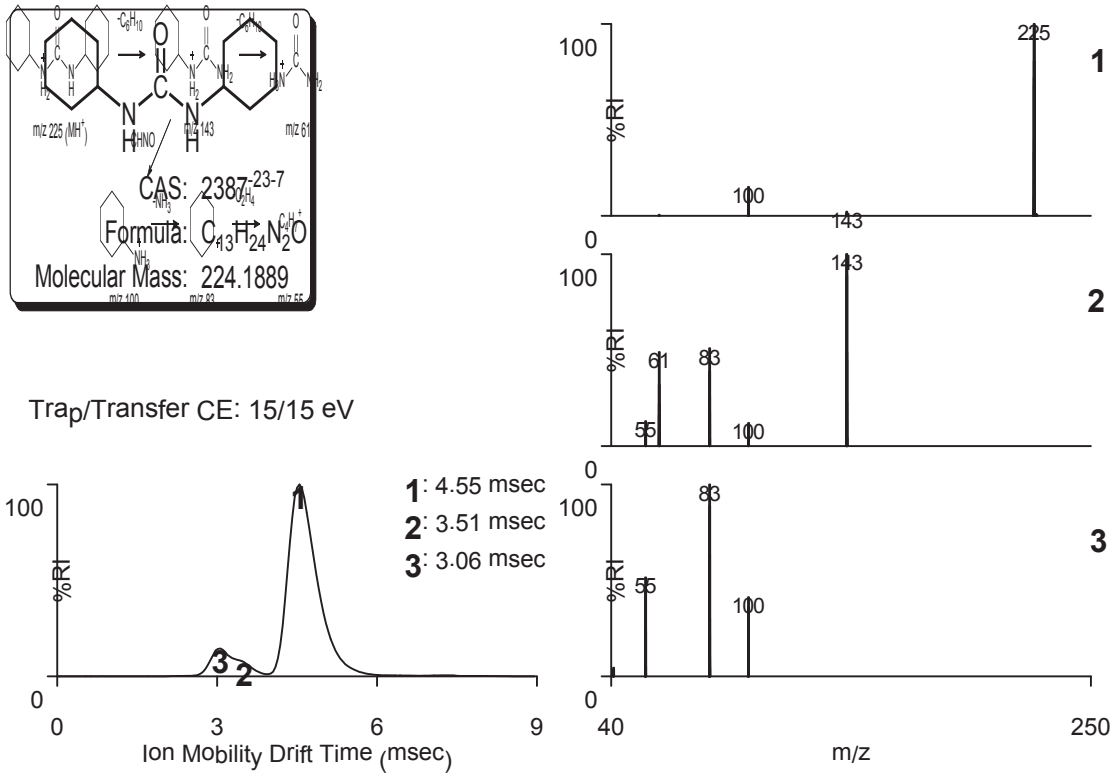

Figure 40: IMS and MS^n data for N,N-dicyclohexylurea (224).

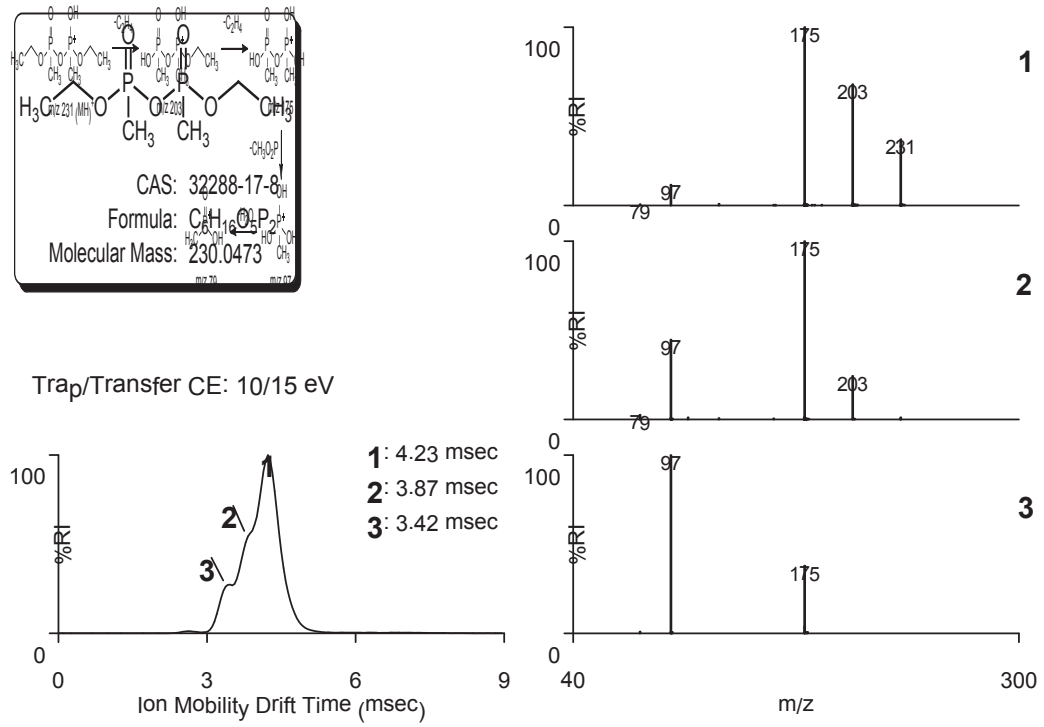

Figure 41: IMS and MS^n data for diethyl dimethylpyrophosphonate (230).

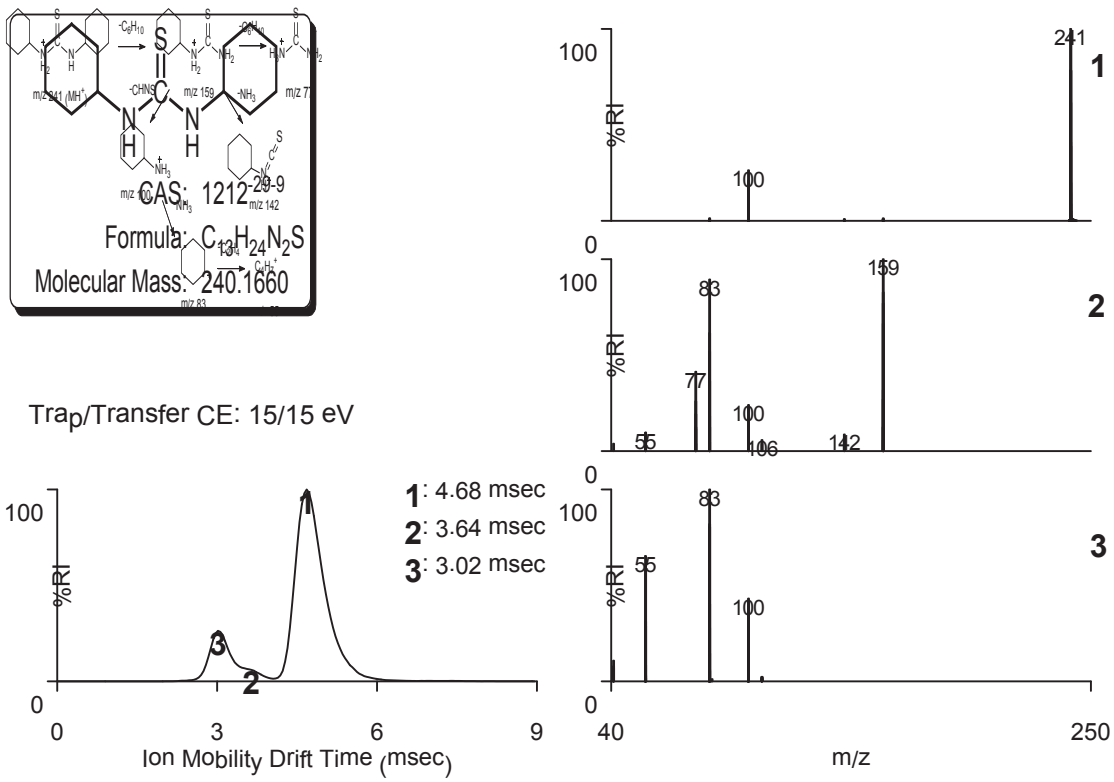

Figure 42: IMS and MS^n data for N,N-dicyclohexylthiourea (240).

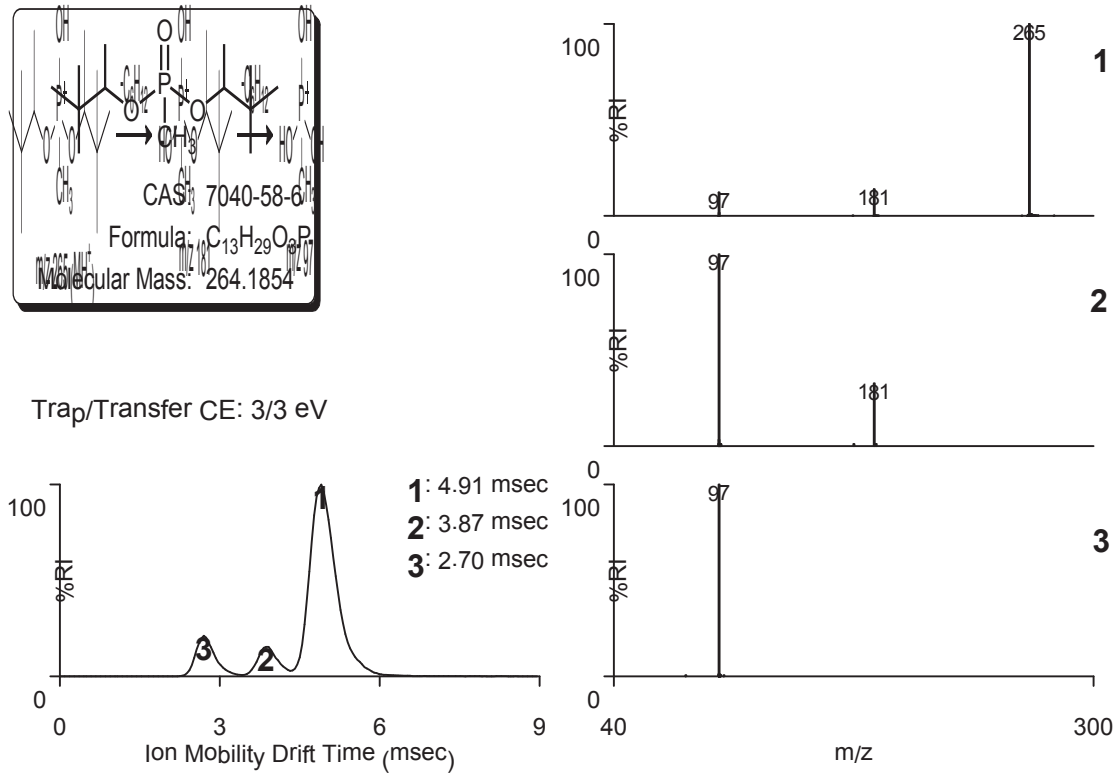

Figure 43: Lower collision energy IMS and MS^n data for dipinacolyl methylphosphonate (264).

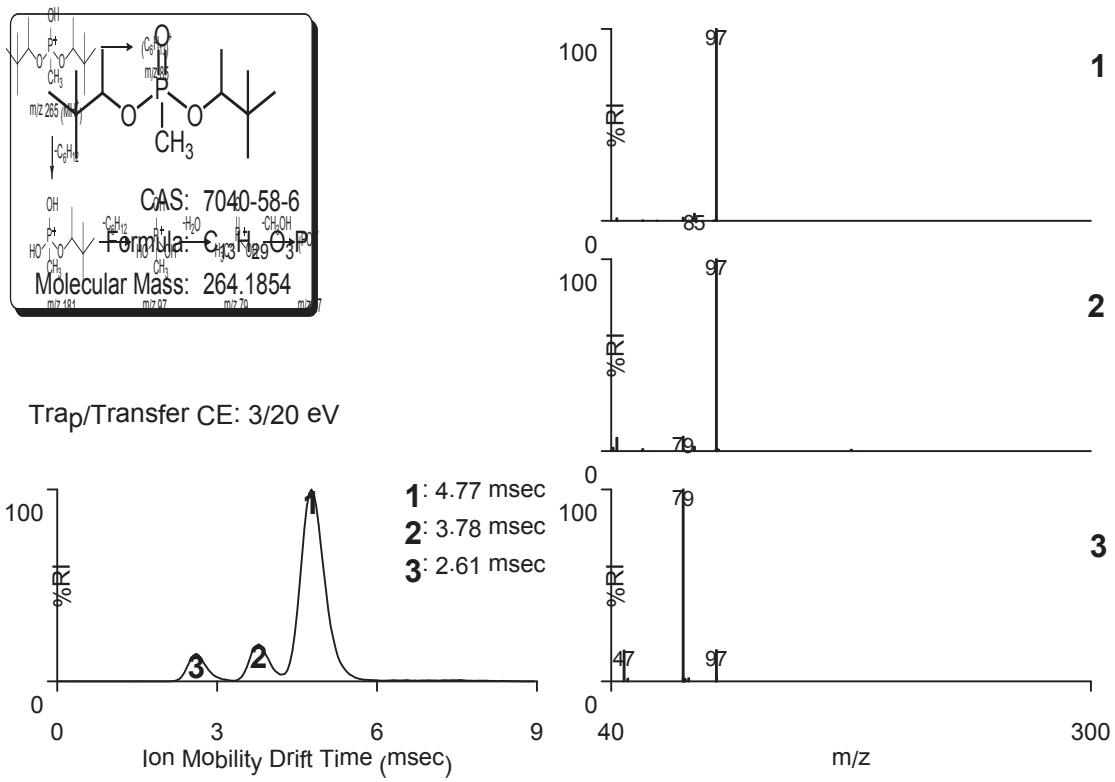

Figure 44: Higher collision energy IMS and MS^n data for dipinacolyl methylphosphonate (264).

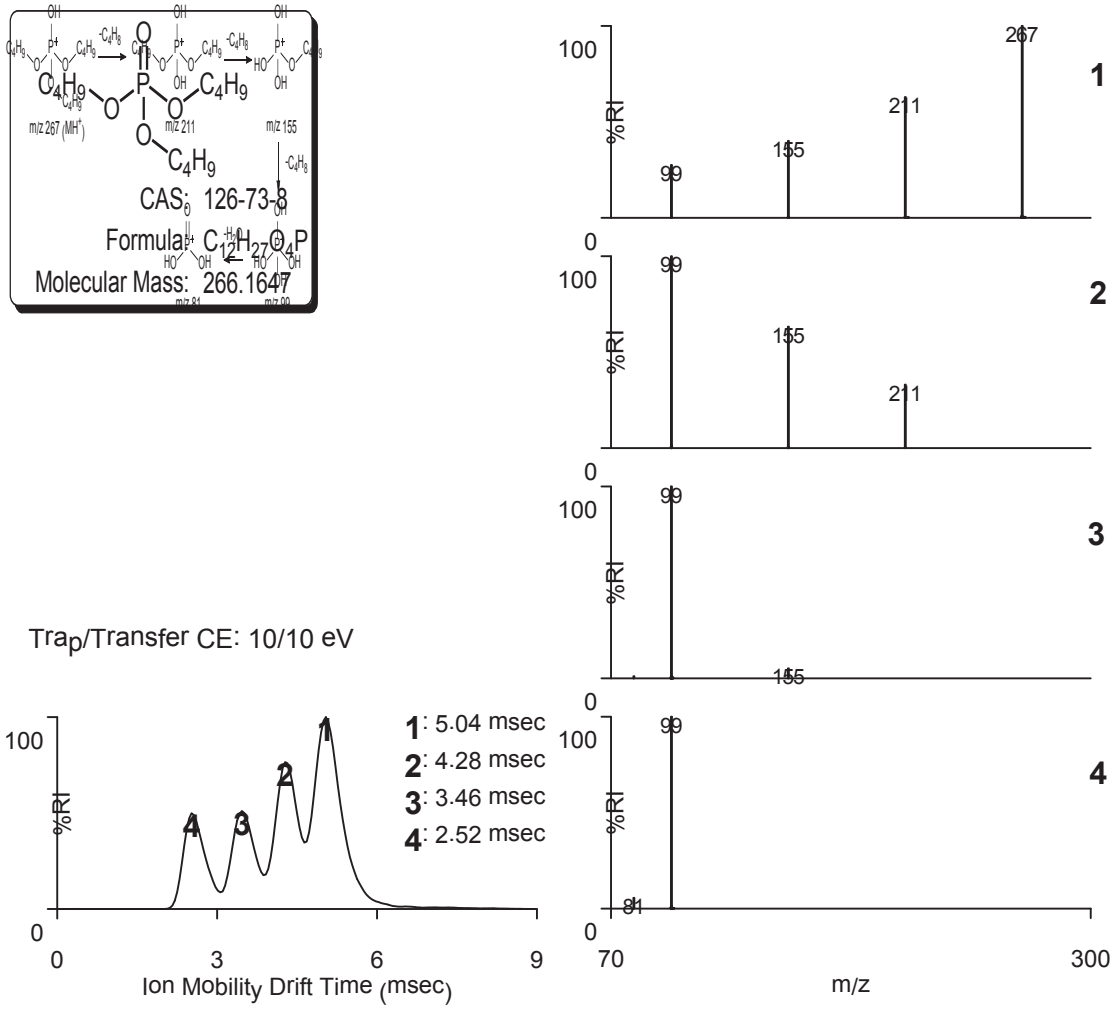

Figure 45: IMS and MS^n data for tributyl phosphate (TBP) (266).

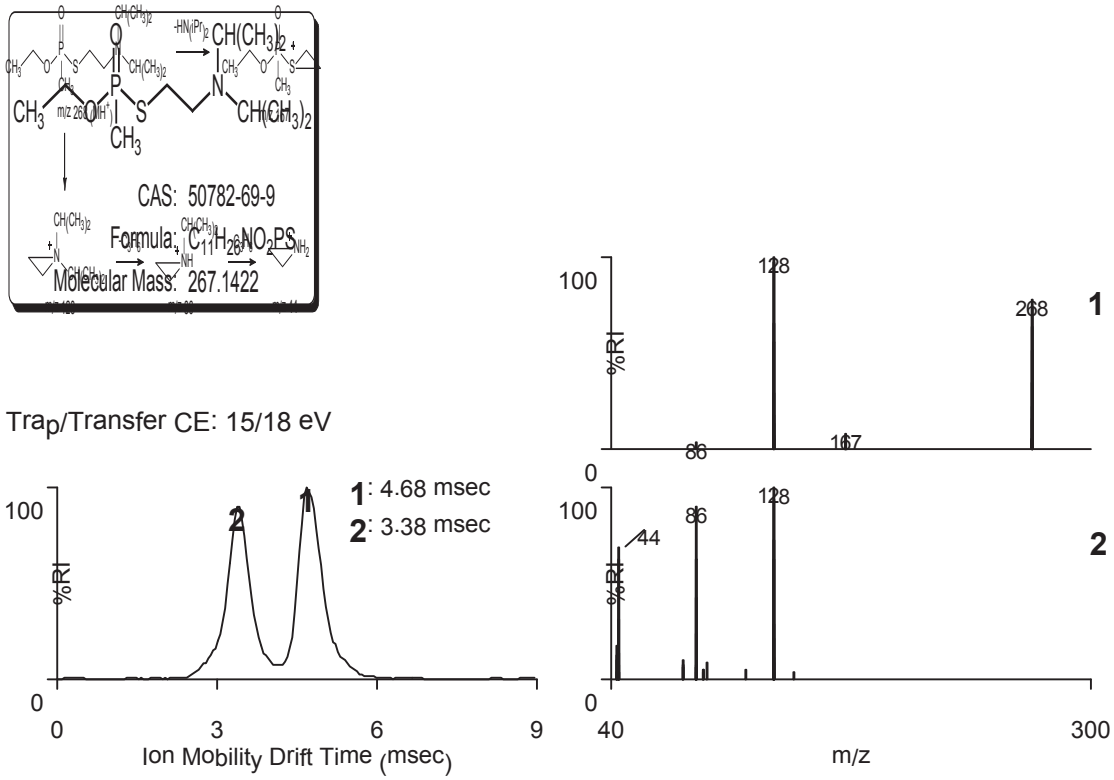

Figure 46: IMS and MS^n data for O-ethyl S-[2-(diisopropylamino)ethyl] methylphosphonothiolate (VX) (267).

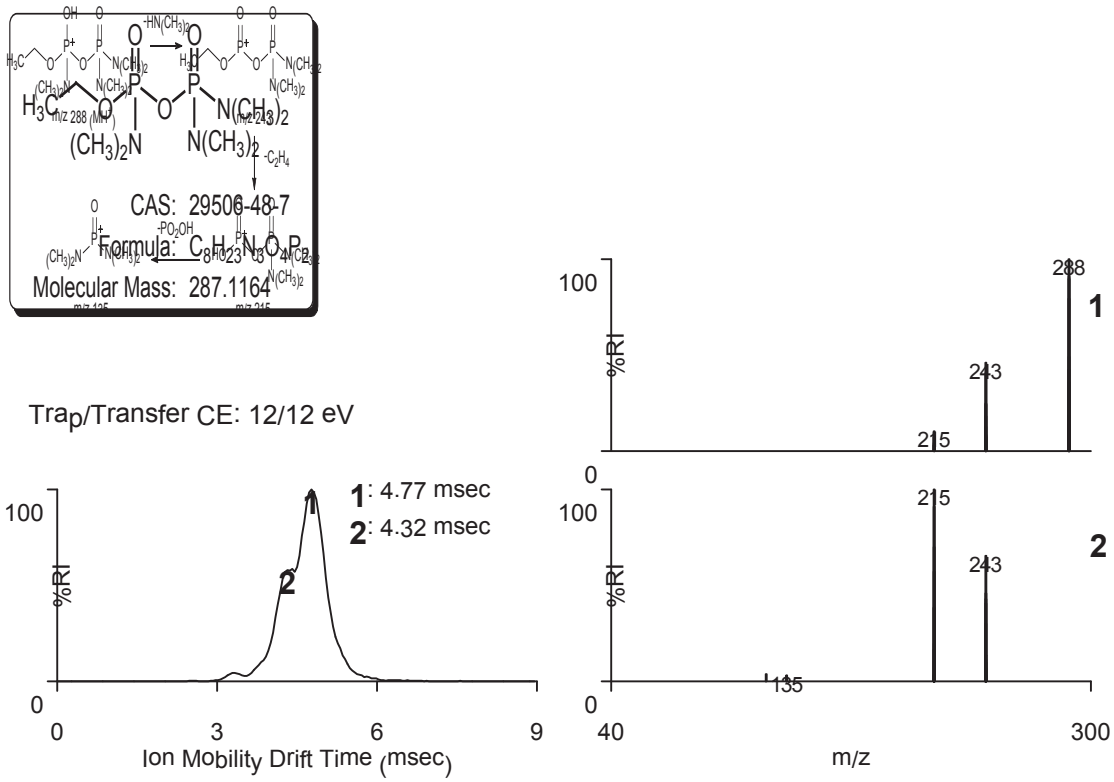

Figure 47: IMS and MS^n data for ethyl dimethylphosphoramidic tetramethylphosphoramidic anhydride (287).

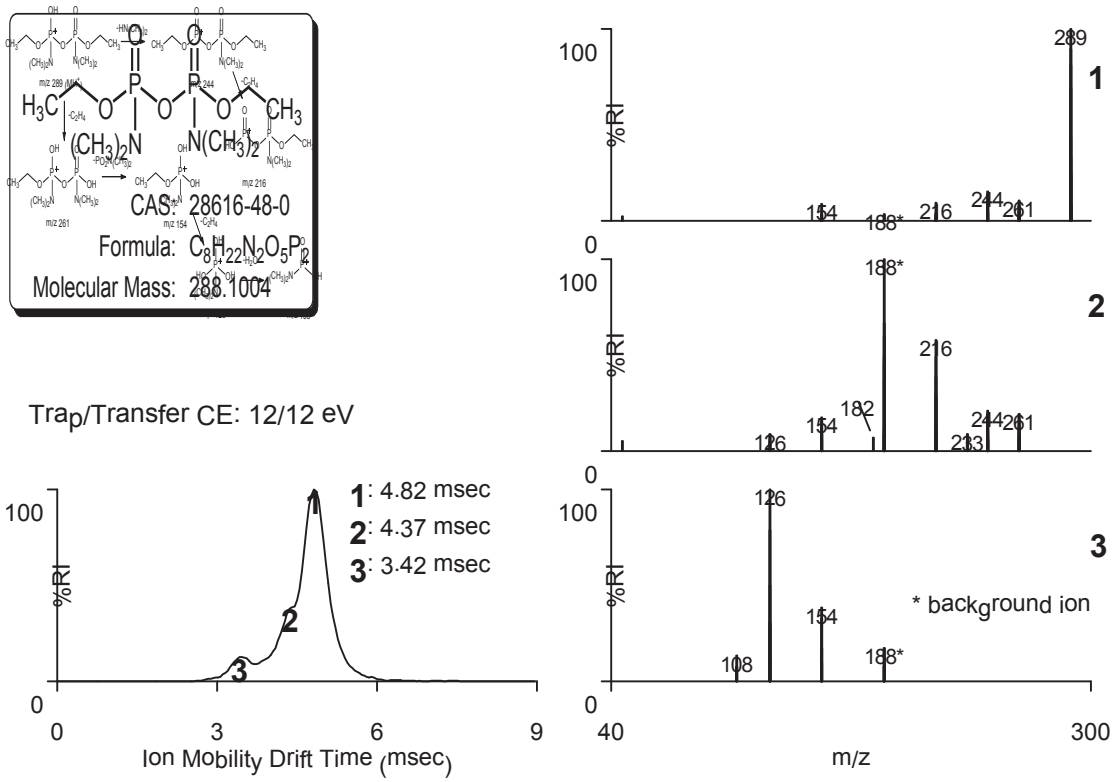

Figure 48: IMS and MS^n data for bis(ethyl dimethylphosphoramidic) anhydride (288).

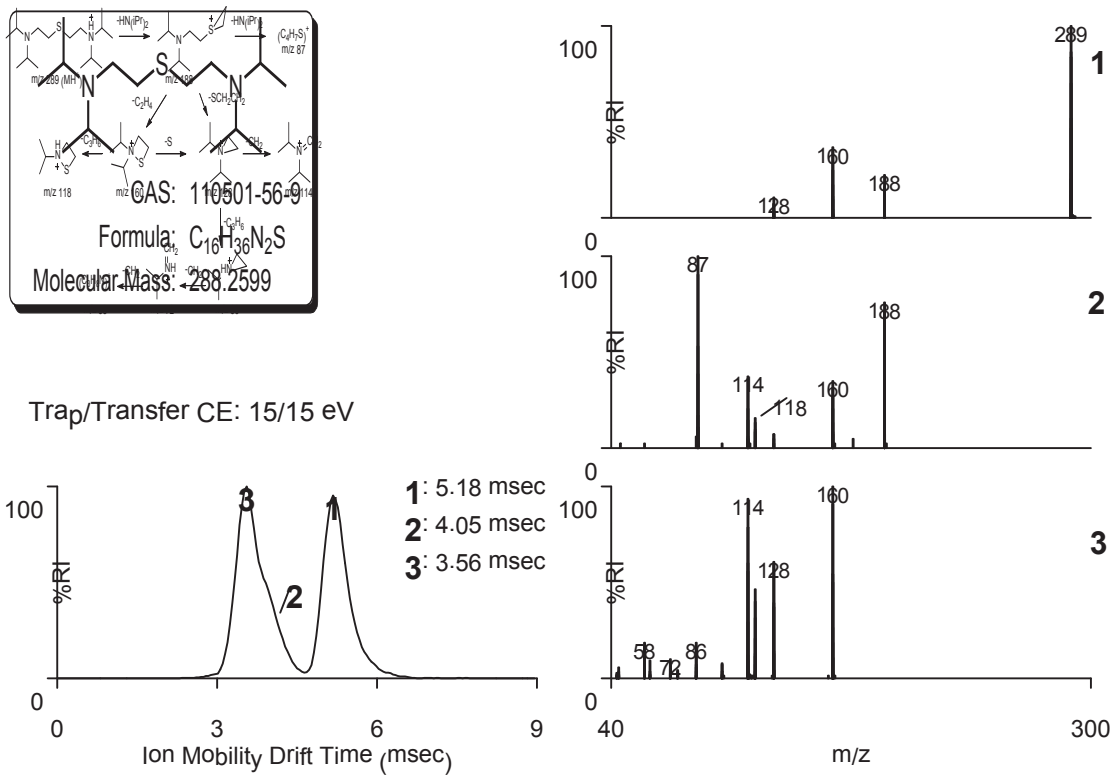

Figure 49: IMS and MS^n data for bis[2-(diisopropylamino)ethyl] sulfide (288).

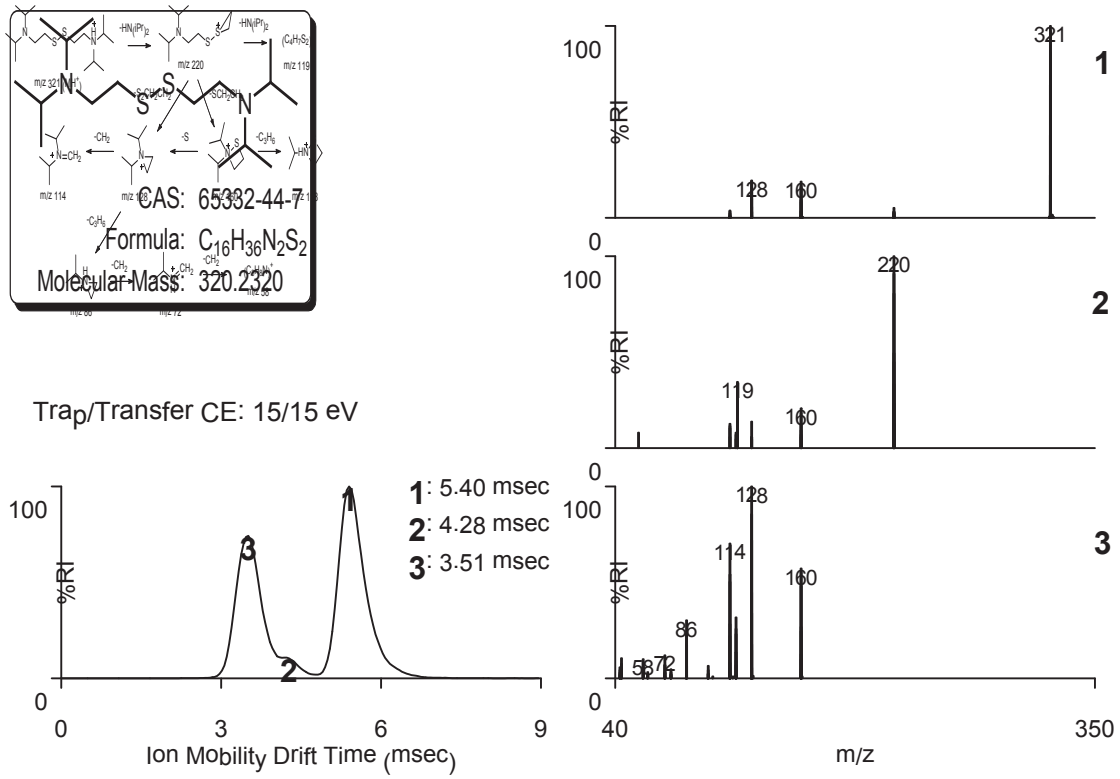

Figure 50: IMS and MS^n data for bis[2-diisopropylamino)ethyl] disulfide (320).

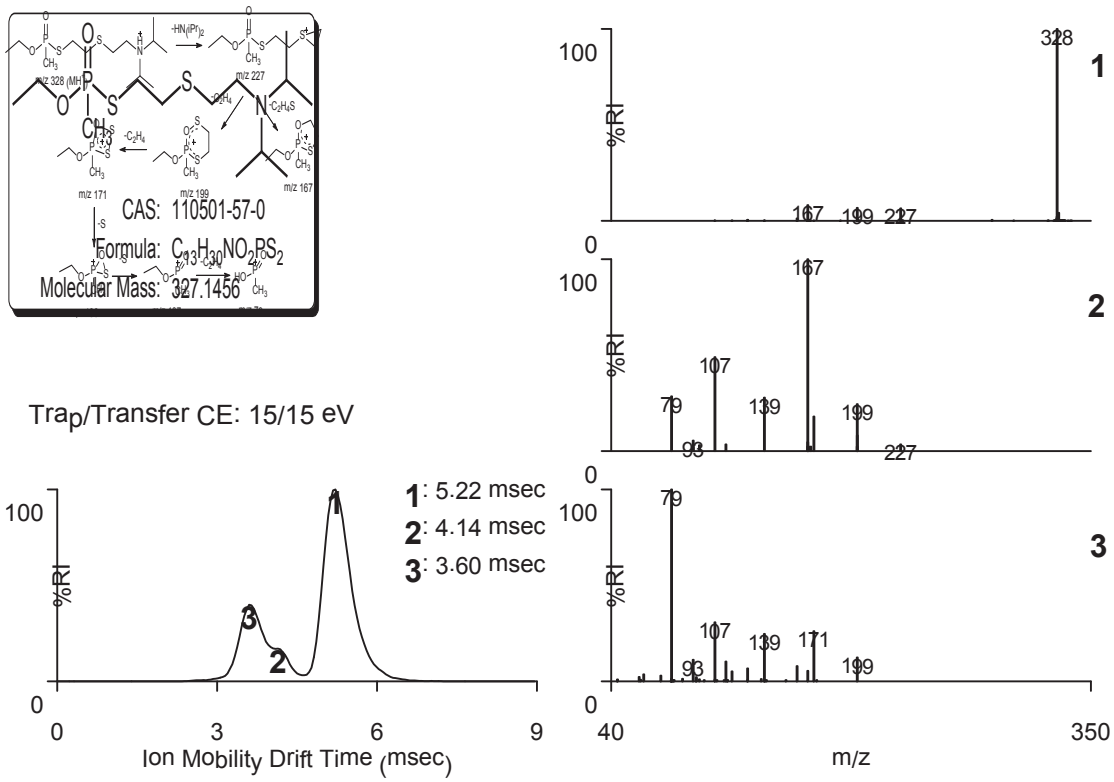

Figure 51: IMS and MS^n data for O-ethyl-S-[5-diisopropylamino)-3-thiapentyl]methylphonothialate (327).

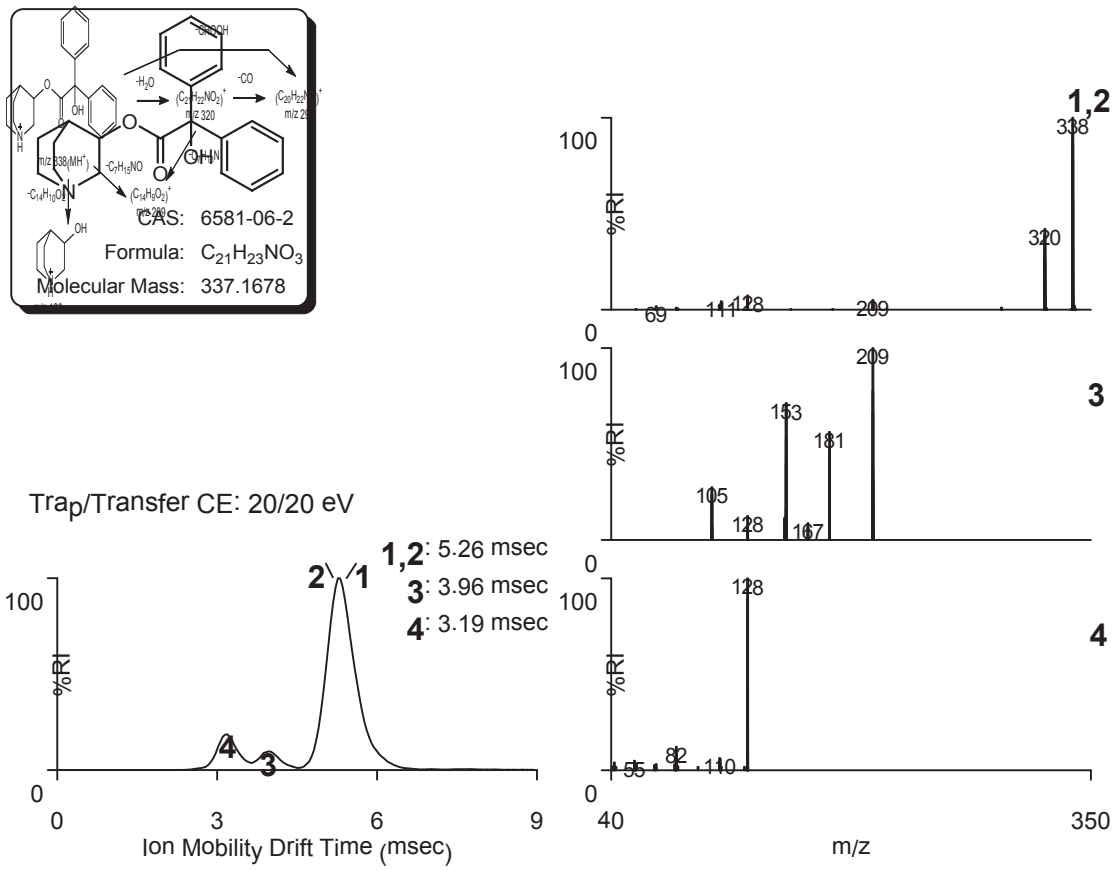

1

2

3

4

Figure 52: Lower collision energy IMS and MS^n data for 3-quinuclidinyl benzilate (BZ) (337).

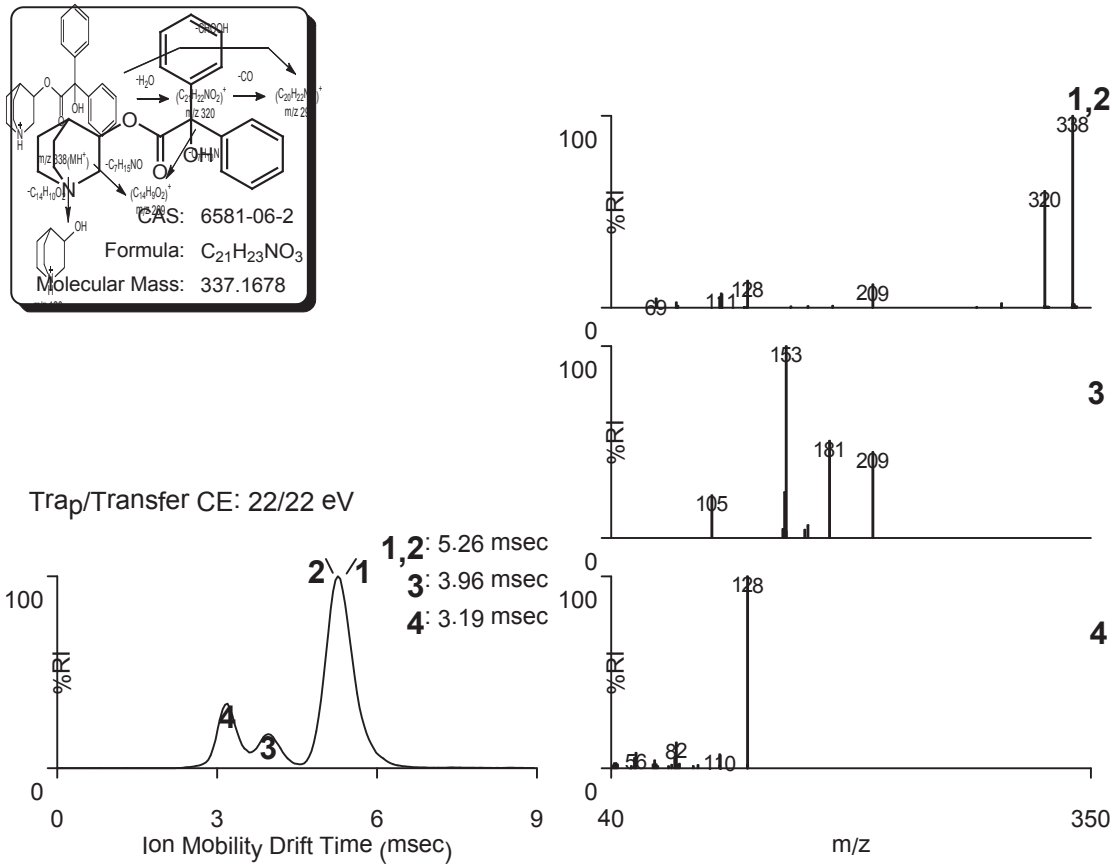

1

2

3

4

Figure 53: Moderate collision energy IMS and MS^n data for 3-quinuclidinyl benzilate (BZ) (337).

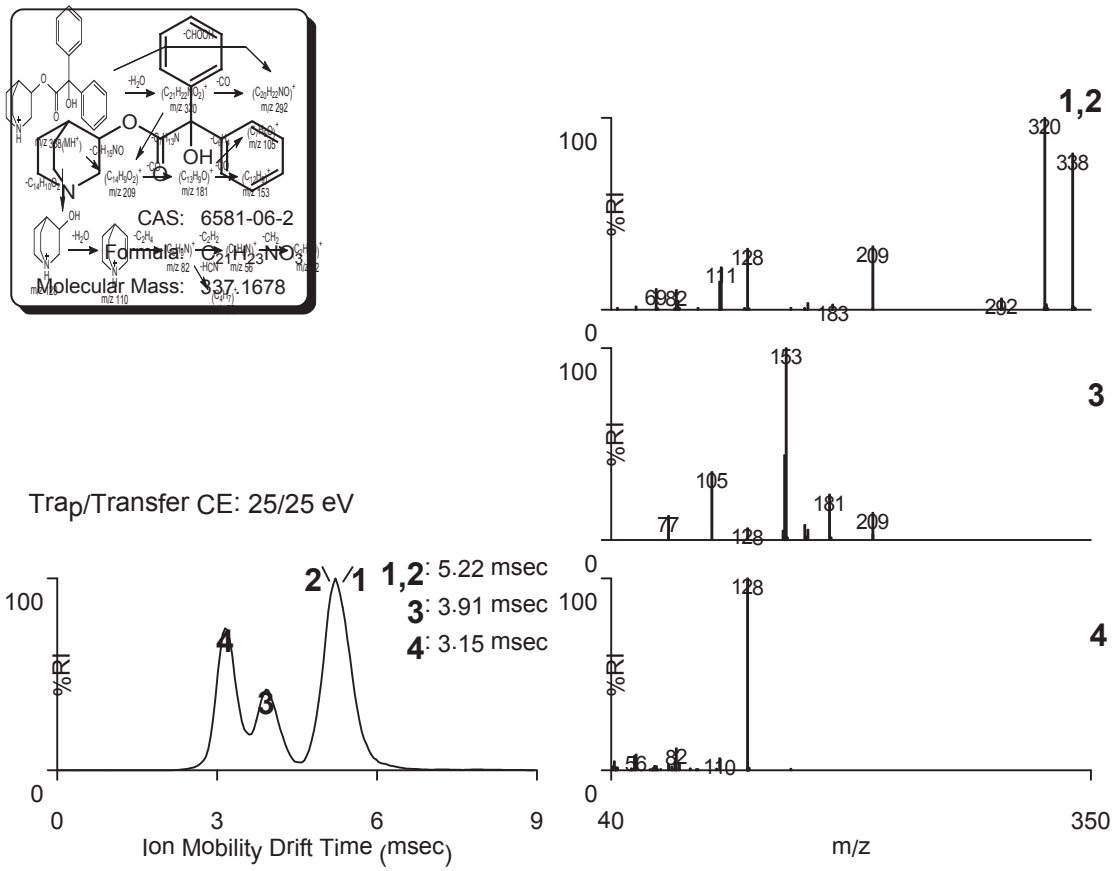

Figure 54: Higher collision energy IMS and MS^n data for 3-quinuclidinyl benzilate (BZ) (337).

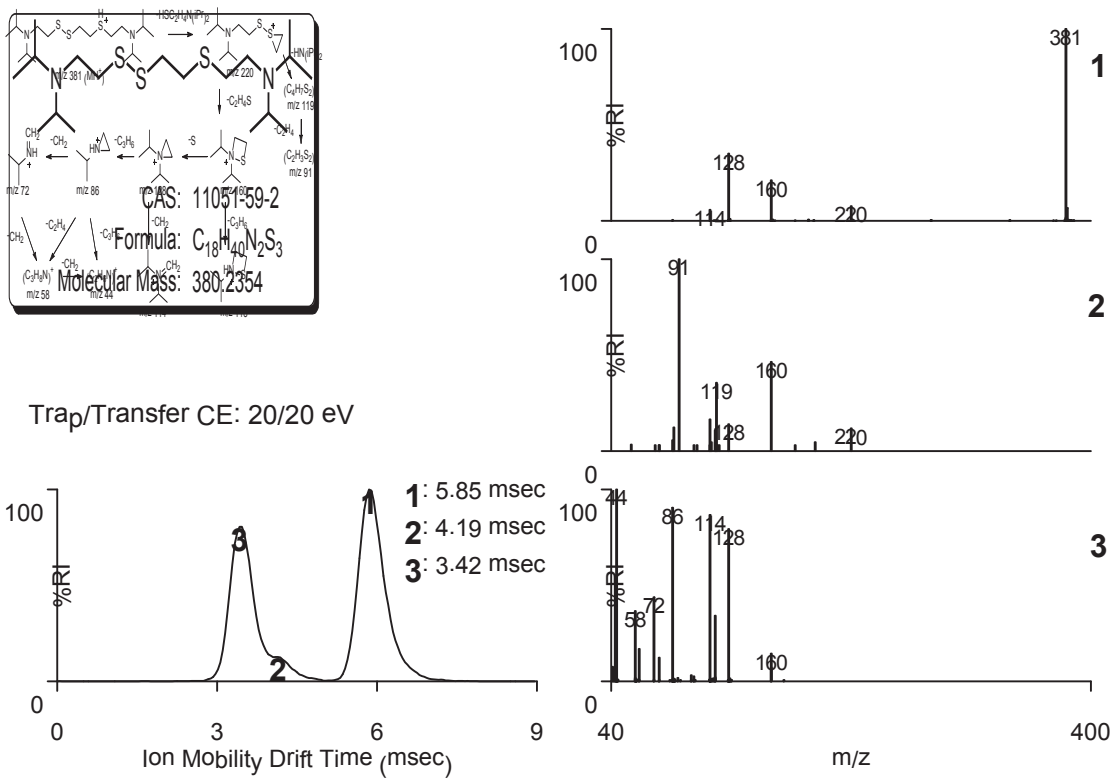

Figure 55: IMS and MS^n data for 1,9-bis(diisopropylamino)-3,4,7-trithianonane (380).

Conclusions

Unambiguous identification of chemical warfare agents requires the acquisition of data from at least two spectrometric/spectroscopic techniques. Usually this would require multiple analyses, often using two different instruments. The Synapt HDMS quadrupole time-of-flight tandem mass spectrometer has the ability to acquire both ion mobility spectrometric (IMS) and tandem mass spectrometric (MS^n where n = 2 or 3) data during a single instrumental analysis. During this study chemical warfare agents, hydrolysis products and related compounds were analysed using the TAP experiment which yields both IMS and MS^n data during a single instrumental analysis. Individual compounds were differentiated on the basis of their acquired IMS profiles and full scanning, high resolution MS^n data, containing evidence of the $[M+H]^+$ ion and typically three or more characteristic product ions were acquired using one or more collision energy settings. Examples of the usefulness of this identification method for chemical warfare agents are provided as well as an application demonstrating the unambiguous identification of the sarin hydrolysis products, isopropyl methylphosphonic acid and methylphosphonic acid, in the fill of an old rocket recovered from the CFB Suffield Military Training Range. This summary report also contains the 55 entry IMS and MS^n database, created following characterization of available chemical warfare agents, hydrolysis products and related compounds.

The data contained in the database may be used for the unambiguous identification of individual compounds contained in the database. Alternatively, data collected using the TAP experimental approach could aid in the structural elucidation of previously uncharacterized compounds or unknowns present in samples selected for chemical warfare agent analysis. Identification of these additional sample components could be significant as their identity may indicate possible synthetic pathway information or aid in identifying the source of the chemical warfare agent.

References

[1] Kientz, Ch.E. (1998). Chromatography and mass spectrometry of chemical warfare agents, toxins and related compounds: state of the art and future prospects. *J. Chromatogr. A*, 814, 1-23.

[2] Munro, N.B., Talmage, S.S., Griffin, G.D., Waters, L.C., Watson, A.P., King, J.F. and Hauschild, V. (1999). The sources, fate, and toxicity of chemical warfare agent degradation products. *Environ. Health Persp*., 107, 933-74.

[3] Black, R.M. and Read, R.W. (2000). Liquid chromatography/mass spectrometry in analysis of chemicals related to the chemicals weapons convention. In R. A. Meyers, (Ed.), Encyclopedia of Analytical Chemistry, John Wiley & Sons Ltd., Chichester, pp 1007-25.

[4] Noort, D., Benschop, H.P. and Black, R.M. (2002). Biomonitoring of exposure to chemical warfare agents: a review. *Toxicol. App. Pharm*., 184, 116-26.

[5] Hooijschuur, E.W.J., Kientz, C.E. and Brinkman, U.A.T. (2002). Analytical separation techniques for the determination of chemical warfare agents. *J. Chromatogr. A*, 982, 177-200.

[6] Black, R.M. and Muir B. (2003). Derivatisation reactions in the chromatographic analysis of chemical warfare agents and their degradation products. *J. Chromatogr. A*, 1000, 253-81.

[7] D'Agostino, P.A (2005). Recent advances and applications of LC-MS for the analysis of chemical warfare agents and their degradation products – A review. *Trends in Chromatography*, 1, 23-42.

[8] Mesilaakso, M. (2005). Chemical weapons convention analysis, Sample collection, preparation and analytical methods. John Wiley & Sons Ltd., Chichester, UK.

[9] Black, R.M. and Read, R.W. Environmental and biomedical sample analysis in support of allegations of use of chemical warfare agents. *Toxin Reviews*, 26, 275-298.

[10] D'Agostino, P.A. (2008). Chemical warfare agents. In M. J. Bogusz, (Ed.), Forensic Science Handbook of Analytical Separation, Vol. 6, Elsevier, Amsterdam, pp 839-872.

[11] D'Agostino, P.A., Hancock, J.R. and Provost, L.R. (2000). Analysis of tabun and related compounds by packed capillary liquid chromatography-electrospray mass spectrometry (LC-ESI-MS), DRES TM 2000-004.

[12] D'Agostino, P.A., Hancock, J.R. and Chenier, C.L. (2003). Comparison of LC-ESI-MS and GC-MS for the analysis of a synthetic tabun sample, DRDC Suffield TM 2003-024.

[13] D'Agostino, P.A., Hancock, J.R. and Chenier, C.L. (2003). Mass spectrometric analysis of chemical warfare agents and their degradation products in soil and synthetic samples, *European J. Mass Spectrom.,* 9, 609-618.

[14] D'Agostino, P.A., Chenier, C.L. and Hancock, J.R. (2001) Identification of sarin and related compounds in snow by packed capillary liquid chromatography-electropsray mass spectrometry (LC-ESI-MS), DRES TM 2001-044.

[15] D'Agostino, P.A., Chenier, C.L. and Hancock, J.R. (2002). Packed capillary liquid chromatography-electrospray mass spectrometry of snow contaminated with sarin, *J. Chromatogr. A*, 950, 149-156.

[16] D'Agostino, P.A., Hancock, J.R. and Provost, L.R. (1999) Packed capillary LC-ESI-MS analysis of O-ethyl S-[2-(diisopropylamino)ethyl] methylphosphonothiolate (VX), Suffield Report No 706.

[17] D'Agostino, P.A., Hancock, J.R. and Provost, L.R. (1999). Analysis of O-ethyl S-[2-(diisopropylamino)ethyl] methylphosphonothiolate (VX) and its degradation products by packed capillary LC-ESI-MS, *J. Chromatogr. A*, 837**,** 93-105.

[18] D'Agostino, P. A., Hancock, J. R., Chenier, C. L. and Jackson Lepage, C. R., (2006). Liquid chromatography electrospray tandem mass spectrometric and desorption electrospray ionization tandem mass spectrometric analysis of chemical warfare agents in office media typically collected during a forensic investigation. *J. Chromatogr. A,* 1110, 86-94.

[19] D'Agostino, P. A., Chenier, C. L., Hancock, J. R. and Jackson Lepage, C. R. (2007). Desorption electrospray ionization mass spectrometric analysis of chemical warfare agents from solid-phase microextraction fibers. *Rapid Commun. Mass Spectrom*., 21, 543-549.

[20] D'Agostino, P.A. and Chenier, C.L. (2010). Desoprtion electrospray ionization mass spectrometric analysis of organophosphorus chemical warfare agents using ion mobility and tandem mass spectrometry. *Rap. Commun. Mass Spectrom*., 24, 1617-1624.

[21] D'Agostino, P.A. and Chenier, C.L. (2010). Desorption Electrospray ionization mass spectrometry (DESI-MS) analysis of organophosphorus chemical warfare agents: rapid acquisition of time-aligned parallel (TAP) fragmentation data, DRDC Suffield TM 2010-047.

[22] D'Agostino, P.A. (2011). DESI-MS/MS of chemical warfare agents and related compounds, In Banoub, J, (Ed), Detection of Biological Agents for the Prevention of Bioterrorism, Springer, The Netherlands, pp 163-179.

[23] Eiceman, G.A. and Karpas, Z. (2005). Ion mobility spectrometry. CRC Press, Boca Raton, Florida.

[24] Asbury, G.R., Wu, C., Siems, W.F. and Hill Jr, H.H. (2000). Separation and identification of some chemical warfare degradation products using electrospray high resolution ion mobility spectrometry with mass selected detection. *Anal. Chim. Acta,* 404, 273-283.

[25] Steiner, W.E., Clowers, B.H., Matz, L.M., Siems, W.F. and Hill, H.H. (2002). Rapid screening of aqueous chemical warfare agent degradation products: ambient pressure ion mobility mass spectrometry. *Anal. Chem.,* 74, 4343-4352.

[26] Steiner, W.E., Clowers, B.H., Haigh, P.E. and Hill, H.H. (2003). Secondary ionization of chemical warfare agent simulants: atmospheric pressure ion mobility time-of-flight mass spectrometry. *Anal. Chem.,* 75, 6068-6076.

[27] Steiner, W.E., Klopsch, S.J., English, W.A., Clowers, B.H. and Hill, H.H. (2005). Detection of a chemical warfare agent simulant in various aerosol matrixes by ion mobility time-of-flight mass spectrometry. *Anal. Chem.,* 77, 4792-4799.

[28] Steiner, W.E., Harden, C.S., Hong, F., Klopsch, S.J., Hill Jr, H.H. and McHugh, V.M. (2006). Detection of aqueous phase chemical warfare agent degradation products by negative mode ion mobility time-of-flight mass spectrometry [IM(tof)MS]. *J. Am. Soc. Mass Spectrom.,* 17, 241-245.

[29] Steiner, W.E., English, W.A. and Hill, H.H. (2005). Separation efficiency of a chemical warfare agent simulant in an atmospheric pressure ion mobility time-of-flight mass spectrometer (IM(tof)MS). *Anal. Chim. Acta,* 532, 37-45.

[30] Kolakowski, B. M., D'Agostino, P.A., Chenier, C. and Mester, Z. (2007). Analysis of chemical warfare agents in food products by atmospheric ionization-high field asymmetric waveform ion mobility spectrometry-mass spectrometry, *Anal. Chem.,* 79, 8257-8265.

[31] D'Agostino, P. A. and Chenier, C. L. (2011). Database of ion mobility and tandem mass spectrometric data: characterization of chemical warfare agents, hydrolysis products and related compounds. DRDC Suffield TM 2011-001.

[32] D'Agostino, P.A., Chenier, C.L. and Hancock, J.R. (2002). Electrospray Mass Spectrometry of Chemical Warfare Agents, Degradation Products and Related Compounds, DRES TR 2002-028.

Annex A Raw datafiles used to prepare Figures 1 to 55

File Names	data file	Function	eV	Peak Scans			
				1	2	3	4
96_MPA.emf	110215-20	2	3/15	57:62			
96_MPA_High eV.emf	110519-13	2	5/20	56:63			
101_VX Products.emf	100517-10	12	10/10	70:76	55:62		
122_TDG_Low eV.emf	110215-05	2	3/3	75:90	59:66		
122_TDG_High eV.emf	110215-09	2	3/10	74:88	61:66-69		
124_VX Products.emf	100517-10	11	8/8	67:74	55:60		
138_iPrMPA.emf	110215-25	2	5/5	73:77	59:63		
138_iPrMPA_High eV.emf	110215-26	2	5/15	73:77	58:63		
140_TMP.emf	110228-11	2	15/15	76:85	57:63		
140_GB.emf	091215-04	4	3/3	72:78	59:63		
140_GB_High eV.emf	091215-04	3	3/20	70:75	55:61		
152_VX Products.emf	100517-10	14	10/10	77:81	66:71	51:57	
153_GA Products.emf	100512-12	10	10/10	75:80	64:70		
162_GA.emf	091215-05	3	7/7	81:83	70:74		
162_GA_Med eV.emf	110126-07	11	7/10	80:83	69:73		
162_GA_High eV.emf	091215-05	4	7/15	81:94	65:74		
178_cyclohexylMPA.emf	110217-06	2	5/5	80:93	56:66		
178_cyclohexylMPA_High eV.emf	110217-19	2	5/20	78:93	53:67		
180_GF.emf	091215-06	4	3/3	79:94	54:70		
180_GF_High eV.emf	091215-06	3	3/20	78:91	53:65		
180_pinMPA.emf	110217-25	2	3/3	81:93	55:69		
180_pinMPA_High eV.emf	110217-27	2	3/20	79:92	54:65		
180_GA Products.emf	100512-12	11	12/12	85:87	74:78	60:67	
181_GA Products.emf	100512-12	12	10/10	82:100	73:77	63:69	
182_TEP.emf	110215-03	2	10/10	87:89	76:79	67:70	55:58:00
182_GD.emf	091215-03	4	3/3	80:89	64:67-(54:58+74:76)	54:59-63:65	
182_GD_High eV.emf	091215-03	3	3/20	83:89	54:60-68:72	65:71-53:60	
189_VX Products.emf	100517-04	15	10/10	90:97	60:66		
194_GA Products.emf	100512-12	15	7/7	86:96	70:80		
195_GA Products.emf	100512-12	17	7/7	90:96	73:80		
196_GA Products.emf	110126-09	15	7/7	91:99	74:81		
208.emf	110303-05	3	3/3	90:106	66:80		
208_High eV.emf	110303-05	4	3/20	87:107	62:78		
209_GA Products.emf	110126-08	16	7/7	91:99	80:86	64:73	
210.emf	110126-08	17	7/7	92:101	80:86	64:74	
224.emf	110308-13	2	7/7	98:105	85:91	69:78	53:62
224_High eV.emf	110307-09	2	10/10	98:105	85:91	70:76	54:62
224_TiPrP.emf	110126-09	18	7/7	95:103	81:88	68:78	54:63
224_TiPrP_High eV.emf	110308-06	2	10/10	98:106	82:89	69:77	54:61
224_VX Products.emf	100517-10	19	15/15	97:109	75:82-62:63	64:69	
230.emf	110223-11	6	10/15	94:98	81:87	71:78	
240_VX Products.emf	100517-10	20	15/15	101:111	78:88	64:69	
264.emf	110301-12	18	3/3	106:115	82:93	56:67	
264_High eV.emf	110301-11	17	3/20	103:111	81:90	54:65	
266_TBP.emf	100504-03	4	10/10	110:117	93:100	72:82	52:62
267_VX.emf	091215-16	2	15/18	101:112	71:82		
287_GA Products.emf	100512-12	13	12/12	106:110	90:99-106:107		
288_GA Products.emf	100512-12	14	12/12	108:112	90:98	73:82	
288_VX Products.emf	100517-09	13	15/15	113:123	88:94	76:81	
320_VX Products.emf	100517-10	16	15/15	117:128	94:102	76:82	
337_BZ.emf	110317-10	2	25/25	112:126	84:94	65:77	
337_BZ_ eV20.emf	110317-15	2	20/20	113:126	86:93	67:76	
337_BZ_ eV22.emf	110317-21	2	22/22	115:123	89:94	67:72	
337_BZ.emf	110317-10	2	25/25	112:126	84:94	65:77	
380.emf	110223-08	2	20/20	126:139	92:101	72:83	

This page intentionally left blank.

DOCUMENT CONTROL DATA

(Security classification of title, body of abstract and indexing annotation must be entered when the overall document is classified)

1. ORIGINATOR (The name and address of the organization preparing the document. Organizations for whom the document was prepared, e.g. Centre sponsoring a contractor's report, or tasking agency, are entered in section 8.)

Defence R&D Canada – Suffield
P.O. Box 4000, Station Main
Medicine Hat, Alberta T1A 8K6

2. SECURITY CLASSIFICATION (Overall security classification of the document including special warning terms if applicable.)

UNCLASSIFIED
(NON-CONTROLLED GOODS)
DMC A REVIEW:GCEC JUNE 2010

3. TITLE (The complete document title as indicated on the title page. Its classification should be indicated by the appropriate abbreviation (S, C or U) in parentheses after the title.)

Database of ion mobility and tandem mass spectrometric data: characterization of chemical warfare agents, hydrolysis products and related compounds

4. AUTHORS (last name, followed by initials – ranks, titles, etc. not to be used)

D'Agostino, P.A.; Chenier, C.L.

5. DATE OF PUBLICATION (Month and year of publication of document.)	6a. NO. OF PAGES (Total containing information, including Annexes, Appendices, etc.)	6b. NO. OF REFS (Total cited in document.)
August 2012	108	32

7. DESCRIPTIVE NOTES (The category of the document, e.g. technical report, technical note or memorandum. If appropriate, enter the type of report, e.g. interim, progress, summary, annual or final. Give the inclusive dates when a specific reporting period is covered.)

Technical Report

8. SPONSORING ACTIVITY (The name of the department project office or laboratory sponsoring the research and development – include address.)

Defence R&D Canada – Suffield
P.O. Box 4000, Station Main
Medicine Hat, Alberta T1A 8K6

9a. PROJECT OR GRANT NO. (If appropriate, the applicable research and development project or grant number under which the document was written. Please specify whether project or grant.)	9b. CONTRACT NO. (If appropriate, the applicable number under which the document was written.)

10a. ORIGINATOR'S DOCUMENT NUMBER (The official document number by which the document is identified by the originating activity. This number must be unique to this document.)	10b. OTHER DOCUMENT NO(s). (Any other numbers which may be assigned this document either by the originator or by the sponsor.)
DRDC Suffield TR 2012-010	

11. DOCUMENT AVAILABILITY (Any limitations on further dissemination of the document, other than those imposed by security classification.)

Unlimited

12. DOCUMENT ANNOUNCEMENT (Any limitation to the bibliographic announcement of this document. This will normally correspond to the Document Availability (11). However, where further distribution (beyond the audience specified in (11) is possible, a wider announcement audience may be selected.))

Unlimited

13. ABSTRACT (A brief and factual summary of the document. It may also appear elsewhere in the body of the document itself. It is highly desirable that the abstract of classified documents be unclassified. Each paragraph of the abstract shall begin with an indication of the security classification of the information in the paragraph (unless the document itself is unclassified) represented as (S), (C), (R), or (U). It is not necessary to include here abstracts in both official languages unless the text is bilingual.)

The unambiguous identification of chemical warfare agents requires the acquisition of data from at least two spectrometric/spectroscopic techniques, a requirement that typically results in multiple analyses on different instrumentation. It is now possible to acquire both ion mobility spectrometric (IMS) and tandem mass spectrometric (MS^n, where n = 2 or 3) data during a single instrumental analysis using the Synapt HDMS. Chemical warfare agents, hydrolysis products and related compounds were analysed using the time-aligned parallel (TAP) fragmentation approach which yields both IMS and MS^n data during a single instrumental analysis. Compounds were characterized and differentiated on the basis of their acquired IMS profiles and high resolution MS^n data, which contained evidence of the $[M+H]^+$ ion and typically three or more characteristic product ions. Examples of the usefulness of this identification method for chemical warfare agents are provided as well as an application demonstrating the unambiguous identification of the sarin hydrolysis products, isopropyl methylphosphonic acid and methylphosphonic acid, in the fill of an old rocket recovered from the CFB Suffield Military Training Range. This summary report also contains a 55 entry IMS and MS^n database, created following characterization of available chemical warfare agents, hydrolysis products and related compounds.

14. KEYWORDS, DESCRIPTORS or IDENTIFIERS (Technically meaningful terms or short phrases that characterize a document and could be helpful in cataloguing the document. They should be selected so that no security classification is required. Identifiers, such as equipment model designation, trade name, military project code name, geographic location may also be included. If possible keywords should be selected from a published thesaurus, e.g. Thesaurus of Engineering and Scientific Terms (TEST) and that thesaurus identified. If it is not possible to select indexing terms which are Unclassified, the classification of each should be indicated as with the title.)

Ion mobility spectrometry, Tandem Mass Spectrometry, Chemical Warfare Agent, Chemical Warfare Agent Hydrolysis Product, Database

Defence R&D Canada

Canada's Leader in Defence and National Security Science and Technology

R&D pour la défense Canada

Chef de file au Canada en matière de science et de technologie pour la défense et la sécurité nationale

www.drdc-rddc.gc.ca